Control in Cogeneration Islanding Systems for Saudi Aramco Processing Facilities

by

Bader Saud Alkhaldi

Bachelor of Science in Electrical Engineering, CSULB, 2006

A THESIS SUBMITTED IN PARTIAL FULFILLMENT OF THE REQUIREMENTS FOR THE DEGREE OF

Master of Science in Engineering

In the Graduate Academic Unit of Electrical and Computer Engineering

Supervisor(s):	Eugene F. Hill, PhD, Electrical and Computer Engineering
	Liuchen Chang, PhD, Electrical and Computer Engineering
Examining Board:	B.G. Colpitts, PhD, Electrical and Computer Engineering,
	G. Holloway, PhD, Mechanical Engineering

This thesis is accepted

Dean of Graduate Studies

THE UNIVERSITY OF NEW BRUNSWICK

May, 2015

©Bader Saud Alkhaldi, 2015

Abstract

The Saudi Aramco Processing Facilities (SAPF) are located in an eastern province of Saudi Arabia. While the plant has three industrial cogeneration units, and is connected to the Saudi national grid via two transmission lines, there is a possibility that both transmission lines will be isolated due to storms or other disturbances. If that happens SAPF would be in an isolated, or islanded, mode of operation. The three units would need to be coordinated to supply the required internal plant power demand in all cases where there initially was export to, or import from, the grid. To achieve this, a model is required that will ensure effective transition from interconnected to islanding mode.

When islanding schemes function properly, the plant can continue operating under its own power generation despite interruptions in electrical supply from the utility grid. Without the implementation of the islanding mode of operation, any disturbance in the grid could cause a blackout, severely disrupting the plant operations, causing revenue loss and gas flaring. A fully functioning islanding scheme refers to the capability of the plant generators to withstand any disturbance to the power system and continue supplying the plant load. Continual balancing of active power generated and consumed is vital for power system security and stability, and to maintain frequency within an acceptable tolerance around nominal system frequency. Due to the large size of individual generators (150 MW each unit, a total of 450 MW) with respect to total in plant load (170 MW), the loss of a generator in a small island system can

cause a large power imbalance and consequently a significant frequency excursion. Achievement of the above goal requires creation of an accurate model for the SAPF cogeneration and electrical network that includes gas turbine, governor, generator and power system. A simple model, the six-parameter linearized model, and the full nonlinear model have been used to represent the synchronous generator in different studies. The governor model is part of the turbine model in gas turbines. The excitation system and the power system stabilizer models have been based on the IEEE Standard. Specific models have been simulated in MATLAB® , and open inclusion of the transmission lines has been done in ETAP® . Critical scenarios that may lead to total blackout of the SAPF have been simulated and analyzed. This thesis provides a justification of future use of special protection systems on the SAPF power system to provide successful transition from interconnection mode of operation to islanding mode of operation during major disturbances. The special protection systems proposed are capable of handling cases of high export to the grid, and also import from the grid. Recommendations and future work are summarized at the conclusion of the thesis.

Acknowledgements

I would like to express my deepest gratitude to Dr. Eugene F. Hill, for his excellent guidance, caring, patience and support while I was doing my thesis.

I am greatly indebted to the Saudi Aramco Processing Facilities management for their financial support.

Many thanks go to SAPF Electrical group for supplying me with all required data from the field. My research would not have been possible without their help.

Finally, a lot of thanks go to my family.

Table of Contents

Abstract ii

Acknowledgments iv

Table of Contents v

List of Tables viii

List of Figures ix

Abbreviations xiii

1 INTRODUCTION 1

1.1 Background 1

1.2 Gas Turbine Cogeneration Operation 4

1.3 Combustion Gas Turbine Types 5

1.4 Development of Models 6

1.5 Islanding Mode of Operation 6

1.6 Objective of the Thesis 7

1.7 Outline of the Thesis 7

2 LITERATURE REVIEW 9

2.1 Introduction 9

2.2 Islanding in Distributed Generation Systems 9

2.3 Islanding in Electric Utility Operation 10
2.4 Islanding in Industrial Plant Cogeneration Applications 11

3 ROWENS MODEL FOR GAS TURBINES 17
3.1 Gas Turbine Model Description 17
3.2 Description of Gas Turbine Parameters 21
3.3 Performance of the Governor System 22

4 SAPF COGENERATION UNIT MODELS USING MATLAB SOFTWARE 24
4.1 MATLAB / SIMULINK 24
4.2 Single Machine Interconnected to an Infinite Bus (SMIB) 25
4.3 Adding the Gas Turbine and Governor to the Interconnected Model . 29
4.3.1 Simulation and Analysis 30
4.4 Adding a Detailed Machine Model and Excitation System 31
4.4.1 Simulation and Analysis 33
4.5 Adding the Power System Stabilizer 41

5 SIMULATION OF SAPF ELECTRICAL SYSTEM USING ETAP SOFTWARE 44
5.1 Introduction 44
5.2 Case Studies and Simulations 45

6 SPECIAL PROTECTION SYSTEM 59
6.1 Introduction 59
6.2 Case Study and Simulations 62

7 CONCLUSIONS AND RECOMMENDATIONS 77
7.1 Summary 77
7.2 Conclusions 78

7.3 Recommendations for SAPF 79
7.4 Recommendations for Future Work 80

A ROWENS MODEL for HDGT INCLUDING IGV **86**

B SYSTEM EQUATIONS **87**

B.1 Moment of Inertia J 87
B.2 Inertia Constant H 87

C SYSTEM PARAMETERS **88**

D CALCULATION OF $K_1 - K_6$ **90**

E SAPF ISLANDING SCENARIOS **92**

F TRANSIENT STABILITY AND OVER-FREQUENCY RELAY ACTIONS **95**

Vita

List of Tables

3.1 Used and Typical Parameters 21

5.1 Over/Under Frequency Relay Setting. 51

6.1 SPS Actions (Case 1) 63

6.2 SPS Actions (Case 2) 68

6.3 Under-Frequency Relay Settings 72

6.4 LSS Setting and Action 72

C.1 Exciter Parameters 89

C.2 PSS Parameters 89

E.1 SAPF Islanding Scenarios 92

F.1 Transient Stability and Over-frequency Relay Actions 95

List of Figures

1.1 Open Cycle Gas Turbine Cogeneration 2

1.2 Single Line Diagram of Electrical System 3

1.3 Black Diagram of GT Major Parts 5

3.1 Rowens Model for HDGT 18

3.2 Response of Mechanical Power, Rotor Speed, Valve Positioner and Exhaust Temperature to changes in Load Torque and Step Change in Speed Reference. 23

4.1 Single Machine Connected to Infinite Bus (SMIB) 25

4.2 Generator Classical Model 27

4.3 Step Change in Mechanical Power 28

4.4 Load Angle Response to Mechanical Power Change 28

4.5 Electrical Power Response to Mechanical Power Change 28

4.6 Speed Response to Mechanical Power Change 29

4.7 Variable Response to Step Change 31

4.8 SMIB Including Excitation System 31

4.9 AC5A Excitation System Model 32

4.10 Case 1: Load Angle, Rotor Speed, Mechanical and Electrical Power, Fuel Demands, Exhaust Temperature and Field and Terminal Voltage. 35

4.11 Case 2: Load Angle, Rotor Speed, Mechanical and Electrical Power, Fuel Demands, Exhaust Temperature and Field and Terminal Voltage. 37

4.12 Case 3: Load Angle, Rotor Speed, Mechanical and Electrical Power, Fuel Demands, Exhaust Temperature and Field and Terminal Voltage. 39
4.13 Case 4: Load Angle, Rotor Speed, Mechanical and Electrical Power, Fuel Demands, Exhaust Temperature and Field and Terminal Voltage. 41
4.14 Load Angle, Rotor Speed, Mechanical and Electrical Power, Fuel Demands, Exhaust Temperature and Field and Terminal Voltage with PSS. 43

5.1 Speed 46
5.2 Bus Voltage 46
5.3 Exciter Current 47
5.4 Reactive Power 48
5.5 Exciter Voltage 48
5.6 Active Power 49
5.7 Mechanical Power 49
5.8 Speed 50
5.9 Bus Voltage 50
5.10 Exciter Current 51
5.11 Reactive Power 52
5.12 Exciter Voltage 52
5.13 Active Power 53
5.14 Mechanical Power 53
5.15 Speed 54
5.16 Bus Voltage 54
5.17 Exciter Current 55
5.18 Reactive Power 55
5.19 Exciter Voltage 56
5.20 Active Power 56

5.21 Mechanical Power 57
5.22 Speed 57
5.23 Bus Voltage 58

6.1 Single Line Diagram of Electrical System 62
6.2 Speed 64
6.3 Mechanical Power (Pm) 65
6.4 Active Power (Pe) 65
6.5 Exciter Voltage 66
6.6 Exciter Current 66
6.7 Reactive Power 67
6.8 Bus Voltage 68
6.9 Speed 69
6.10 Mechanical Power (Pm) 69
6.11 Active Power (Pe) 70
6.12 Exciter Voltage 70
6.13 Exciter Current 71
6.14 Reactive Power 71
6.15 Bus Voltage 72
6.16 Exiter Current 73
6.17 Reactive Power 73
6.18 Exciter Voltage 74
6.19 Active Power 74
6.20 Mechanical Power 75
6.21 Speed 75
6.22 Bus Voltage 76

A.1 Rowens Model for HDGT Including IGV 86

D.1 A One Machine Infinite Bus Power System 90

List of Symbols, and Abbreviations

SAPF	Saudi Aramco Processing Facilities.
SEC	Saudi Electricity Company.
CGT	Combustion Gas Turbine.
HRSG	Heat Recovery Steam Generator.
GEN	Generator
Co-Gen	Cogeneration.
CB	Circuit Breaker.
PSS	Power System Stabilizer.Power System Stabilizer
Area EPS	Area Electrical Power System (Grid).
Local EPS	Local Electrical Power System.
PCC	Point of Common Coupling.
TCS	Turbine Control System.
SPS	Special Protection System.
MW	Megawatt a Unit of Power.
MVAR	Mega Volt Ampere Reactive.
i	Armature Current.
PU	Per Unit.
IB	Infinite Bus.
K_S	Synchronizing Torque Coefficient.
K_D	Damping Torque Coefficient.

SG	Synchronous Generator.
P_e	Electrical Power.
P_m	Mechanical Power.
P	Active Power.
Q	Reactive Power.
V_t	Terminal Voltage.
E_{FD}	Exciter Field Voltage.
X	Reactance.
V_{IB}	Infinite Bus Voltage.
H	Inertia of the Machine.
T	Torque in Per Unit.
ω_r	Nominal Value of the Rotor Angular Velocity.
f_{osc}	Frequency of Oscillation
$\Delta\delta$	Variation of the Rotor Angle.
$\Delta\omega$	Variation of the Rotor Angular Velocity.
$\Delta_{\Psi fd}$	Field Flux Variation.
$X_{d'}$	Direct Transient Reactance.
X_d	Direct Axis Synchronous Reactance.
X_q	Quadrature Axis Synchronous Reactance.
E_f	Internal Voltage.

Chapter 1

INTRODUCTION

1.1 Background

The Saudi Aramco Processing Facilities (SAPF) are located in an eastern province of Saudi Arabia. The processing facilities consist of three processing plants-gas production, oil production and power generation. The oil plant is capable of processing 500,000 barrels per day (BPD) of Arabian light crude oil blend. The gas plant processes one billion standard cubic feet a day (SCFD) of associated gas and 1.8 billion SCFD of non-associated gas. The power plant contains three industrial cogeneration units (combustion gas turbines). Each unit is designed to generate 148.95 MW (nominally 150 MW) of electrical power. Steam is also produced as a by-product by a heat recovery steam generator (HRSG) for use in the gas plant, as shown in Figure 1.1.

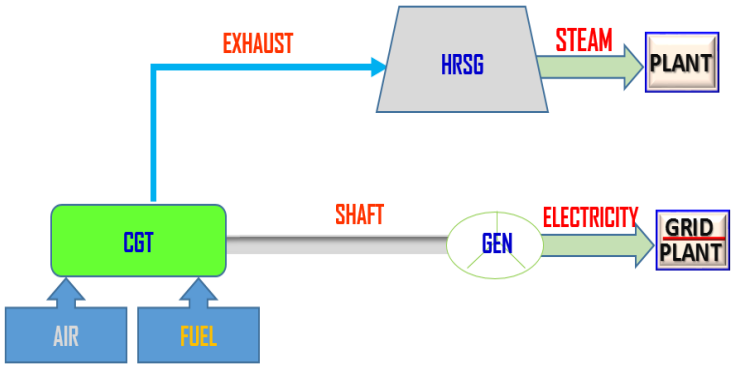

Figure 1.1: Open Cycle Gas Turbine Cogeneration

Both the gas plant and the oil plant in the SAPF facility require many electrical motor compressor loads and other large electrical drives, often called the internal plant load. While it may vary with ambient temperature and loading conditions, the internal plant load is normally 100-200 MW. With a potential power plant generation of 450 MW, there is an opportunity for the SAPF to export the excess power to the national grid to support it. Therefore 250-350 MW could be exported to the national grid. SAPF main substation contains a 115 kV double-bus bar type switchgear equipped with circuit-breaker sectionalizers and couplers. The circuit breakers contain insulated gas (Sulfur Hexafluoride, SF6). The main substation is connected to the main power grid by two 115 kV transmission lines as shown in Figure 1.2.

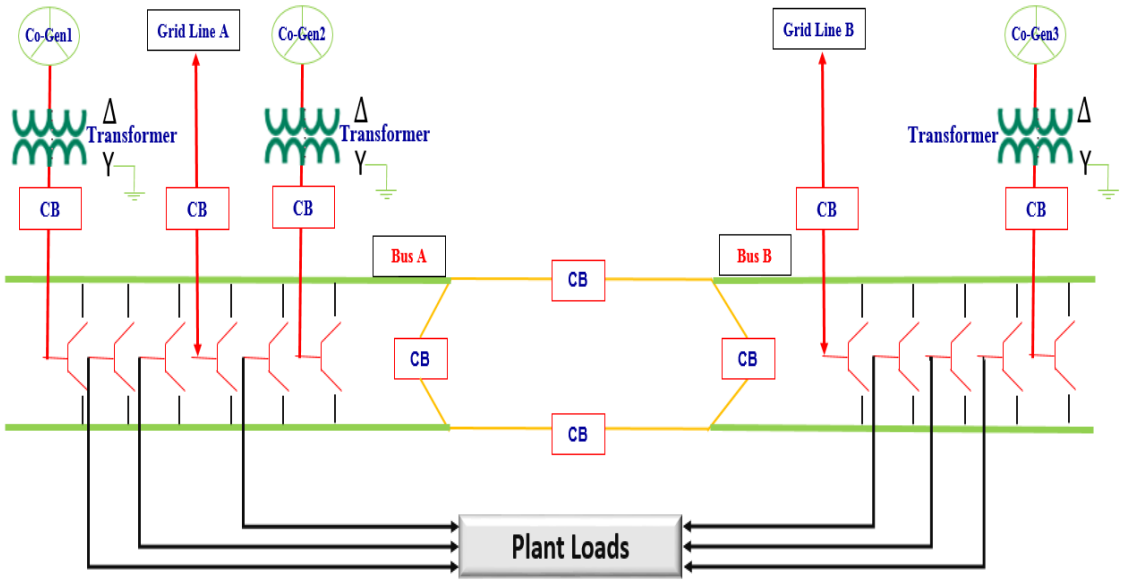

Figure 1.2: Single Line Diagram of Electrical System

There are three modes of operation to supply the plant electrical load. First, the load can be supplied from the Saudi Arabian grid, referred to as "import mode"in this thesis. Secondly, they can be supplied from the SAPF cogeneration plant while it is connected with the grid, referred to as "interconnected mode". Finally, they can be supplied solely from the SAPF cogeneration units, referred to as isolated or "islanded mode".

Combustion gas turbines burn natural gas as the primary fuel. Each SAPF gas turbine is direct coupled to a two-pole generator, which is rated at 175.24 MVA at a power factor of 0.85 lagging. The generator-rated three-phase voltage is 16.5 kV at 60 Hz. Each 175.24 MVA unit is connected to the main substation by a 115 kV underground cable through a 200/250 MVA step-up transformer and a 123 kV SF6-circuit breaker. The cogeneration gas-turbine auxiliary power is supplied from the plant 0.48 kV distribution system for start-up. A 4.16 kV starting motor is initially used to get the gas turbine shaft rotating. The 0.48 kV and 4.16 kV systems are independently supplied by the national grid. Once the gas turbine is operational, these systems are supplied by the cogeneration units. The plant electrical

system is designed to be isolated from the utility and maintain operation in the event of severe utility under-voltage or under-frequency conditions, or on loss of the two 115 kV connections to the power grid. Plant-connected loads consist primarily of synchronous motors, induction motors and static loads. Most motors operate below rated horsepower. SAPF management requires the cogeneration facility to maintain or improve plant electric and steam system availability. Accordingly, it was determined that an electrical study would be necessary to ensure that operation of the cogeneration facility will meet management objectives. The research of this thesis meets this requirement, with special emphasis on maximizing cogeneration system availability and minimizing the effect of transient disturbances on plant production.

1.2 Gas Turbine Cogeneration Operation

The gas turbine generation system is based on the Brayton cycle of thermodynamics, in which atmospheric air is compressed and mixed with fuel for combustion heating. The compressed and heated combustion products are expanded through a turbine which produces sufficient shaft power to drive the compressor and electrical generator. The turbine exhaust is at an elevated temperature which can be further raised by the exhaust gas. As shown in Figure 1.1 a gas turbine system utilizes the Brayton cycle, in which the compressor takes air in from the atmosphere and drives it into the combustor under increased pressure. This process also increases the air temperature. A diffuser is used to express the air into a combustion chamber, which is under constant pressure. The diffuser decreases the velocity of the air so that it can be utilized effectively in the combustor. Fuel is injected and burned in the combustion chamber, which results in a slight pressure drop. The exhaust gas output of the chamber has excess oxygen and a high temperature. The gas turbine sets the maximum gas temperature, depending on the effectiveness of the cooling blades. The mechanical work

results from the exhaust gases, which have high pressure and temperature, driving the compressor and electrical generator. The high temperature exhaust gas from the turbine is directed to a generator for production of plant process steam.

1.3 Combustion Gas Turbine Types

Combustion gas turbines are the prime mover acting as a source of mechanical power that will be converted to electrical power. As a prime mover, gas turbines are preferred because of their low capital cost per unit of output. They are more compact than steam and hydraulic turbines, and are quick to start up and reach synchronous speed, which makes them useful as peaking units in utility applications. Natural gas turbines also have advantages from an environmental perspective. The design of the gas turbine includes a single shaft and a twin shaft. This thesis focuses on a single shaft combustion gas turbine, in which the compressor is connected to the turbine by a single shaft. The benefits of this system are that it is easy to operate and is not costly in terms of overall investment. It is also more reliable than turbines that have a twin shaft unit, in which one shaft has higher pressure and runs at a higher speed, while the other shaft runs under lower pressure at a lower speed.

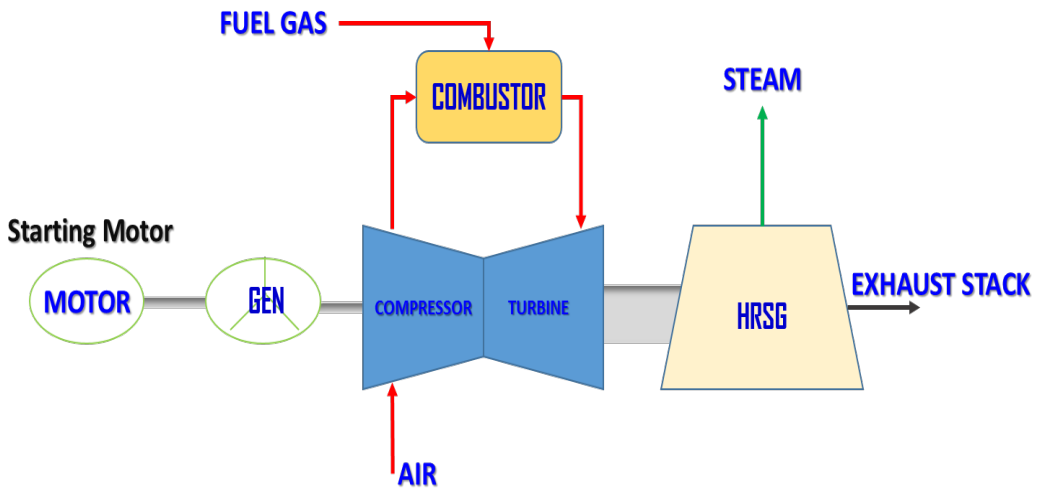

Figure 1.3: Black Diagram of GT Major Parts

1.4 Development of Models

Depending on the area of the world, original equipment manufacturers (OEMs) have built and operated gas plants under agreements with local authorities. More recently OEMs have built plants on a turn-key basis. Under such arrangements, the OEMs are also responsible for system studies related to the successful operation of the plant, and for analyzing and simulating plant upsets and disturbances. Because the OEMs are in a competitive market, much of their information is declared to be proprietary. A dynamic stability study of the SAPF cogeneration facility has not been undertaken by plant personnel. No models were provided by the OEM for this thesis work. The exciter and power system stabilizer models have been constructed based on IEEE standards and guides. The governor and turbine models have been developed using Rowens models [1, 2], as outlined in the literature review Chapter 2. The generator model has been based on materials described in textbooks, as detailed in Chapter 4.

1.5 Islanding Mode of Operation

It is obvious that the uninterrupted operation of the gas and oil production plants within the SAPF is of paramount importance. This requires successful operation in the interconnected and islanded modes, and, more importantly, successful transition from one mode to the other. The IEEE Standard on Interconnecting Distributed Resources with Electric Power Systems [3] introduces the terminology, and describes islanding as "a condition in which a portion of a local electrical power system (EPS) is energized solely by one or more local generators through the associated point of common coupling (PCC) while that portion of the local EPS is electrically separated from the rest of the Area EPS ".

1.6 Objective of the Thesis

The objective of this thesis is to develop a successful model of the electrical power system for transition from "interconnected mode" to "islanded mode" for the SAPF in Saudi Arabia. This thesis assesses the operating conditions of the three cogeneration units during any disturbing circumstances, and identifies appropriate control logic that will enable a turbine control system (TCS) to distinguish between the interconnected and islanded modes of operation. A simulation, using Rowens model [1] of the three gas turbines with governor controls, IEEE models for excitation systems and power system stabilizers and generator models, is carried out in MATLAB® software. ETAP® software is used to model the full transmission system and the in-plant load. This project analyzes the performance of the three cogeneration units during the transition from interconnected mode to islanded mode of operation and ensures that the units can generate the required power to reach a stable operation condition. This will ensure that there is no failure of the electrical power supply to the facility plants, and will prevent trip to the plants (total blackout). Should they be necessary, Special Protection Systems (SPSs) will be proposed to assure successful transition to the islanded mode of operation.

1.7 Outline of the Thesis

Chapter 1 introduces the Saudi Aramco Processing Facilities (SAPF), provides brief details about cogeneration systems, and sets out the objective of the thesis. Chapter 2 includes a literature review. Chapter 3 describes Rowens model for gas turbines, provides a description of gas turbine models and parameters, and shows some simulation results. Chapter 4 includes a full model of a gas turbine using MATLAB® software and details of the major components, presents simulation of some special operational scenarios, and briefly discusses the results. Chapter 5 provides a full model of the

SAPF electrical system using ETAP® software and presents the results for variable operating conditions. Chapter 6 describes a Special Protection System. Chapter 7 concludes the thesis with a summary, recommendations and future work. Chapter 8 contains the references.

Chapter 2

LITERATURE REVIEW

2.1 Introduction

It is critically important in terms of maintaining a revenue stream that the SAPF successfully transitions from interconnected mode to islanded mode. Islanding is a very broad term which has specific meaning depending on the power system. In distributed generation systems, islanding often requires disconnection of a generator. Power generated by utility companies is mainly transmitted to remote loads, so islanding conditions can mean full load rejection on the generator. On the other hand, gas and petrochemical plant companies use cogeneration in-house to supply their own plant load needs, exporting excess power to the national grid, or importing it if required. Partial load rejection or load shedding is a possible consequence of islanding.

2.2 Islanding in Distributed Generation Systems

IEEE 1547-2003, Standard for Interconnecting Distributed Resources with Electric Power Systems [4], is the first in the 1547 series of interconnection standards. It includes general requirements, response to abnormal conditions, power quality, is-

landing, and test specifications as well as requirements for design, production, installation evaluation, commissioning, and periodic tests. Historically the practice in utilities was to stop Distributed Generations (DG) from operating in case of loss of the grid. Addressing islanding issues, and recognizing the broad penetration of DG into the power system [5] argues that there should be a distinction between intentional and unintentional islanding. In a paper, Vieira et al [6] note that the IEEE distributed resources interconnection guide recommends that a DG must not be disconnected due to small frequency variations. If the relay is set to meet this requirement, it may not detect islanding conditions within the required time. On the other hand, if the relay is set to be sensitive enough for anti-islanding protection, it may also trip the DG due to small frequency variations. The authors compared the action of frequency relays versus vector surge relays in handling this problem. In another paper Vieira et al noted that, as a standard practice, anti-islanding protection systems of synchronous generators employ frequency-based relays. On the other hand, anti-islanding protection systems of induction generators are equipped with voltage-based relays. They went on to develop dynamic models of frequency-based and voltage-based relays for distributed generation protection [7].

2.3 Islanding in Electric Utility Operation

An early IEEE Working Group Report in 1983 [8] examined thermal plant response to partial load rejections as would happen during islanding. They considered fundamental factors such as overall plant control, boiler level and pressure control, governor action, the response of power plant auxiliary systems, and the possibility of steam bypass of the turbine and going directly to the condenser. Researchers have noted that in disturbances some generators have an inherent nature to tend to oscillate at, or near, the same frequency, and they have focused on those generators which oscillate

slowly. They have called this slow coherency-based islanding [9]. Two categories for islanding have been identified, controlled and uncontrolled. Uncontrolled islanding is described as the process by which an interconnected power system separates into unplanned islands as a result of a severe disturbance. Meanwhile, controlled islanding is an advanced plan to separate a severely disturbed power system into self-healing islands that are characterized by minimum load-generation unbalance and slowly-coherent generators. They have proposed a process called a decision tree for island detection and identification [10]. The authors in [11] used decision trees for transient stability prediction. Diao et al [12] looked at the use of decision trees to assist in the formation of controlled islands as a means of preventing cascading events.

2.4 Islanding in Industrial Plant Cogeneration Applications

The remainder of the literature review deals with those references which will, to a greater or lesser extent, be used directly in the research work of this thesis. Chen et al published a paper in 2010 [13] on the transient stability analysis of an industrial cogeneration system in the Science Park housing a segment of the semiconductor industry in Taiwan. They point out that the importance of the semiconductor industry leads to a much higher requirement for power service quality and reliability than for general customers. Therefore, keeping the reliability and stability of power service for the Science Park becomes quite an important issue. The cogeneration in the Science Park consists of three gas turbines and one steam turbine, with a total capacity equal to about 38% of the SAPF. The authors describe various operating scenarios, and note that a load shedding scheme is implemented when the generated power is less than the internal load, in order to avoid a plant blackout during the islanding mode of operation.

In 1983, W. I. Rowen [1], of the General Electric Company in the United States published a now-classic paper on gas turbine modelling in studies of electrical power systems. This was based on a basic simple-cycle, single-shaft gas turbine, using a control system of speed, temperature and acceleration controls, along with upper and lower fuel limits. In the simplified mathematical model, a low-value selector identifies which of the three control signals requires the least fuel, based on information from the outputs of the three control signals. The minimum signal is thus given priority, and subjected to upper and lower fuel demand limits. As the lower limit is required to sustain adequate fuel flow to prevent flame-out in the gas turbine combustor, it is more important than the upper limit which is used as a backup to temperature control. The signal that is identified as most efficient is the fuel demand signal, which controls the output of the combustor by driving the fuel valve actuator. The generator and compressor are driven by the hot gases from the combustion chamber that have expanded in the turbine. The application of this model to generator-drive applications is limited, however, due to the allowable speed range of 95 to 107 percent of rated speed.

The limitations of constant compressor inlet guide vane angle and ambient temperature, as well as narrow turbine speed range, were addressed by Rowen in 1992 [2] by an upgrade of the model. Using a single-shaft gas turbine for variable-speed mechanical drive service requires careful coordination of the prime mover, and this publication provides essential information to perform dynamic studies to ensure that the coordination of the prime mover is achieved. The 1992 control scheme is similar to the single-shaft gas turbine mathematical model of 1983, but goes further by focusing on axial flow compressor inlet guide vane control. By fully opening the inlet guide vanes at start-up for the simple cycle, they become fixed over the normal operating cycles which makes the model similar to that published in 1983.

Yee et al [14] did a comparative analysis and reconciliation of gas turbine models for

stability studies focusing specifically on Rowens model and the IEEE Model. References [15] and [16] refer to simplification of the gas turbine model and its control system using Rowens model. Typical parameters of the governor, fuel system, temperature system, and turbine were utilized, providing some simulation results relating to disturbances. Utility experience with gas turbine testing and modelling is presented in [16].

Rowens model with inlet guide vanes (IGV) was used in this 2013 study for identification and control of a heavy duty gas turbine(HDGT), in order to build a model that is suitable for controller testing [17]. Neural networks were used for identification purposes. The gas turbine studied in this paper is a single-shaft machine with a 200 MVA generator, which uses natural gas as fuel and can service both simple cycle and combined cycle. The rated speed is 3000 RPM that can maintain a frequency of 50 Hz. In [18] two types of governors were identified, the GE Speedtronic Governor Control and Woodward Governor Retrofit. The model structure provided was Rowens model. The Speedtronic governors were found to be adequate and, with minor modification, a similar model structure was used for the Woodward retrofit governors. A simple procedure, based on actual operating data, is used for estimating the parameters of Rowens model for practical HDGTs [19]. These parameters could be used in dynamic studies for many purposes. Two more parameters of HDGT were used in addition to Rowens parameters. Mahat et al [20] showed three governor control forms: speed droop control, isochronous control and isochronous control with feedback. An IEEE Type ST1 excitation system model was used for the gas turbine generator (GTG). Performance of each controller was studied, with results of both islanded and grid-connected conditions.

Textbooks by Kundur [21] and Yu [22] describe both nonlinear and linear models for large electric generators. A widely used linear model is based on the so-called Heffron Phillips parameters, and these are applicable for a synchronous machine connected to

an infinite bus system and operating in closed loop. A method for identifying these parameters is given in [23]. Because the majority of online data used for identification is gathered when the machine is connected to the power system and operating in closed loop, this problem is a practical one of significance. Errors in the parameter estimates result from the use of open-loop identification techniques. This resource suggests that using the joint input-output closed-loop subspace identification technique will overcome this problem.

IEEE Standard 421.5-2005 is an outstanding resource for excitation systems. It provides models which can be used in transient stability studies for all excitation systems manufactured by OEMs world-wide from the earliest use of excitation systems up to the present. The IEEE Type ST1 static excitation system referred to above is an example. A brushless excitation system for synchronous machine with hybrid rotor is introduced in this paper. While not very common in Canada at these MVA levels, nevertheless a brushless excitation system is used on each of the three generators at the SAPF. Feng et al [24] look at the performance of brushless excitation systems [25], while Feng et al [24] show an improved genetic algorithm for estimation of the parameters of a brushless excitation system. In this reference, a brushless excitation system IEEE Type AC1A was considered.

IEEE Standard 421.5-2005 is also an outstanding resource for power system stabilizer (PSS) models, because PSSs always work through the excitation system. Sumina et al [26] compared the operation of a variety of IEEE type stabilizers used in synchronous generator excitation systems. The operation of an IEEE PSS1A stabilizer with an input signal of generator active power was compared to the operation of the IEEE PSS2B stabilizer. This latter stabilizer is based on the integration of accelerating power, with the signal obtained from rotor rotation speed and generator active-power input signals. The digital excitation control system of the generator was implemented in the case of both stabilizers. A study in 2010 [27] investigated stability enhancement

using a power system stabilizer. Results of the simulation demonstrate that adding a coordinated PSS to the model contributes to the improvement of the dynamic stability of the power system, while effectively suppressing low frequency oscillation. In [28] a detailed power system stabilizer PSS4B model was examined. The study provides the advantages along with the parameter settings of the power system stabilizer model, and includes the implementation method on an excitation regulator. Kamwa et al [29] systematically assessed, and compared, an IEEE PSS2B and a PSS4B stabilizer in order to identify the primary differences in their behavior based on their intrinsic design characteristics.

In 1994, an IEEE Working Group on Prime Mover and Energy Supply Models for System Dynamic Performance Studies published a paper on dynamic models for combined cycle plants for power system studies [30]. These studies include gas turbines, waste heat recovery boilers, and steam turbines. This publication illustrates development of models designed for use in system dynamic performance studies to simulate the response of the combined cycle plant. Sharma modeled an island grid [31]. The results in this study show the difference between simulation and actual measurements in a steel plant with the loss of 40 MW and 80 MW arc furnace loads. Although there were some differences between measured and simulated results, the research can be deemed successful as there were two positive outcomes: a validated model of the power system and a system for portable data acquisition. The power system model has allowed the utility to monitor the relationship between load rejection and frequency variation based on operations at the steel mill.

Khan et al [32] performed a simulation of a large electrical power system using ETAP software. Based on the outcomes, analysis and monitoring can be conducted on overloading of power/distribution transformers, line conductor and cable current carrying ability, power factors, supply demand gaps, voltage drops, transmission losses, active and reactive power flows, voltage and current magnitudes, as well as Total Harmonic

Distortion in voltage and current. The complete power system can be simulated, and utilities can integrate different grids as they are actually connected using this approach. An additional benefit is that utilities can use this simulation in their planning and development sectors.

Chen et al [33] analyzed an industrial plant with a 62 MW load. The plant also had four 10 MW cogeneration units which provided steam to the plant and generated 27 MW of power. The remaining 35 MW of load had to be supplied by the grid. A condensing type cogeneration unit with 40 MW capacity was added to the system in 1998 [33]. Due to disturbances on the bulk power system, they were concerned with coordination of the tie line protection and the setting of load shedding relays in order to maintain the supply of crucial loads in the industrial plant.

Sengupta et al [34] developed a PC based frequency monitoring system, and also a frequency relay for protection of the power system.

Chapter 3

ROWENS MODEL FOR GAS TURBINES

3.1 Gas Turbine Model Description

Rowens model of a heavy duty gas turbine (HDGT) provides an accurate model to study the dynamics of this torque production, as it is a basic isolated operation model of a unit against load. The purpose of this chapter is to describe and demonstrate the fundamentals of gas turbine operation. The original Rowens model appeared in his 1983 paper [1], as shown in Figure 3.1. It entails a simplified block diagram for a single shaft, heavy duty gas turbine with its control and fuel systems. The original Rowens model consists of a governor speed control, acceleration control, and temperature control.

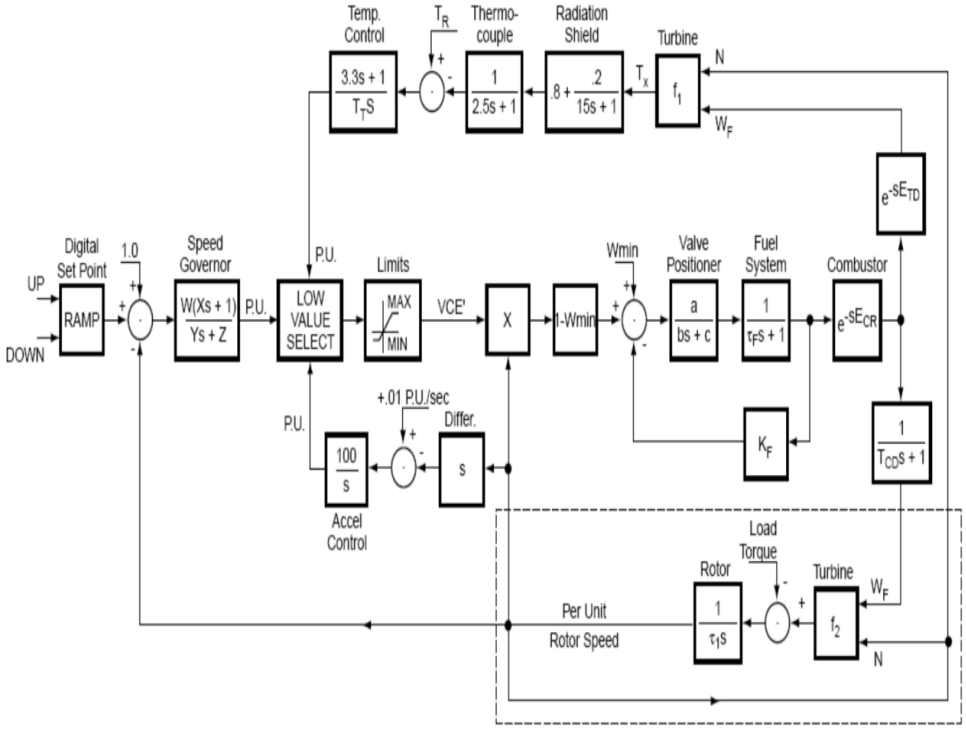

Figure 3.1: Rowens Model for HDGT

Governor speed control

This is the main control used during normal operation. Governors can operate in either droop or isochronous mode. The speed governor block shows the parameters 'w', 'x', and 'y', where 'w' is a gain equal to one divided by governor droop. For a governor droop of 4%, w = 25.'z' is the indicator of the governor mode with a value of 0 for isochronous mode and 1 for droop mode. As is well known, in droop mode as the load increases the speed or frequency decreases. A typical speed droop value is 4% which means that when the machine is fully loaded the speed will decrease from set point by 0.04 x 60 Hz, or 2.4 Hz. The output signal from the speed governor goes to the minimum value select gate.

Acceleration control

This is designed to be used mainly during gas turbine start-up or on load rejection, to limit the rate of rotor acceleration. This control would prevent an overspeed of the gas

turbine that might damage the shaft.The acceleration control block shows that the gas turbine speed signal goes through a differential block to obtain the acceleration value. This is then compared to an acceleration limit, and an error signal is obtained. That signal is the input to the acceleration control block. The output signal goes to the minimum-select value gate.

Temperature control

This is important to control the gas turbine if the temperature of the exhaust surpasses a fixed maximum setting. Under normal conditions, in order to secure a balance of the power in a steady state, the mechanical power output of the gas turbine increases due to speed governor action when the load increases. This results in an increase in the temperature of the exhaust. If the rise exceeds the maximum stated value, the signal of the temperature control will be lower than that of the speed governor. The temperature control impacts on how the turbine responds, based on a minimum select value. Another factor is ambient temperature. An increase in the ambient temperature will cause an increase in the temperature of the exhaust, with the temperature control reducing the amount of fuel consumption. A decrease in the ambient temperature will cause a decrease in the temperature of the exhaust, but with no corresponding drop in fuel consumption. The speed governor control becomes the active control.

A reduction in the input air increases the fuel-to-air ratio, with a resultant increase in the temperature of the exhaust gases. The temperature control is activated as the temperature of the output gas increases. This reduces the amount of fuel that is input until the ratio of air to fuel returns to an optimum point. The ambient temperature and pressure are the main components which affect the generated power of the gas turbine. An increase in the ambient temperature causes an increase in the temperature in the compressor, which consequently reduces the pressure in the compressor and the turbine, which in turn, reduces the output.

Rowens model consists of a number of components including function blocks F1 & F2, simple time delays, transport delay ETD, combustion reaction time delay ECR and compressor discharge volume TCD as shown in Figure 3.1. F1 is an expression to calculate the temperate of the exhaust gases, while F2 is an expression to calculate the output torque of the turbine. Both F1 and F2 are dependent on speed (N) and fuel flow (WF). The fuel system provides energy input to the gas turbine proportional to the output of the command signal (VCE) times the unit speed (N). The model includes a fuel demand signal limiter, although in normal operation the maximum is not reached. This demand signal limiter may be used as a temperature control backup in the case where an increase in exhaust temperature could lead to activation of temperature control and a decrease in the flow of fuel.

As discussed in his paper in 1992, Rowen [2] modified the original model to include the inlet guide vanes (IGV), which is the fourth control shown in Figure A.1 of Appendix A.

The inlet guide vane (IGV) control program depends on which type of operation is chosen, simple cycle or combined cycle. The function of the IGV control is based on compressor inlet temperature and gas turbine speed during start-up. The IGV angle is regulated by this control to maintain high exhaust temperature in partial load. For a full load, the IGV angle is opened as a result of an increase in exhaust temperature. In the case of unloading, the shutdown control will reach the minimum fuel limit. To maintain a constant exhaust temperature, a further control is used to regulate the IGVs which is important to satisfy the thermal load demand from the heat recovery of exhaust gases in a cogeneration plant. To regulate the temperature of the exhaust gases, the IGV controller will adjust the guide vanes to modify the air inlet flow. Although this loop is unnecessary for the analysis of the primary frequency control of the gas turbine, it is critically important to the heat recovery system that will meet the thermal load demand of the cogeneration plant.

3.2 Description of Gas Turbine Parameters

Table 1 shows a comparison of the parameters of typical and SAPF gas turbines. It was possible in most cases to obtain exact values of the SAPF cogeneration parameters. In a few instances, typical plant parameters had to be used.

Table 3.1: Used and Typical Parameters

Parameter	Parameter Description	Used Parameters	Typical
W	Gain =1/Droop (PU MW/PU speed)	25	16.7
X	Governor lead time constant (S)	0	0.6
Y	Governor lag time constant (S)	0.05	1.0
Z	Governor mode	1	1
MAX	Demand upper limit (PU)	1	1.5
MIN	Demand lower limit (PU)	0	-0.1
a	Valve positioner	1	1
b	Valve positioner	0.2	0.05
c	Valve positioner	1	1
WMIN	Minimum fuel flow	0.23	0.23
TF	Fuel control time constant (S)	0.02	0.4
KF	Fuel system feedback	0	0
ECR	Combustion reaction time delay (S)	0	0.01
ETD	Turbine and exhaust delay (S)	0	0.04
TCD	Compressor discharge volume time constant	0.5	0.2
TR	Turbine rated exhaust temperature (F)	1086	950

Parameter	Parameter Description	Used Parameters	Typical
TT	Temperature controller integration rate (F)	500	450
F1	Function to calculate the exhaust temperature	TX= TR-700 (1-WF)+550*(1-N)	SAME
F2	Function to calculate the torque output	1.3*(WF-0.23) +0.5*(1-N)	SAME
TI	Inertia (2*H)	16	15.64

3.3 Performance of the Governor System

The simulation conditions are for the system in an isolated or islanded mode of operation. A governor speed droop of 4% is assumed. Two disturbances are simulated.

1. 50% load torque increase at 5 seconds.

2. 0.04 PU step change increase in speed reference at 50 seconds.

The results are shown in Figure 3.2. As expected, when the electrical load increased by 0.5 PU the mechanical power output increased by 0.5 PU. Also as expected when the governor speed reference increased by 0.04 PU the mechanical power did not increase, but just oscillated a little and settled down at 0.5 PU. The rotor speed acted as expected also. When the load increased the speed decreased to 0.98 PU, a drop of 2% since the load only increased by 50%. When the speed reference increased by 4% or 0.04 PU, the rotor speed responded with the expected actual speed increase of 0.04 PU. The valve positioner action leads the mechanical power response by a second or two, as expected. The exhaust temperature started at 410 (^oF), and reached a final steady state value of near 680 (^oF).

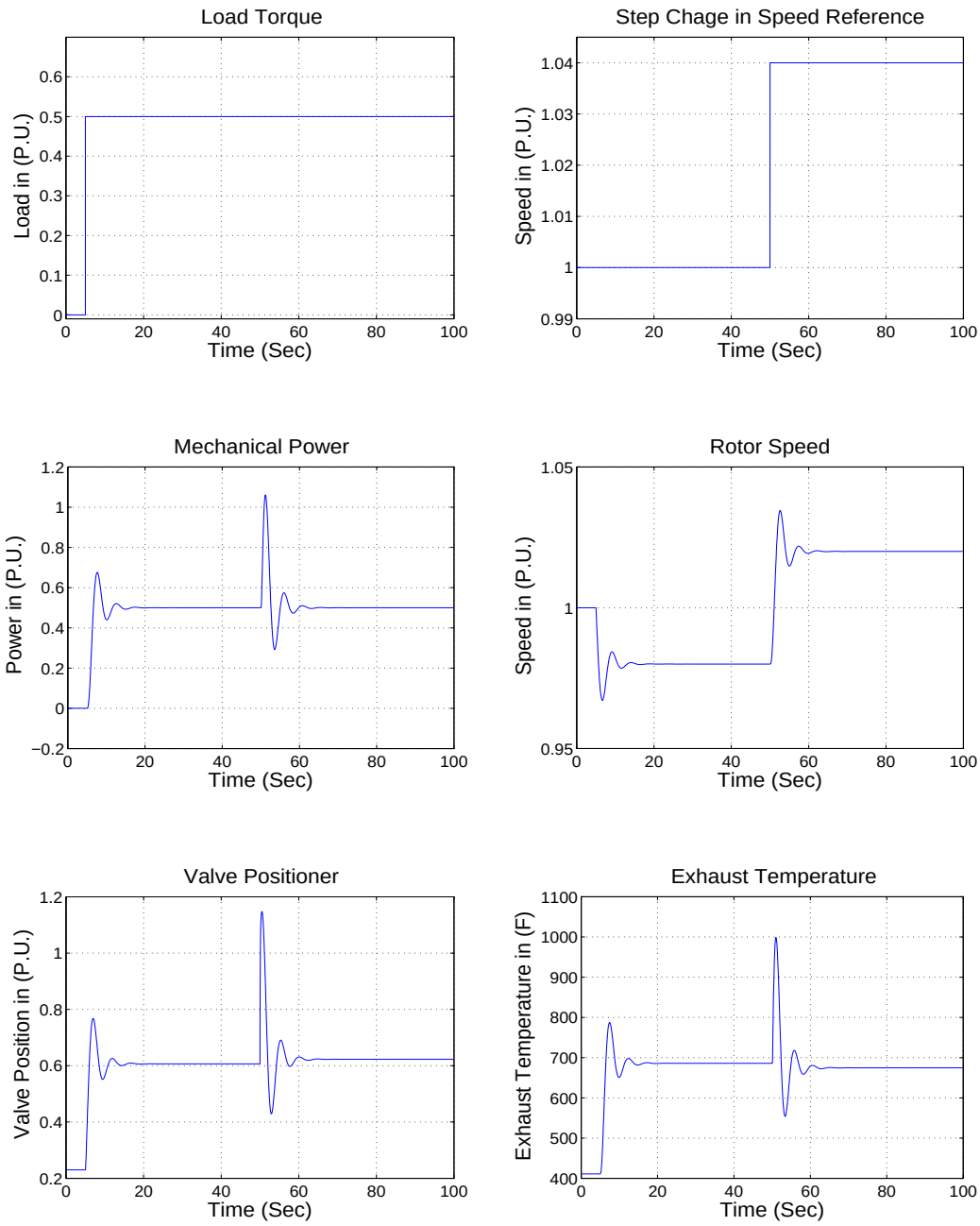

Figure 3.2: Response of Mechanical Power, Rotor Speed, Valve Positioner and Exhaust Temperature to changes in Load Torque and Step Change in Speed Reference.

Chapter 4

SAPF COGENERATION UNIT MODELS USING MATLAB SOFTWARE

4.1 MATLAB / SIMULINK

MATLAB includes Simulink software which provides the opportunity to model, simulate and analyze dynamic systems in a graphical environment. There are a number of reasons why Simulink is useful to undertake analysis of a power system, for example:

a. It brings the researcher closer to the physical reality of the power system as they go through the process of constructing the Simulink models.

b. It enables one to start with the simplest form of the power system, and to build thus understanding the effects of complexity.

c. It enables identification of special effects such as inertia, the machine model and the excitation system.

d. Commercial power system simulation software normally provides pre-structured

models for power system components, which may be a simplification of the original model.

e. It allows for identification of modes associated with individual power system components.

f. It will allow eigenvalue analysis (which although not part of this thesis could be an area for future research).

g. Simulink has traditionally been used as the software for tuning controllers.

4.2 Single Machine Interconnected to an Infinite Bus (SMIB)

Capacitances in a transmission line model are not part of the power transfer across the line. The transmission line resistance, while important for loss calculations, has very little influence on voltage drop calculations and stability studies. As well as, a reactance X can represent the per unit model of a synchronous machine, a transformer and a transmission line. A simple model of a power system is shown in Figure 4.1.

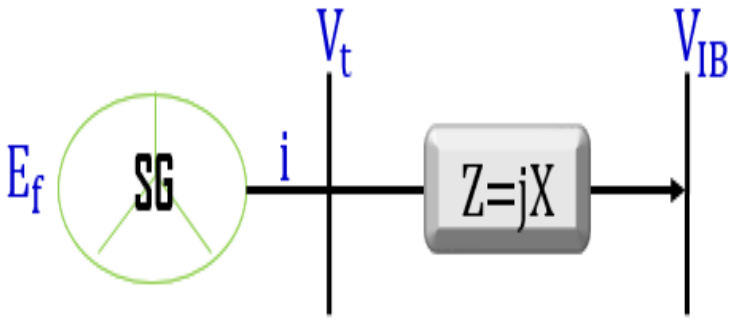

Figure 4.1: Single Machine Connected to Infinite Bus (SMIB)

The power flow across the power system, which is the electrical power provided by

the synchronous generator, is given in the well-known expression:

$$P = \frac{E_f V_{IB}}{X} sin\,(\delta) \tag{4.1}$$

where δ is torque angle and X is equivalent reactance.

$$\delta = \angle E_f - \angle V_{IB} \tag{4.2}$$

For up to approximately 25 degrees the sine of the angle is equal to the angle in radians, so that the expression may be linearized using a synchronizing coefficient.

$$K_S = \frac{E_f V_{IB}}{X} \tag{4.3}$$

$$P_e = \frac{E_f V_{IB}}{X}\delta = K_S\ \delta \tag{4.4}$$

The Swing Equations for a single machine connected to an infinite bus are:

$$\frac{2H}{\omega_o}\frac{d^2\delta}{dt^2} = P_m - P_e \tag{4.5}$$

$$\frac{1}{\omega_o}\frac{d\delta}{dt} = \Delta\omega \tag{4.6}$$

H is the inertia constant of the turbine-generator in MW.Seconds/MVA, K_S is the synchronizing torque coefficient in per unit torque per radian. $\omega_o = 377$ electrical radians per second and through integration converts the per unit speed $\Delta\omega$ to the load angle in radians. $\Delta\omega$ is the change in per unit speed, about synchronous speed, and mechanical power P_m and electrical power P_e are per unit.

The block diagram representing these equations is shown in Figure 4.2

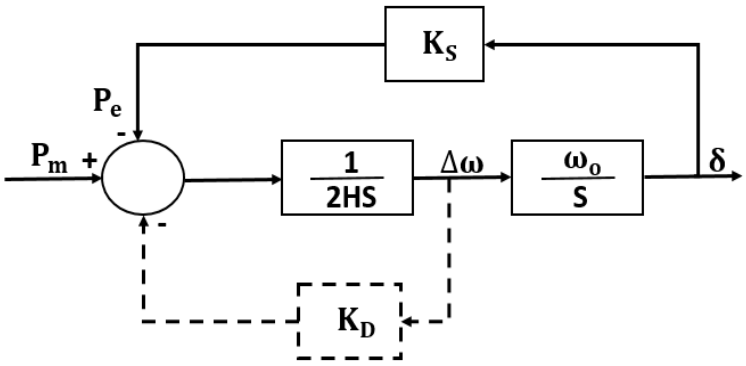

Figure 4.2: Generator Classical Model

Neglecting K_D a transfer function may be written relating the angle δ and P_m as:

$$\frac{\delta}{P_m} = \frac{\omega_o}{2HS^2 + \omega_o K_S} \tag{4.7}$$

Assuming a step change in P_m, the time response will be governed by the poles of the transfer function as follows:

$$S_1, S_2 = \pm j\sqrt{\frac{K_S \omega_o}{2H}} \tag{4.8}$$

$$\omega_{osc} = \sqrt{K_S \frac{\omega_o}{2H}} \quad rad/sec \tag{4.9}$$

$$f_{osc} = \frac{1}{2\pi}\sqrt{K_S \frac{\omega_o}{2H}} \quad Hz \tag{4.10}$$

Appendix B includes the inertia constant equation for SAPF machines, H = 8.03 seconds.

The transmission reactance X = 1.262 PU giving a $K_S = 0.792$ PU and $f_{osc} = 0.686$ Hz. The response of the load angle, electrical power, and speed to a step change in mechanical power is shown below:

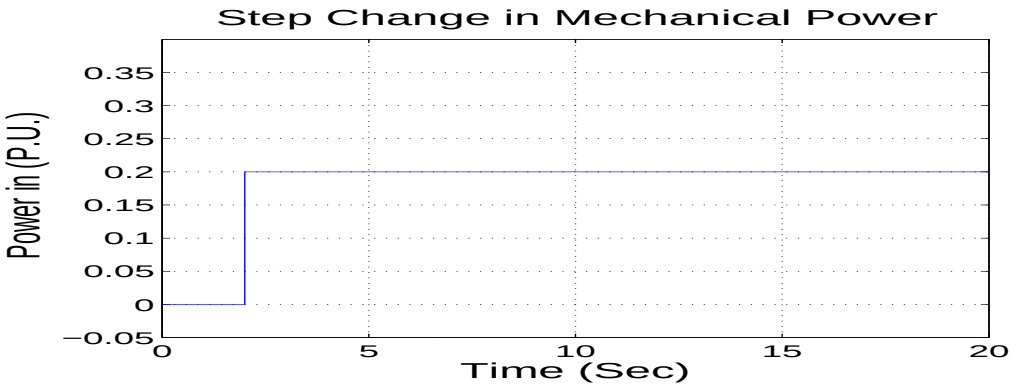

Figure 4.3: Step Change in Mechanical Power

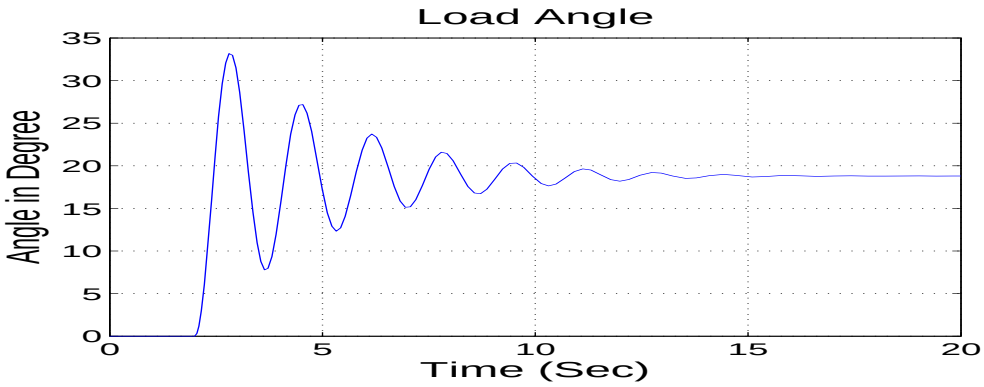

Figure 4.4: Load Angle Response to Mechanical Power Change

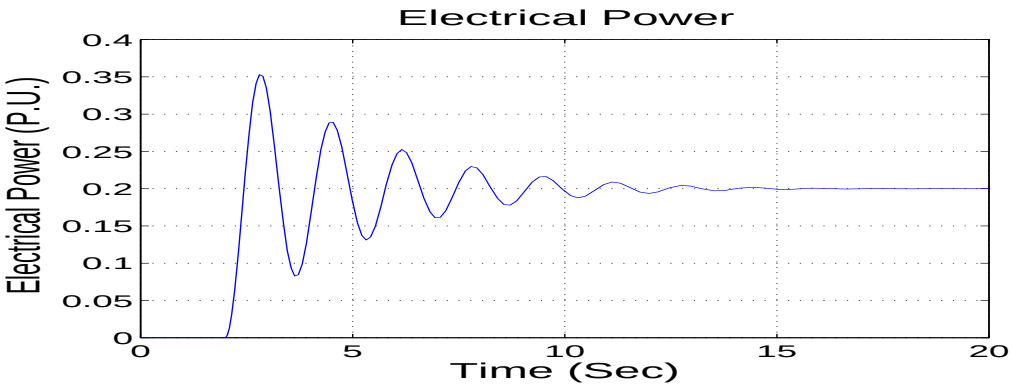

Figure 4.5: Electrical Power Response to Mechanical Power Change

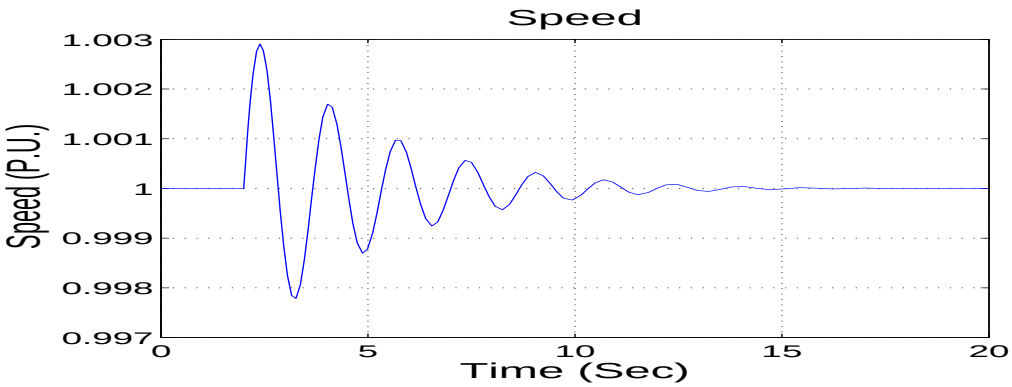

Figure 4.6: Speed Response to Mechanical Power Change

As shown above, three points are emphasized.

1. The synchronizing coefficient K_S is the simplest possible model for a synchronous generator.

2. As shown in Figure 4.2, dotted in the block diagram, there is normally some damping K_D in the power system which causes the 0.686 Hz machine oscillations to damp out. This is often referred to as the synchronous mode of oscillation.

3. The step change in P_m obviously causes an accelerating force on the turbine-generator rotating mass, and the speed oscillates during transients, but the speed comes back to 60 Hz in the steady state. This confirms that the model validly and accurately represents a single machine against an infinite bus because by definition there is no disturbance which happens in one machine which can change the frequency of the infinite bus in the steady state.

4.3 Adding the Gas Turbine and Governor to the Interconnected Model

Chapter 3 presented the detailed model for the gas turbine and its governor. At that time the turbine generator was considered as operating in the isolated mode.

Responses were shown for various machine and governor variables for a step change in load on the turbine generator. The graphs from chapter 3 are not repeated here. The operation of the simple generator model connected to an infinite bus will be considered here.

4.3.1 Simulation and Analysis

A disturbance was introduced by changing the speed reference from 1-1.01 PU at 2 seconds. With the synchronous generator connected to the grid, transiently there are small oscillations in the rotor speed. P_m increased from 0 - 0.25 PU corresponding to the speed reference change and settled down after 8 seconds of the disturbance. P_e follows the P_m as normal action, and the rotor speed oscillated for around 12 seconds, then stabilized at synchronous speed.Valve positioner and temperature behaved as expected.

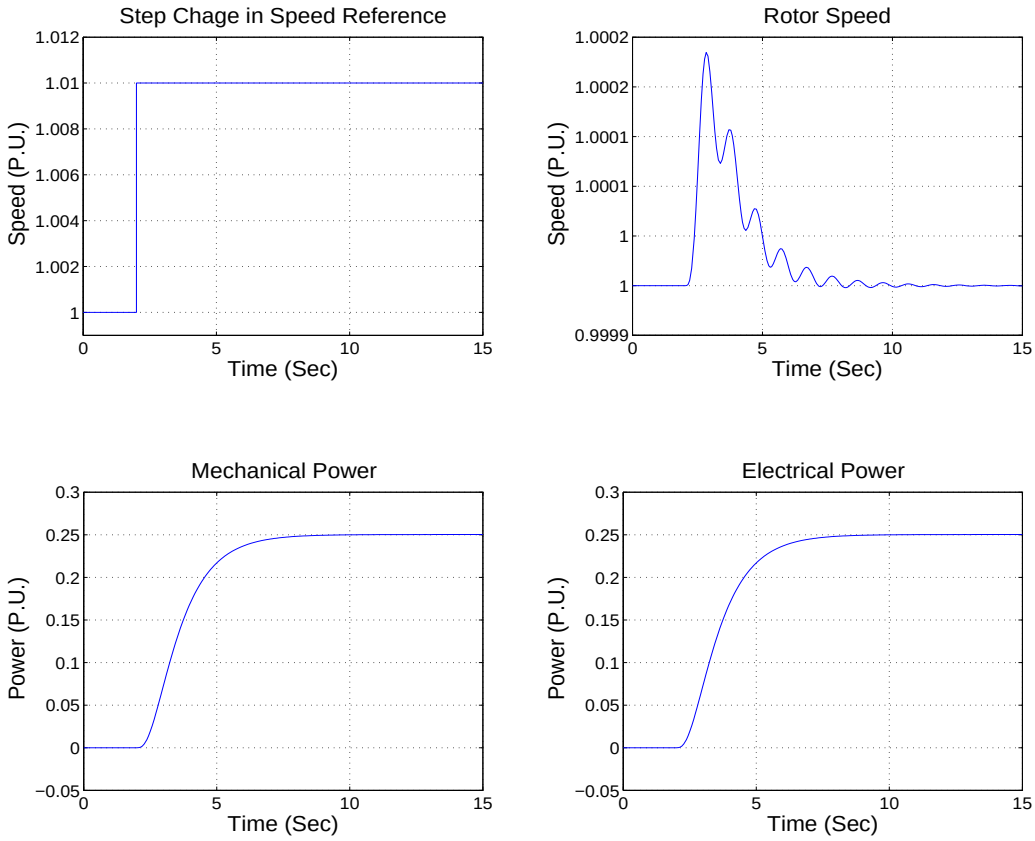

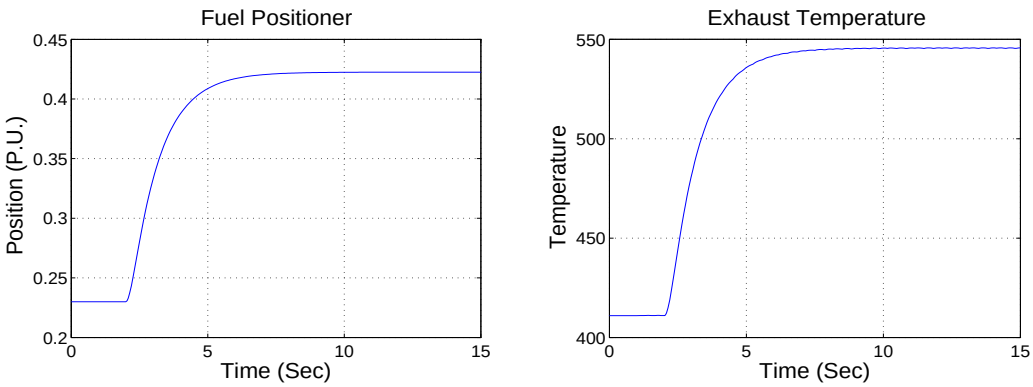

Figure 4.7: Variable Response to Step Change

4.4 Adding a Detailed Machine Model and Excitation System

Heffron and Phillips [23] were the first to propose a detailed linearized model for a synchronous generator, later used by Concordia and Demello [35] in their classic work on power system stabilizers (PSS). Simply because of the parameters involved, it has become known as the K1-K6 model. Figure 4.8 shows the K1-K6 model proposed by Heffron and Phillips. The parameters are calculated for a specific operating point of MW, MVARs and generator terminal voltage.

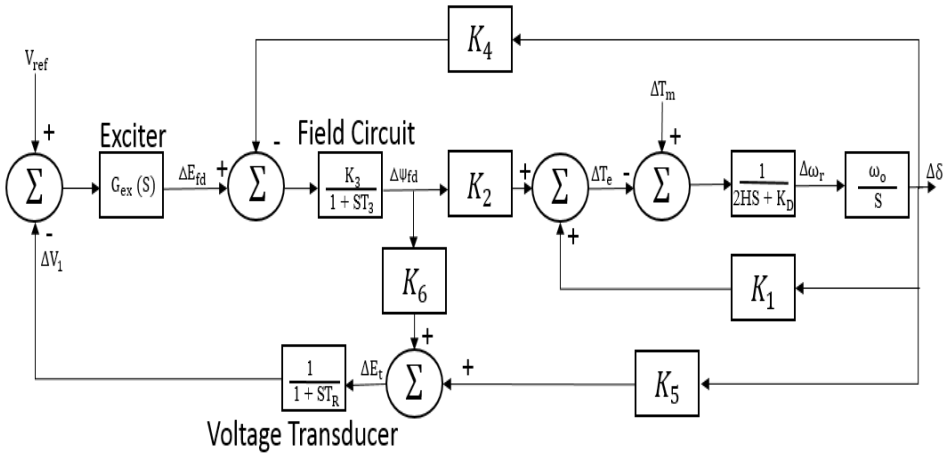

Figure 4.8: SMIB Including Excitation System

The parameters in Figure 4.8 are defined as follows:

K1: Changes in the electrical torque will result in a change in rotor angle, given constant flux linkages on the d-axis.

K2: Changes in electrical torque will result in d-axis flux linkages, given constant rotor angle.

K3: Impedance factor.

K4: A change in the rotor angle will have a demagnetizing effect.

K5: A change in terminal voltage along with a change in the rotor angle.

K6: A change in terminal voltage along with a change in flux linkage.

The detailed expressions for calculating K1-K6 are available in [21] and [22]. The synchronous machine parameters for calculating K1-K6 are showing in Appendix C. Appendix D includes the equations for K1-K6.

IEEE Standard 421.5-2005 shows exciter models for every type of exciter in existence. The SAPF exciter is a brushless type, and is best represented by the IEEE AC5A model, it is shown in Figure 4.9. The parameters for the AC5A exciter model are shown in Appendix C.

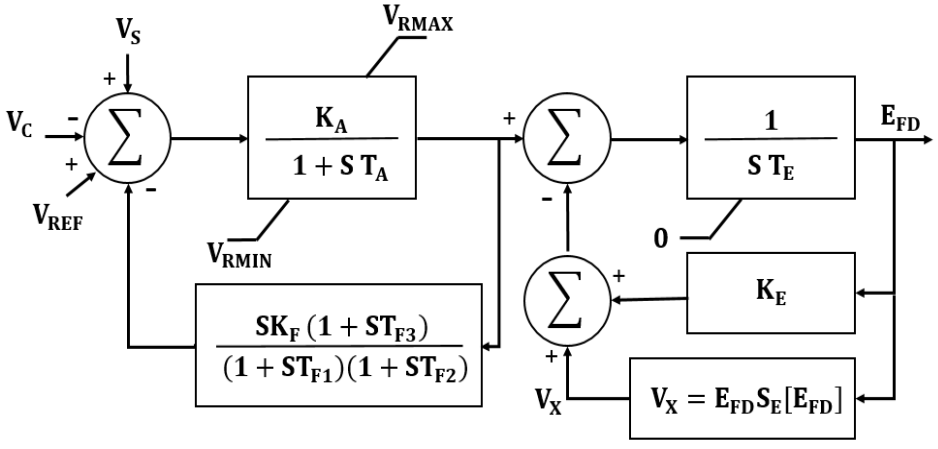

Figure 4.9: AC5A Excitation System Model

4.4.1 Simulation and Analysis

Two disturbances have been introduced in this power system consisting of a synchronous generator connected to an infinite bus through an external reactance. The speed reference in the governor was decreased from 1.04 to 1.03 PU at 10 seconds, and the generator terminal voltage reference was increased by 4%, or 0.04 at 30 seconds. Four operating case scenarios were simulated.

Case 1:

MW and MVAR out of the generator, with a strong grid.

The governor droop is 4%. Since the governor speed reference was decreased by 1%, the mechanical power and electrical power decreased by 25% or 0.25 PU in the steady state, which is clearly shown on the graphs. The load angle in the original steady state was 43.8 degrees. When the load was decreased from 1 to 0.75 PU, the load angle decreased as expected to a new steady state value of 32.8 degrees at 18 seconds. Furthermore, when the strength of the electrical system was increased by increasing the generator terminal voltage, the load angle oscillated for a few cycles but again decreased to a new stable point of 26.6 degrees at 40 seconds. Because the generator is synchronized with the grid, the speed momentarily oscillated for both disturbances but quickly went back to its original value as expected for an infinite bus. The turbine quantities of the valve positioner and temperature were greatly impacted by the load decrease with the exhaust temperature decreasing from 950 to 815 F^o. However, as expected they barely responded to the change in generator terminal voltage. Turning to the exciter, it responds vigorously to the call for an increase in generator terminal voltage by transiently driving the exciter voltage E_{FD} to about 430%, or 4.3 PU. Since the Automatic Voltage Regulator (AVR) is a proportional controller, the actual change in generator terminal voltage in the steady state is only about 3.6% arising from the step change of 4% in the terminal voltage reference value.

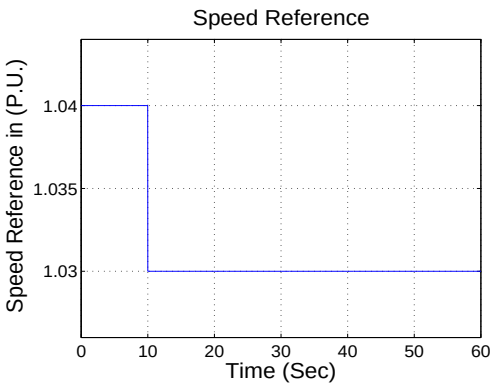
Speed Reference
Speed Reference in (P.U.)
1.04
1.035
1.03
0
10
20
30
40
50
60
Time (Sec)

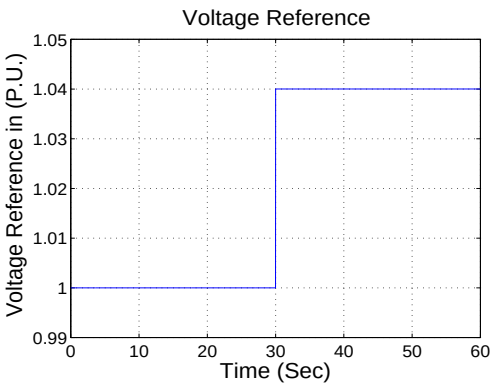
Voltage Reference
Voltage Reference in (P.U.)
1.05
1.04
1.03
1.02
1.01
1
0.99
0
10
20
30
40
50
60
Time (Sec)

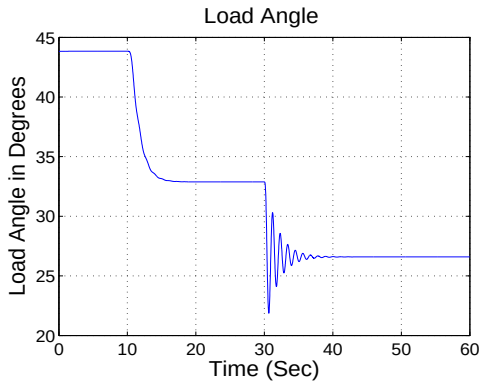
Load Angle
Load Angle in Degrees
45
40
35
30
25
20
0
10
20
30
40
50
60
Time (Sec)

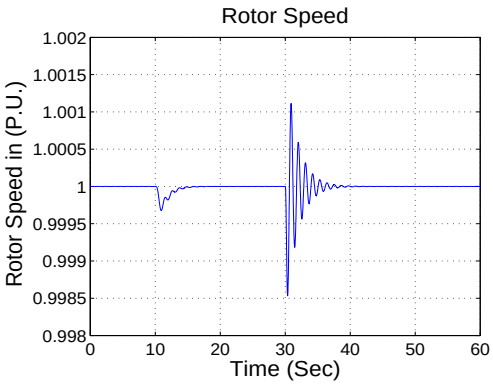
Rotor Speed
Rotor Speed in (P.U.)
1.002
1.0015
1.001
1.0005
1
0.9995
0.999
0.9985
0.998
0
10
20
30
40
50
60
Time (Sec)

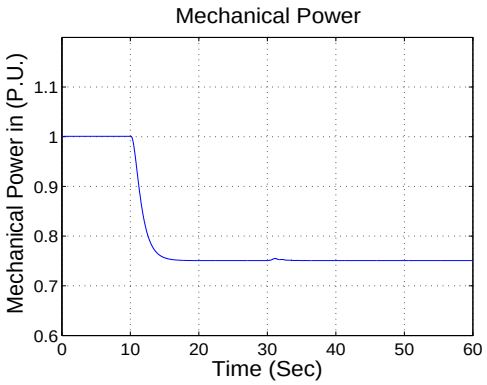
Mechanical Power
Mechanical Power in (P.U.)
1.1
1
0.9
0.8
0.7
0.6
0
10
20
30
40
50
60
Time (Sec)

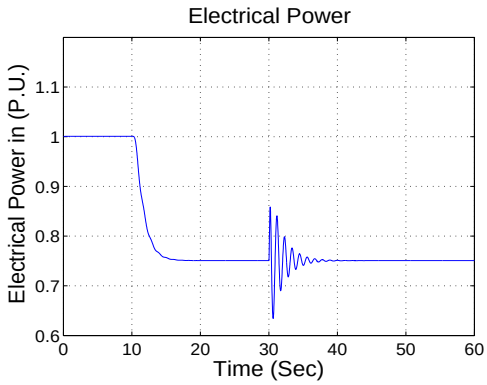
Electrical Power
Electrical Power in (P.U.)
1.1
1
0.9
0.8
0.7
0.6
0
10
20
30
40
50
60
Time (Sec)

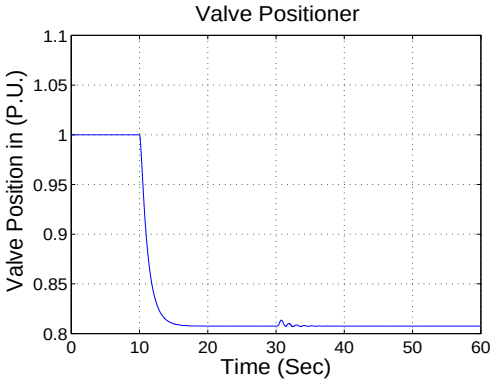
Valve Positioner
Valve Position in (P.U.)
1.1
1.05
1
0.95
0.9
0.85
0.8
0
10
20
30
40
50
60
Time (Sec)

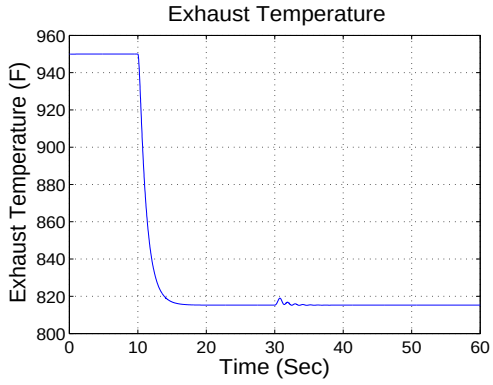
Exhaust Temperature
Exhaust Temperature (F)
960
940
920
900
880
860
840
820
800
0
10
20
30
40
50
60
Time (Sec)

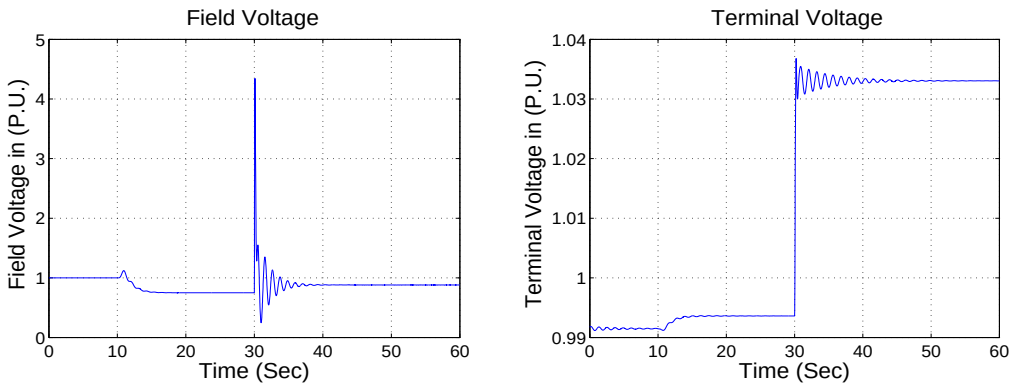

Figure 4.10: Case 1: Load Angle, Rotor Speed, Mechanical and Electrical Power, Fuel Demands, Exhaust Temperature and Field and Terminal Voltage.

Case 2

MW and MVAR out of the generator, with a weak grid.

The SAPF plant is connected to the Saudi Arabian grid (Called Saudi Electrical Company) through two short 5 km, 115 kV, transmission lines. One scenario of a weaker grid would be the loss of one of the 115 kV transmission lines. At the 115 kV point of interconnection, the grid is very strong, and there could be a number of transmission lines whose loss would weaken the grid. A number of different scenarios were tried, some of which caused an instability in the operation. The one case shown here is with the external reactance between the generator and the infinite bus increased from 0.257 PU to 0.400 PU, which when considering the additional factor of generator reactance, only resulted in a stability reduction of about 11%. The results generally follow the pattern of Case 1, except that any oscillations in the various quantities arising from the disturbances lasted for about 20 cycles rather than 9 cycles.

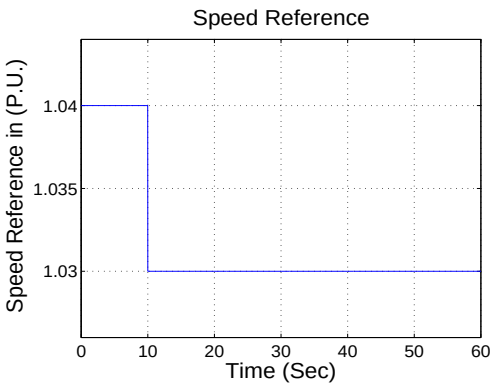
Speed Reference
Speed Reference in (P.U.)
1.04
1.035
1.03
0
10
20
30
40
50
60
Time (Sec)

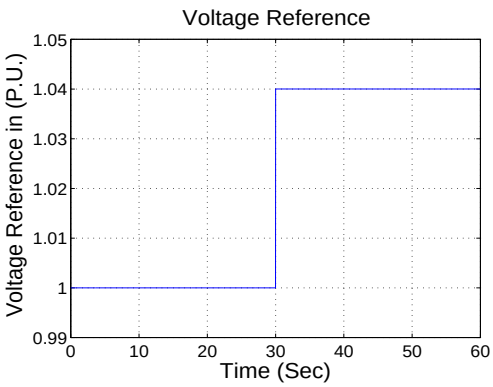
Voltage Reference
Voltage Reference in (P.U.)
1.05
1.04
1.03
1.02
1.01
1
0.99
0
10
20
30
40
50
60
Time (Sec)

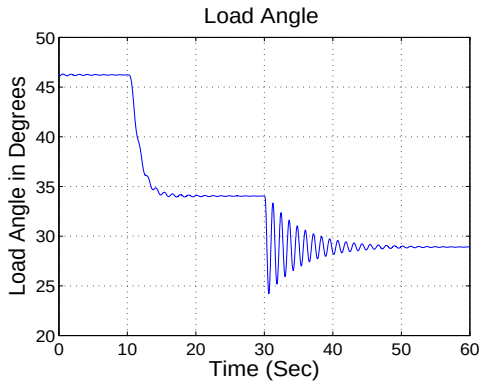
Load Angle
Load Angle in Degrees
50
45
40
35
30
25
20
0
10
20
30
40
50
60
Time (Sec)

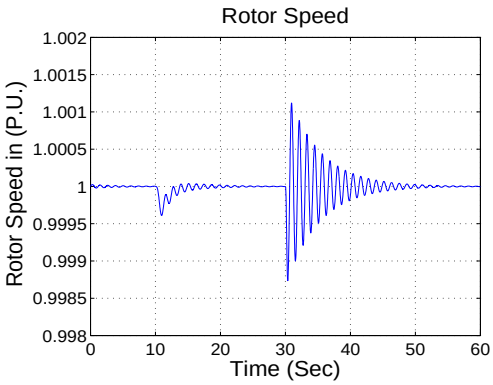
Rotor Speed
Rotor Speed in (P.U.)
1.002
1.0015
1.001
1.0005
1
0.9995
0.999
0.9985
0.998
0
10
20
30
40
50
60
Time (Sec)

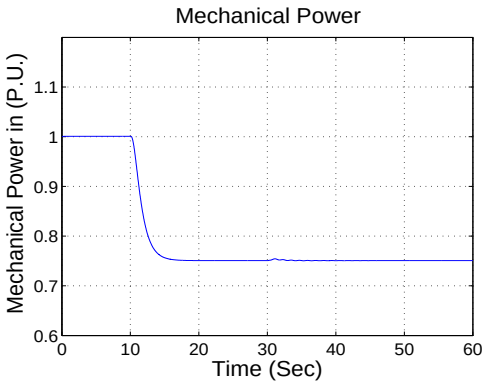
Mechanical Power
Mechanical Power in (P.U.)
1.1
1
0.9
0.8
0.7
0.6
0
10
20
30
40
50
60
Time (Sec)

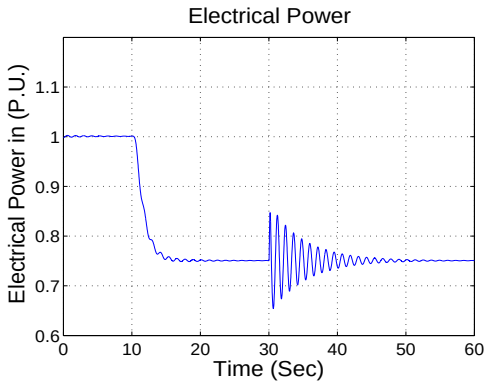
Electrical Power
Electrical Power in (P.U.)
1.1
1
0.9
0.8
0.7
0.6
0
10
20
30
40
50
60
Time (Sec)

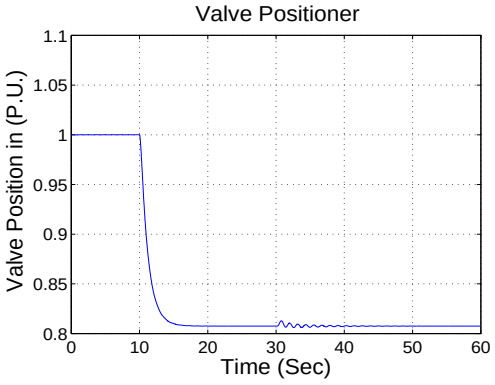
Valve Positioner
Valve Position in (P.U.)
1.1
1.05
1
0.95
0.9
0.85
0.8
0
10
20
30
40
50
60
Time (Sec)

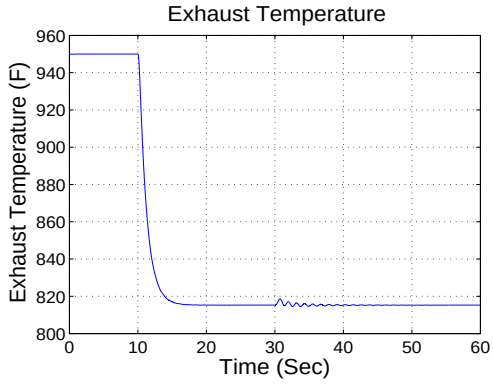
Exhaust Temperature
Exhaust Temperature (F)
960
940
920
900
880
860
840
820
800
0
10
20
30
40
50
60
Time (Sec)

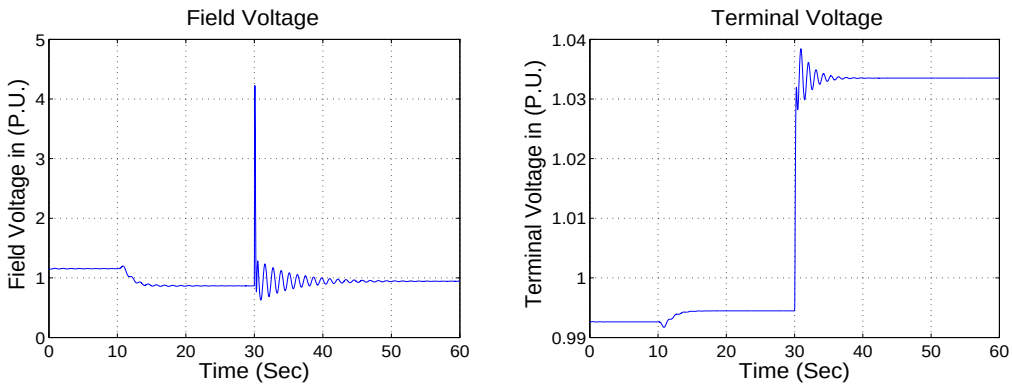

Figure 4.11: Case 2: Load Angle, Rotor Speed, Mechanical and Electrical Power, Fuel Demands, Exhaust Temperature and Field and Terminal Voltage.

Case 3

MW out of the generator and MVAR into the generator, with a strong grid.

In order for a generator to take in MVAR, it must be under-excited. This tends to weaken the magnetic coupling between the rotor of the generator and the infinite bus. Therefore as expected the original steady state machine angle was 52.77 while in the comparable Case 1 it was only 43.82 degrees. As a result of both disturbances the new steady state load angle was 34 degrees, giving an incremental change of 18.77 degrees. For the comparable Case 1, the incremental change due to both disturbances was only 17.22 degrees. Intuitively one would think that the oscillations would last longer in this case than in the comparable Case 1. However, that did not happen. Here the oscillations lasted for about 5 cycles while in the comparable Case 1 the oscillations lasted about 9 cycles. Kundur [21] shows that high-gain exciters in combination with the loading conditions can have a significant impact on both the synchronizing torque coefficient and the equivalent damping coefficient.

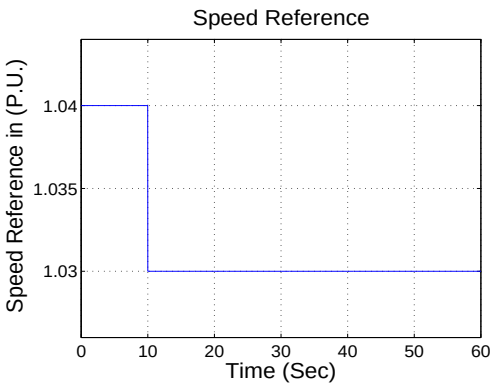
Speed Reference
Speed Reference in (P.U.)
1.04
1.035
1.03
0
10
20
30
40
50
60
Time (Sec)

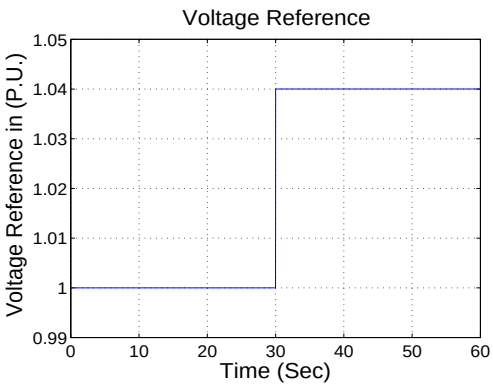
Voltage Reference
Voltage Reference in (P.U.)
1.05
1.04
1.03
1.02
1.01
1
0.99
0
10
20
30
40
50
60
Time (Sec)

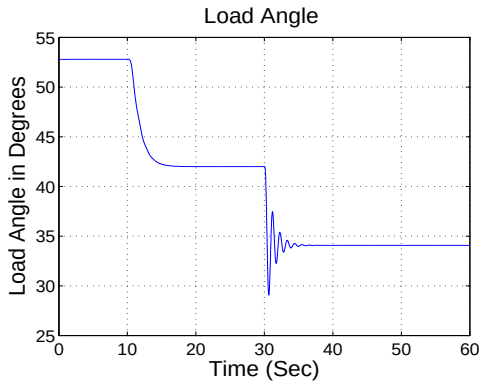
Load Angle
Load Angle in Degrees
55
50
45
40
35
30
25
0
10
20
30
40
50
60
Time (Sec)

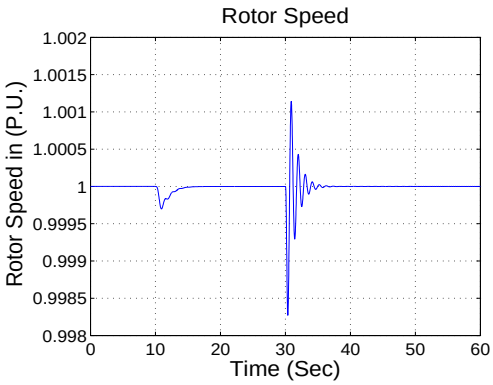
Rotor Speed
Rotor Speed in (P.U.)
1.002
1.0015
1.001
1.0005
1
0.9995
0.999
0.9985
0.998
0
10
20
30
40
50
60
Time (Sec)

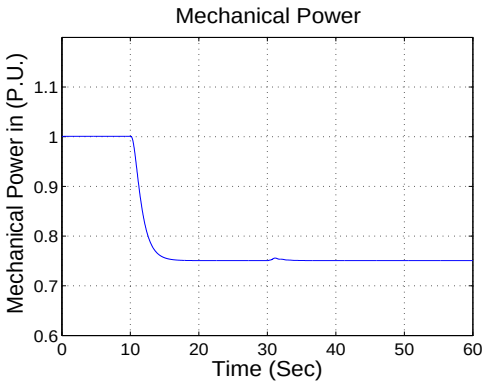
Mechanical Power
Mechanical Power in (P.U.)
1.1
1
0.9
0.8
0.7
0.6
0
10
20
30
40
50
60
Time (Sec)

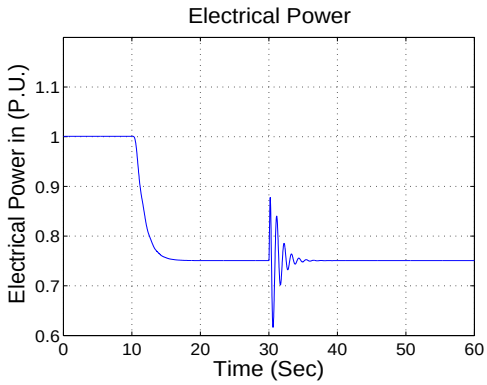
Electrical Power
Electrical Power in (P.U.)
1.1
1
0.9
0.8
0.7
0.6
0
10
20
30
40
50
60
Time (Sec)

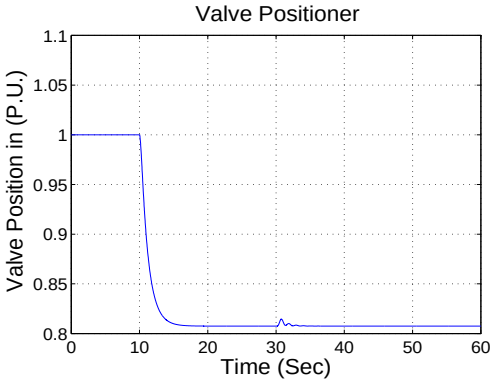
Valve Positioner
Valve Position in (P.U.)
1.1
1.05
1
0.95
0.9
0.85
0.8
0
10
20
30
40
50
60
Time (Sec)

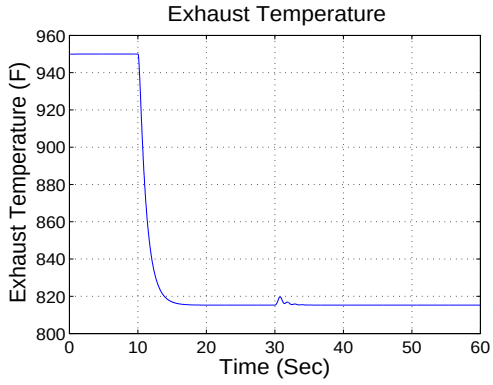
Exhaust Temperature
Exhaust Temperature (F)
960
940
920
900
880
860
840
820
800
0
10
20
30
40
50
60
Time (Sec)

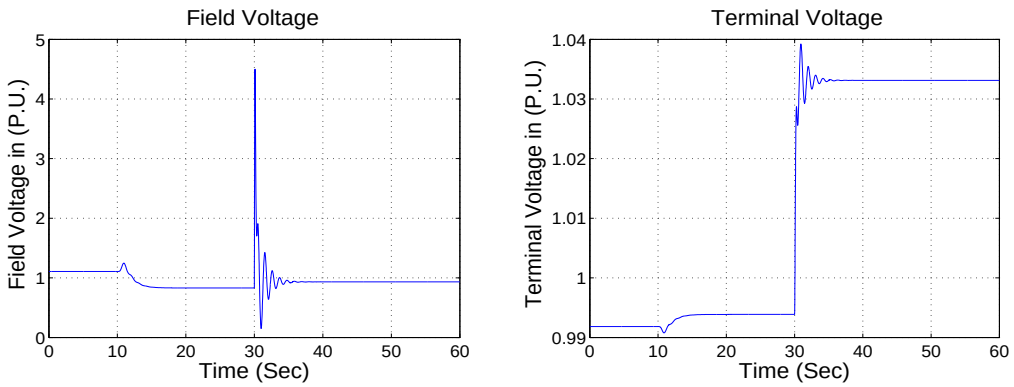

Figure 4.12: Case 3: Load Angle, Rotor Speed, Mechanical and Electrical Power, Fuel Demands, Exhaust Temperature and Field and Terminal Voltage.

Case 4

MW out of the generator and MVAR into the generator, with a weak grid.

All the patterns for this Case are consistent with the previous three cases. Again, contrary to intuition there was more damping in this case than in the comparable Case 2 where there were MVAR out of the generator (requiring an over-excited generator) and a weak grid. This was a fortuitous circumstance where the combination of an optimal exciter gain tuned for the loading conditions produced a higher effective damping coefficient.

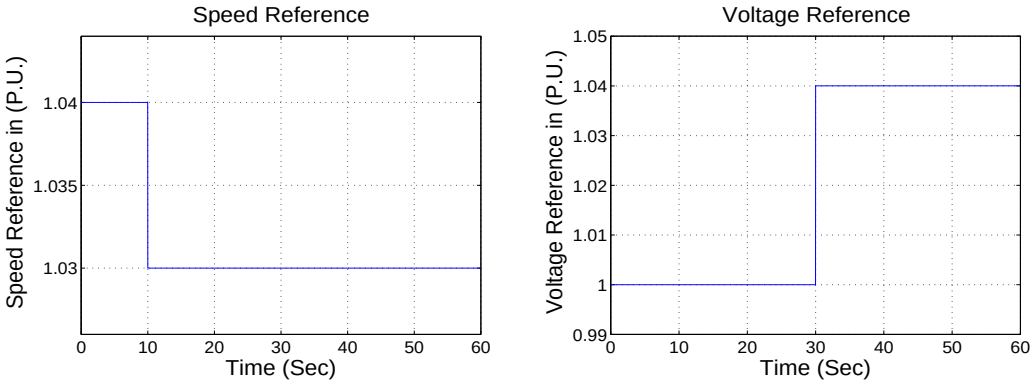

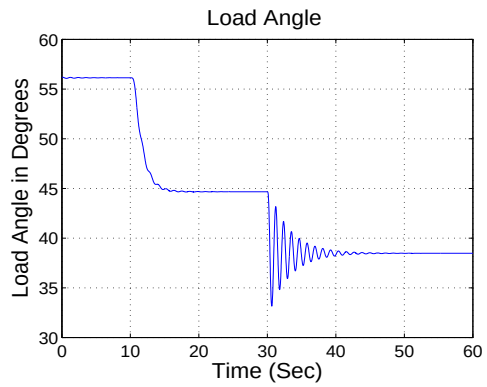
Load Angle
Load Angle in Degrees
Time (Sec)

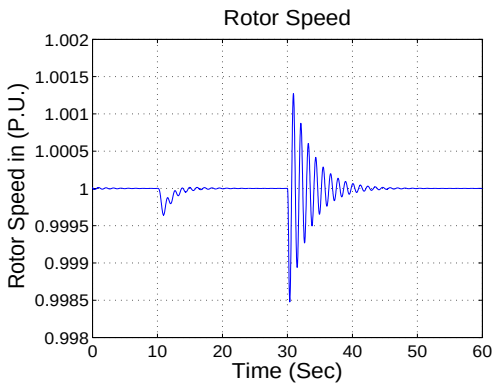
Rotor Speed
Rotor Speed in (P.U.)
Time (Sec)

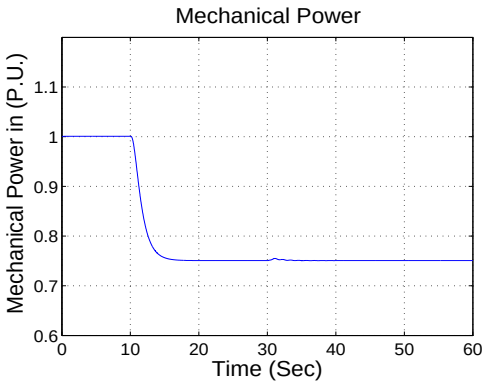
Mechanical Power
Mechanical Power in (P.U.)
Time (Sec)

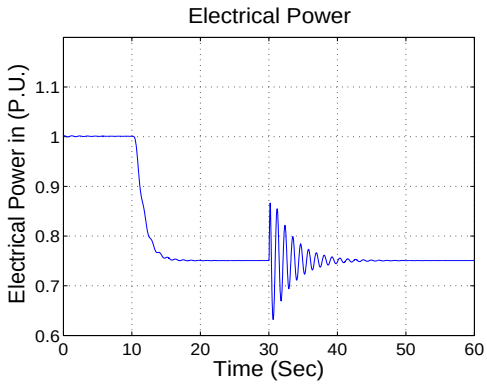
Electrical Power
Electrical Power in (P.U.)
Time (Sec)

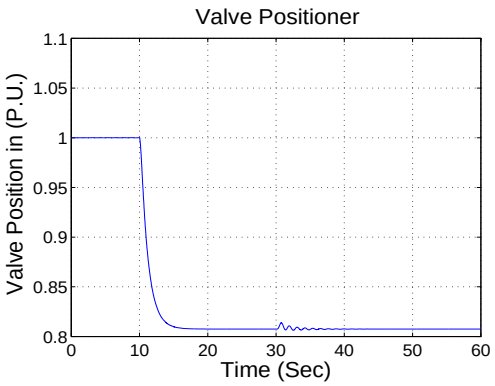
Valve Positioner
Valve Position in (P.U.)
Time (Sec)

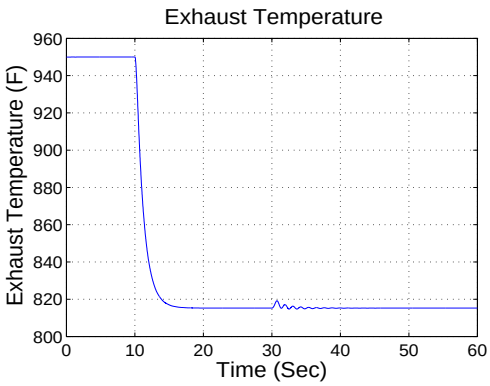
Exhaust Temperature
Exhaust Temperature (F)
Time (Sec)

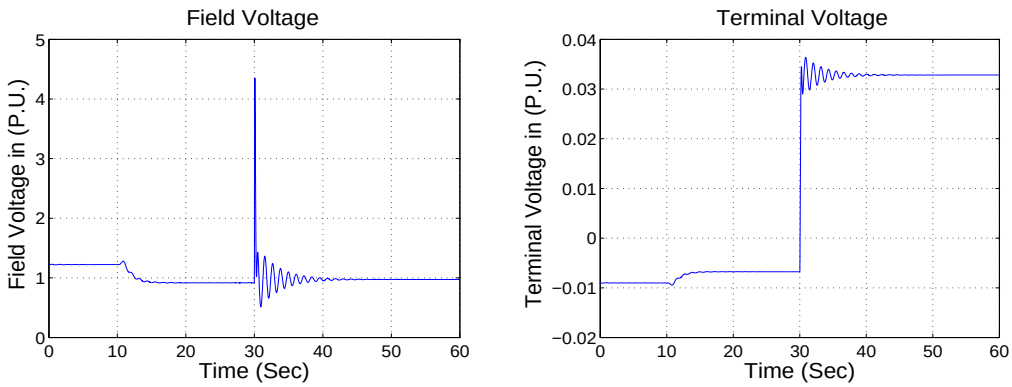

Figure 4.13: Case 4: Load Angle, Rotor Speed, Mechanical and Electrical Power, Fuel Demands, Exhaust Temperature and Field and Terminal Voltage.

4.5 Adding the Power System Stabilizer

The power system stabilizer (PSS) is a device which operates through the excitation system of the synchronous generator with the purpose of increasing the damping. In Canada often transmission distances are quite long which results in a less stable power system. Consequently it is almost standard practice to require PSS for generators. As indicated in the above four cases, the SAPF generators behaved in a very stable manner without a PSS. Furthermore, in the plant itself it was the recommendation of the OEM not to activate the PSS. For completeness it was decided to add a power system stabilizer to the SAPF model to see the effect on Case 1.The PSS parameters are shown in Appendix C, no attempt was made to optimize the parameters of the PSS, and only typical parameters were used. By making reference to specific variables such as rotor speed in this section and in Case 1, it can be seen that the PSS reduces the oscillations by one or two cycles but does not have a significant influence of the envelope of decay. If properly tuned, the PSS should have a prominent influence on the envelope of decay of the various variables. The figures below show the performance of the system with the PSS.

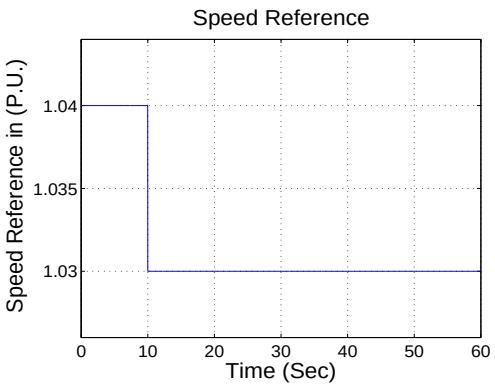
Speed Reference
Speed Reference in (P.U.)
1.04
1.035
1.03
0
10
20
30
40
50
60
Time (Sec)

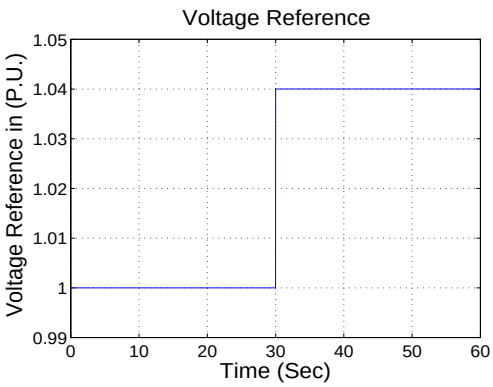
Voltage Reference
Voltage Reference in (P.U.)
1.05
1.04
1.03
1.02
1.01
1
0.99
0
10
20
30
40
50
60
Time (Sec)

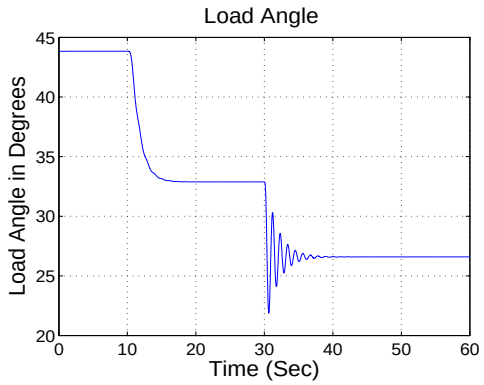
Load Angle
Load Angle in Degrees
45
40
35
30
25
20
0
10
20
30
40
50
60
Time (Sec)

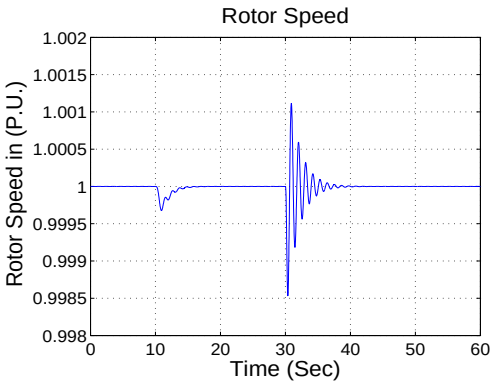
Rotor Speed
Rotor Speed in (P.U.)
1.002
1.0015
1.001
1.0005
1
0.9995
0.999
0.9985
0.998
0
10
20
30
40
50
60
Time (Sec)

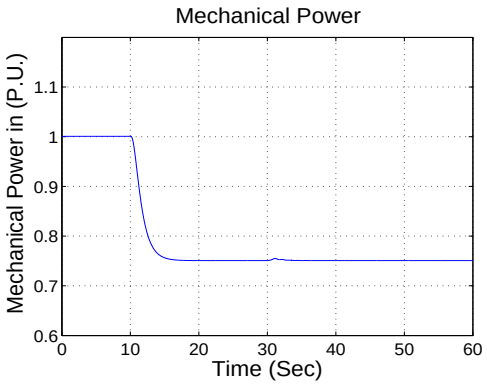
Mechanical Power
Mechanical Power in (P.U.)
1.1
1
0.9
0.8
0.7
0.6
0
10
20
30
40
50
60
Time (Sec)

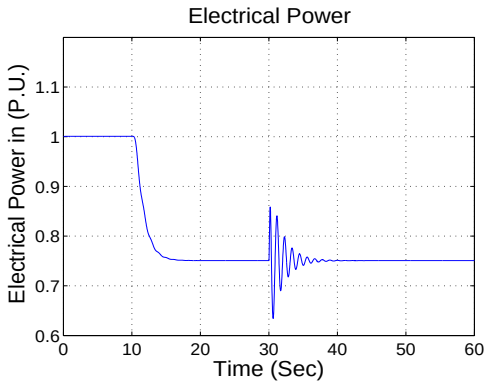
Electrical Power
Electrical Power in (P.U.)
1.1
1
0.9
0.8
0.7
0.6
0
10
20
30
40
50
60
Time (Sec)

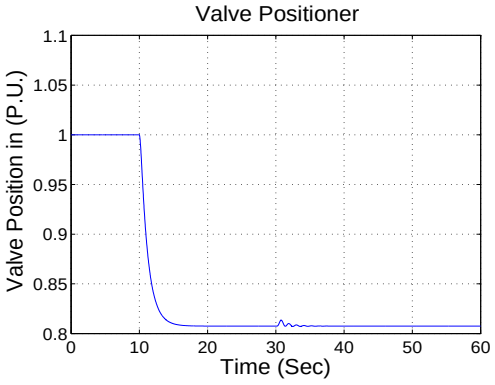
Valve Positioner
Valve Position in (P.U.)
1.1
1.05
1
0.95
0.9
0.85
0.8
0
10
20
30
40
50
60
Time (Sec)

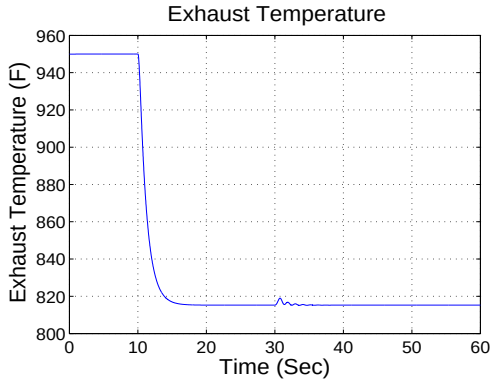
Exhaust Temperature
Exhaust Temperature (F)
960
940
920
900
880
860
840
820
800
0
10
20
30
40
50
60
Time (Sec)

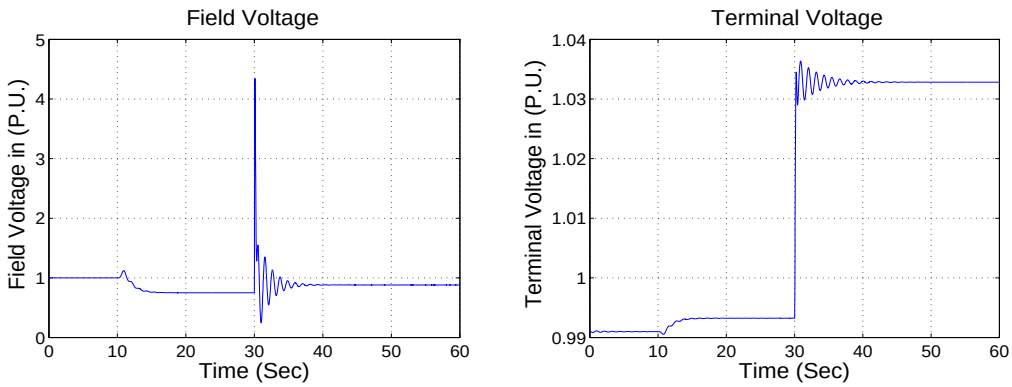

Figure 4.14: Load Angle, Rotor Speed, Mechanical and Electrical Power, Fuel Demands, Exhaust Temperature and Field and Terminal Voltage with PSS.

Chapter 5

SIMULATION OF SAPF ELECTRICAL SYSTEM USING ETAP SOFTWARE

5.1 Introduction

Worldwide there is a host of commercial software packages capable of carrying out the fundamental power system studies of load flow, fault analysis, and transient stability. The Electrical Transient Analyzer Program (ETAP®) is used in this thesis.
Commercial power system transient stability software is important for a number of reasons.

1. It allows full modelling of individual transmission lines, and allows for contingencies such as at the opening of one or both transmission lines.

2. Circuit breakers can be placed in location in the power system to allow isolation of components during faults.

3. Bus structures can be fully modelled (Bus A and Bus B configuration).

4. Detailed load models can be chosen according to the load type.

5. Relaying, particularly that used for under-frequency load shedding, is available in the software.

6. Over-frequency relay protection of the power system is available in the software.

7. It allows for implementation of special protective logic such as that employed in Special Protection Systems (SPS).

5.2 Case Studies and Simulations

The SAPF is a processing plant. It seeks to maximize its profits. One way of achieving the optimum revenue stream is through the achievement of the highest possible reliable power supply. The SAPF has three gas fired synchronous generators, each with a rated nominal capability of 150 MW, which can supply the nominal plant load of 170 MW. The plant load can also be supplied from the grid through the two 115 kV transmission lines. Power system electrical faults can always happen. Load changes can occur in the plant. Stated succinctly, optimum plant reliability is by definition operation in one steady state, suffering a disturbance and moving through it, and successfully reaching a new stable steady state. Plant operating experience allows a researcher to know the likely plant scenarios which can occur. Appendix E table (E.1) is a summary of the most likely scenarios that can take place in the SAPF electrical power system.

Four of the cases were selected to represent important scenarios:

Case 1

This is a case of zero import and zero export. At 0.5 seconds both transmission lines to the grid opened. Because of the initial perfect load-generation balance, the opening of the transmission lines causes no electrical disturbance. This is essentially

a non-event, and there are no changes in any of the power system variables. For illustration, only the graphs of generator speed and bus voltage are shown.

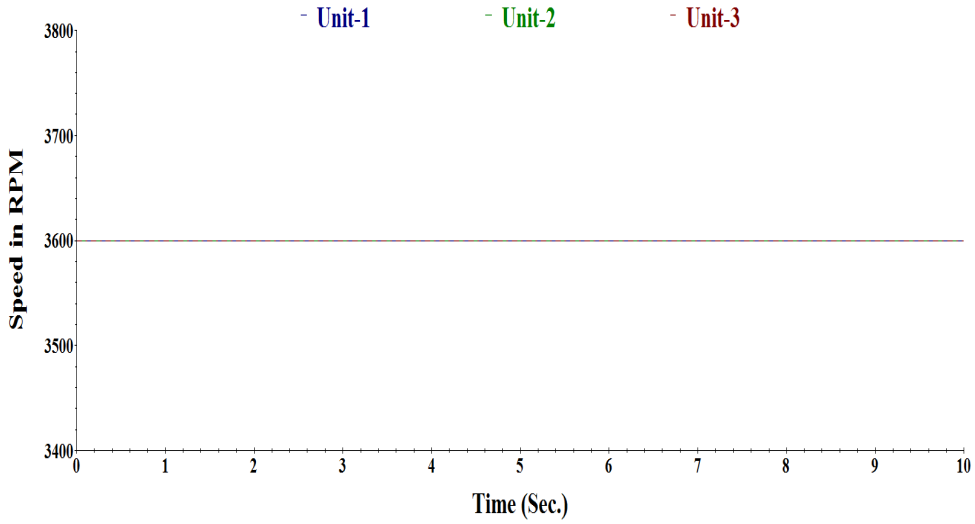

Figure 5.1: Speed

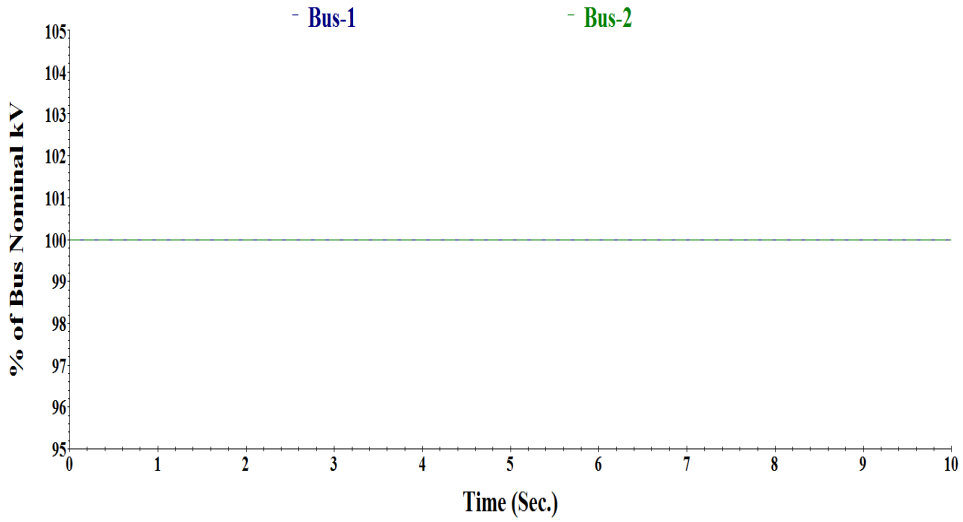

Figure 5.2: Bus Voltage

Case 5

In this case unit 3 was out of service. Unit 1 and unit 2 were on-line each generating 52 MW. The total plant load was 204 MW, with the result that there was an import

of 100 MW from the gird. The load shedding system (LSS) was not activated. The results are as expected. Each generator picked up 50 MW of the load originally supplied by the grid. This caused an increased voltage drop in the generator, so the generator exciter voltage and the generator exciter current both increased to maintain the generator terminal voltage. There was a small overshoot in the mechanical power, but it was very stable. There was a transient decrease in the generator speed of about 50 RPM, or 1.38%, but it quickly arrived at a new steady state. These results demonstrate that the SAPF, with only two units operating, would be able to survive the loss of the grid when it was supplying 100 MW to the plant.

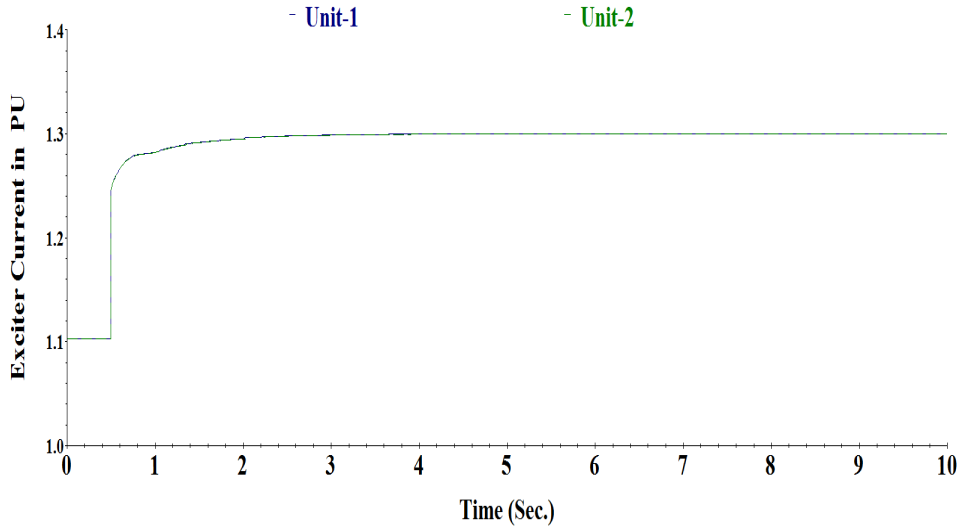

Figure 5.3: Exciter Current

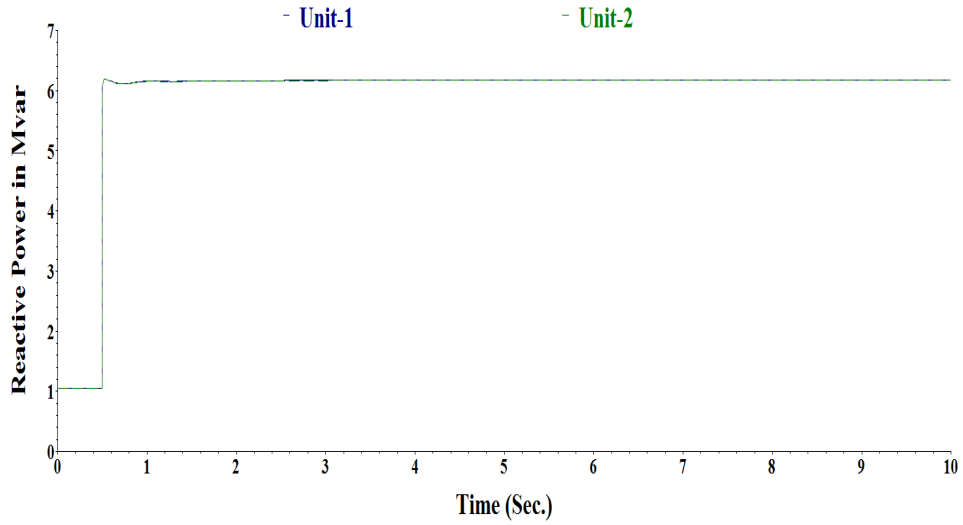

Figure 5.4: Reactive Power

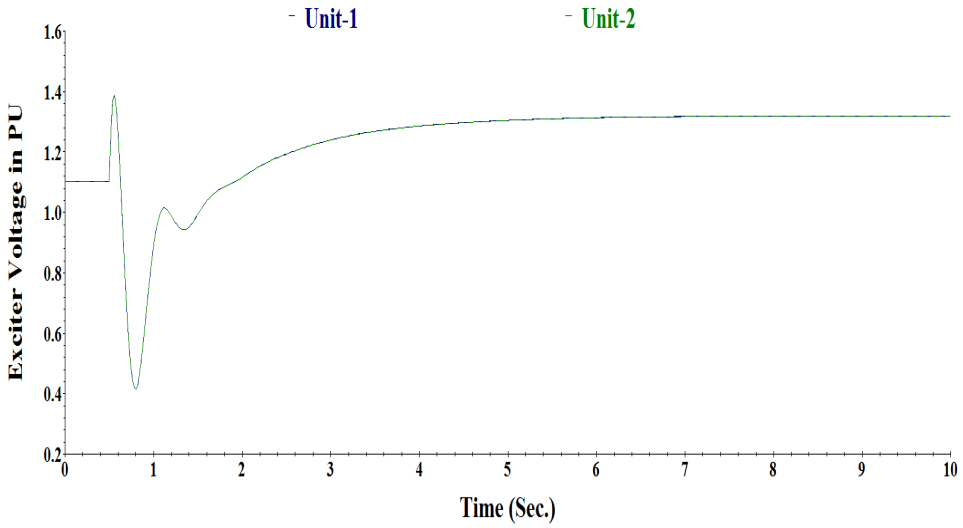

Figure 5.5: Exciter Voltage

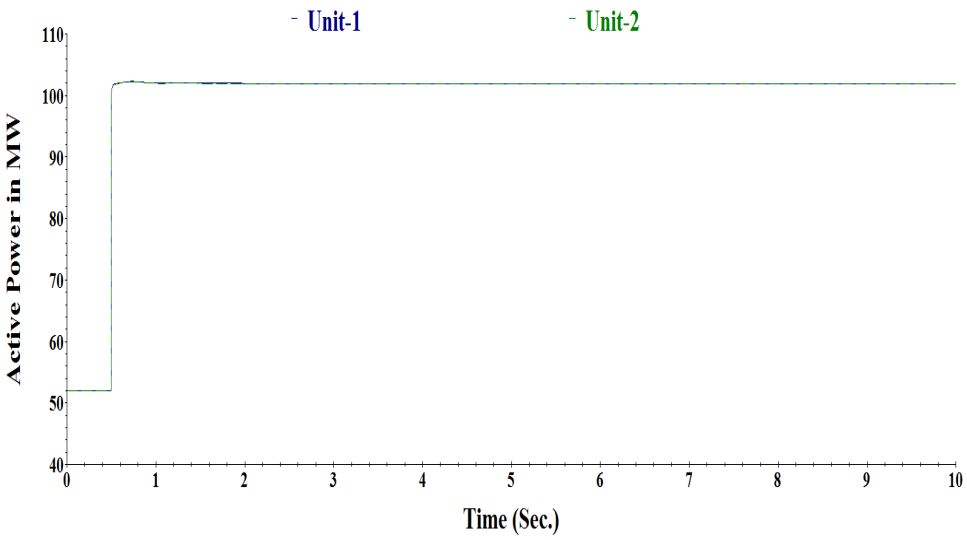

Figure 5.6: Active Power

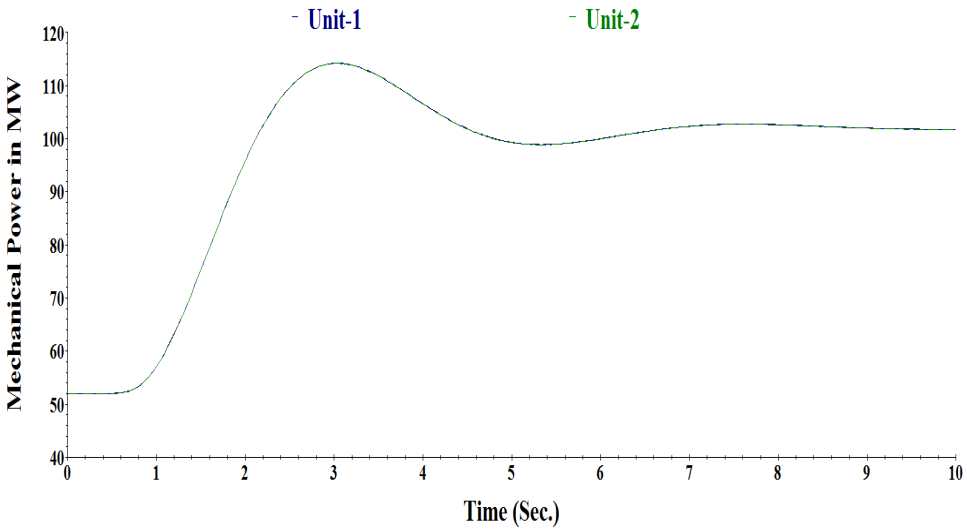

Figure 5.7: Mechanical Power

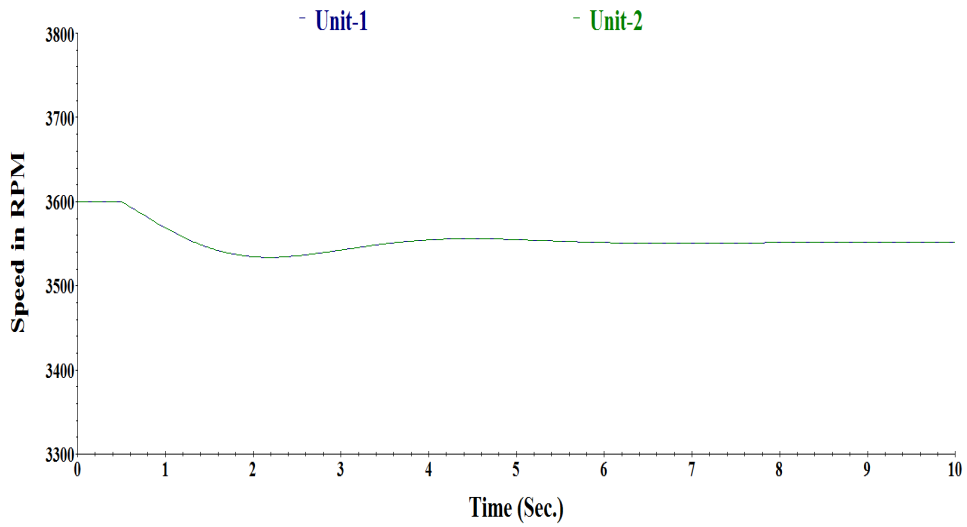

Figure 5.8: Speed

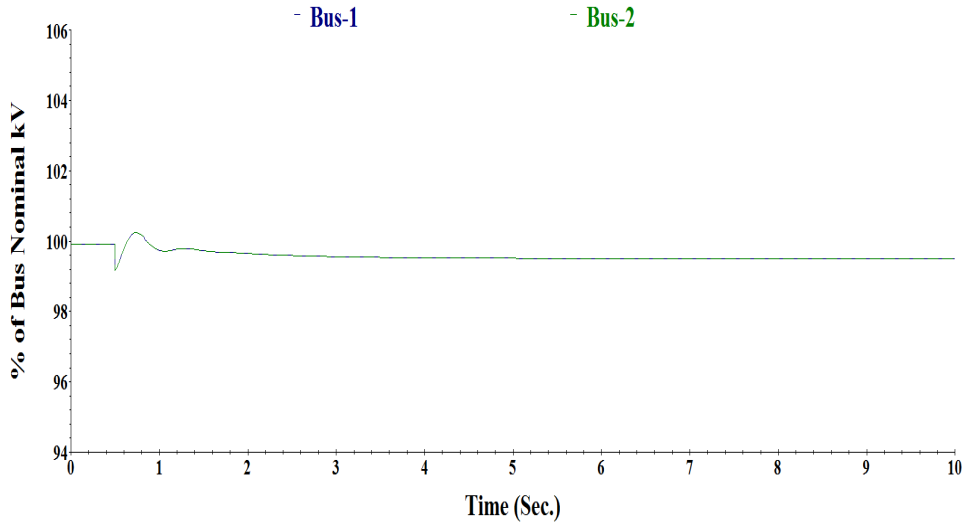

Figure 5.9: Bus Voltage

Case 10

All three units were on-line with each one generating 150 MW. The total plant load was only 100 MW, with the consequence that there was an export of 350 MW to the grid. Both transmission lines opened at 0.5 seconds. The turbine mechanical power momentarily dipped to almost zero MW, but quickly settled out at the expected value of 33.3 MW for each unit. However, during the disturbance there was a transient speed

swing to about 3750 RPM at 3 seconds, which is 104.2% speed. The new steady state speed was 3710 RPM, which is 103.05%. The over-frequency relay protection was set at 103%, with a time delay of 35 seconds as shown in the following table. All three units tripped at 40.5 seconds due to over-frequency relay action. The table below shows over/under frequency relay settings.

Table 5.1: Over/Under Frequency Relay Setting.

Device	Setting (%)	Time Delay (Sec)
Over-Frequency, relay	103	35 (meaning that the unit has to be above 103% for 35 consecutive, uninterrupted seconds after which the unit will trip on Over Frequency protection)
Under-Frequency, relay	94	0.1

Appendix F table (F.1) shows more details on transient stability and over-ferquency relay actions.

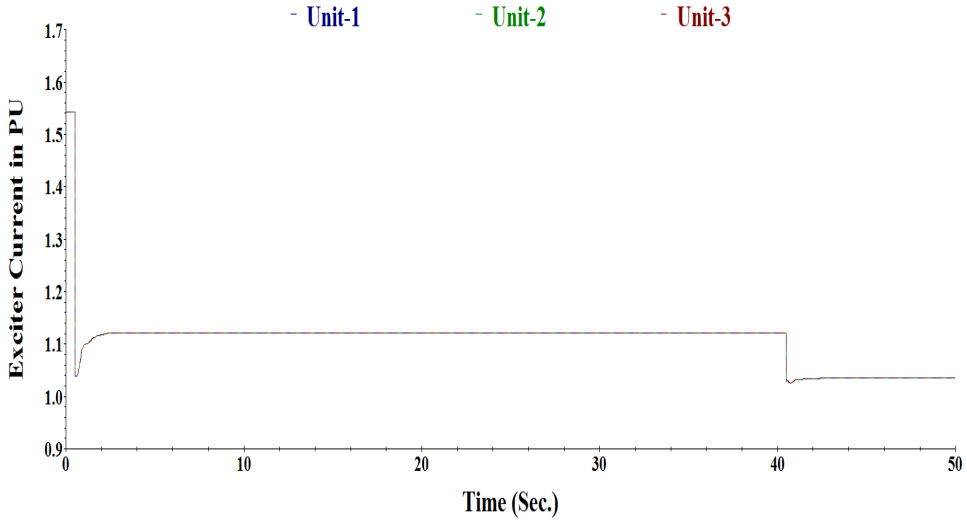

Figure 5.10: Exciter Current

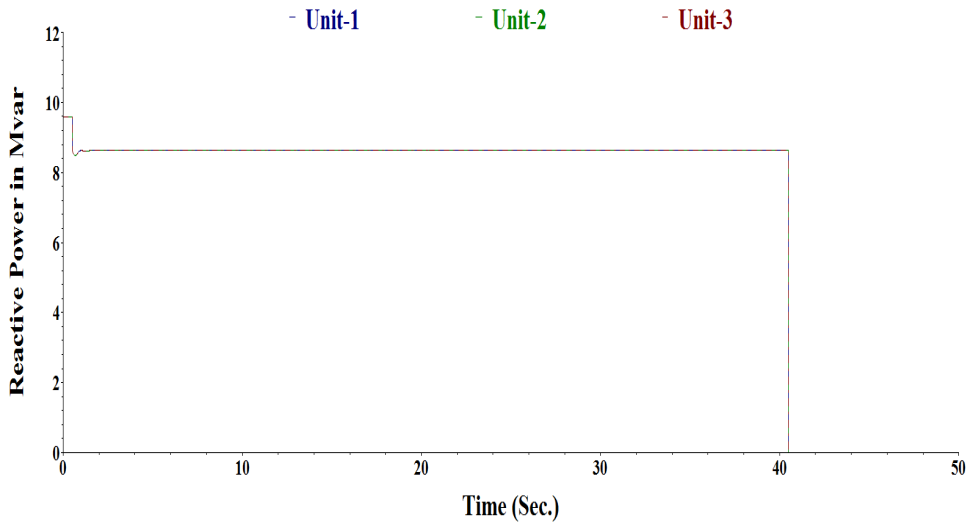

Figure 5.11: Reactive Power

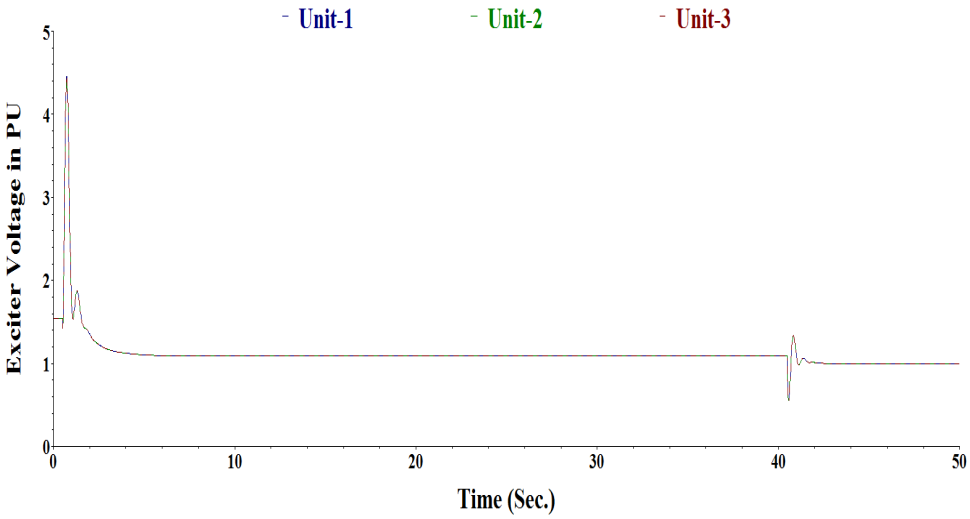

Figure 5.12: Exciter Voltage

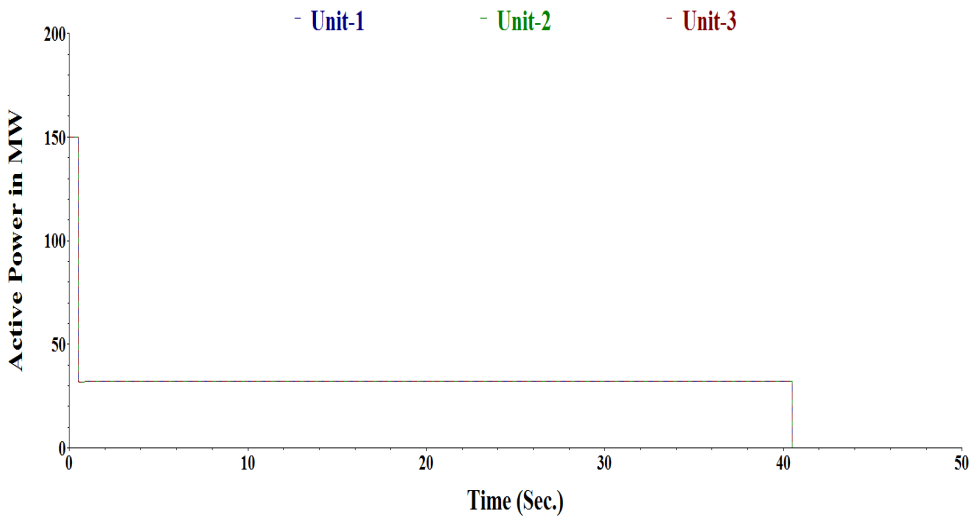

Figure 5.13: Active Power

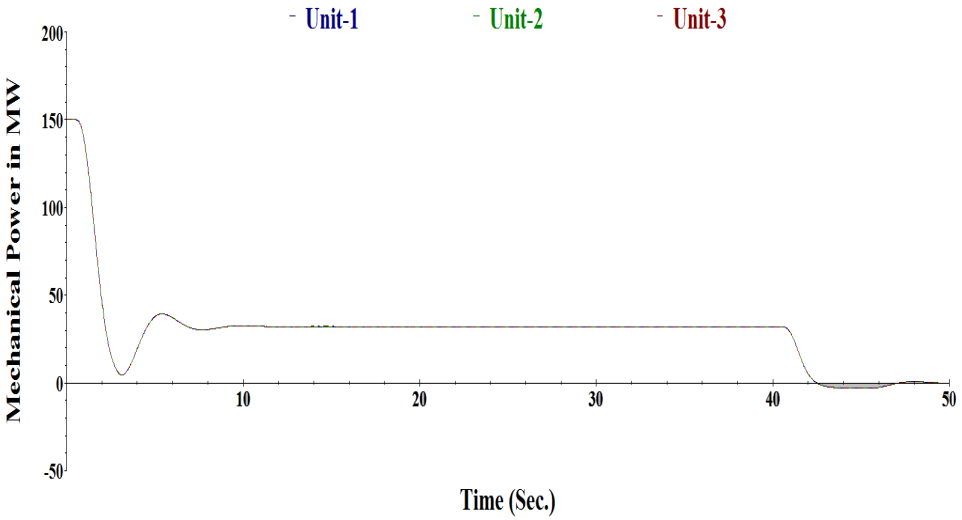

Figure 5.14: Mechanical Power

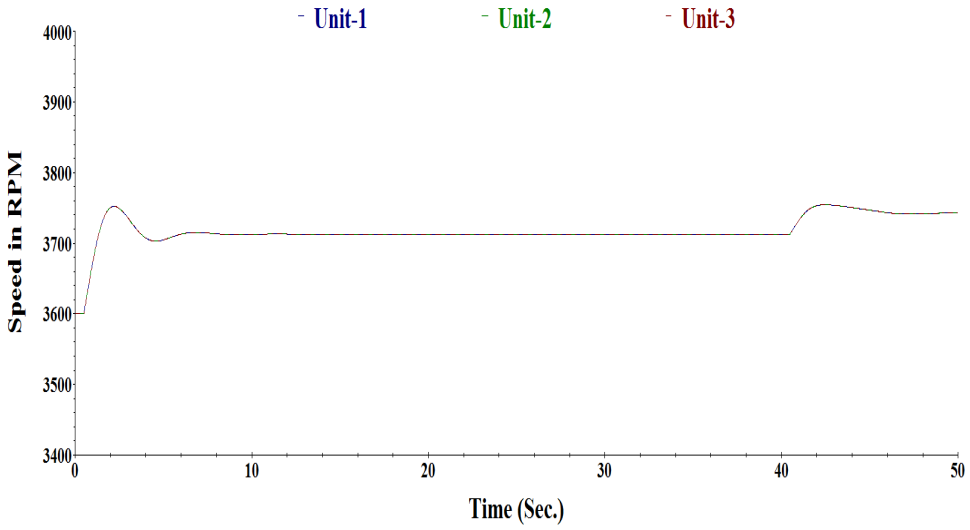

Figure 5.15: Speed

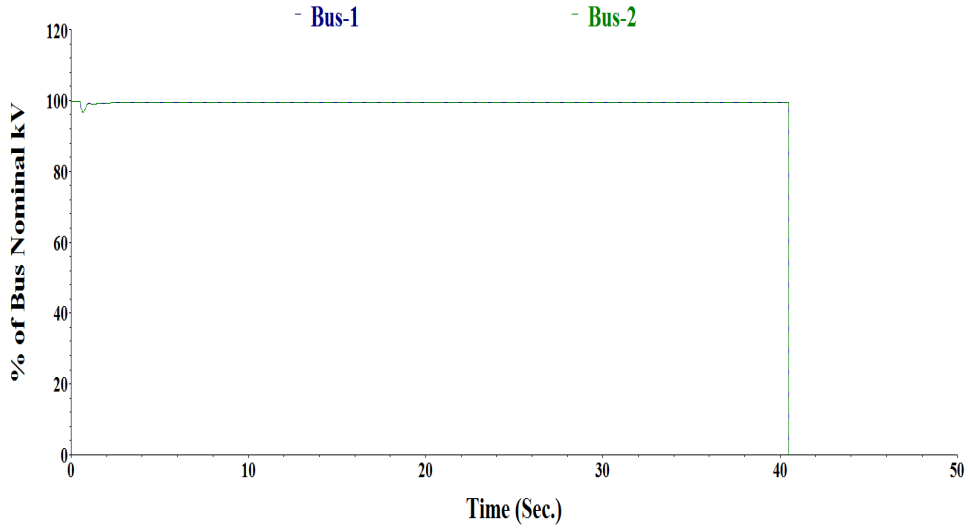

Figure 5.16: Bus Voltage

Case 11

All three units were online, each one generating 150 MW. The plant demand was 170 MW, with an export of 280 MW to the grid. When both grid lines opened, all units faced a load rejection of 92.4 MW, which caused the speed to be increased from 3600 to 3675 RPM (102 %). This is below the over-frequency relay setting, so the system remained intact.

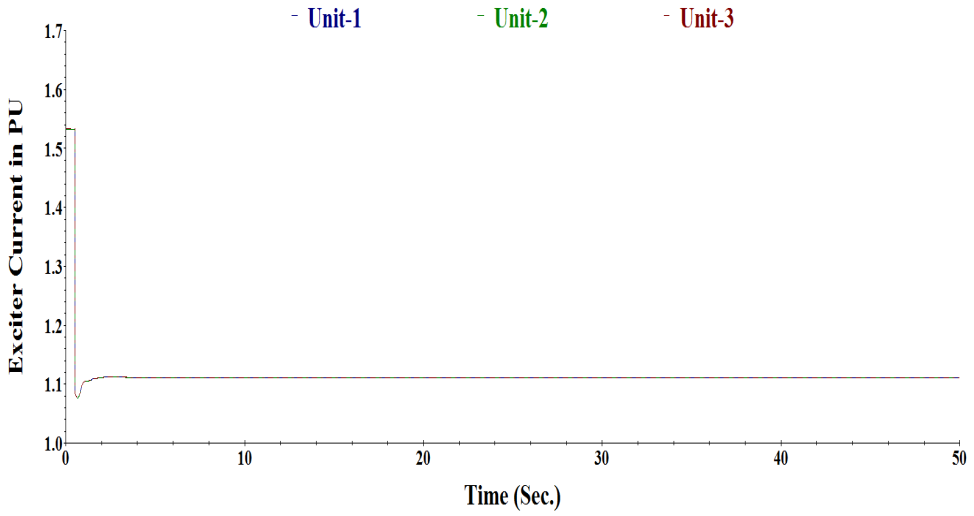

Figure 5.17: Exciter Current

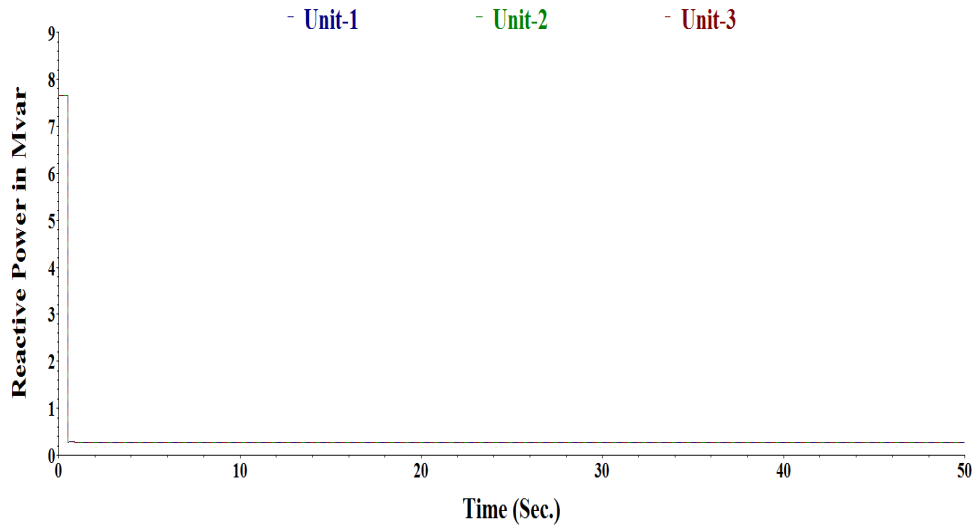

Figure 5.18: Reactive Power

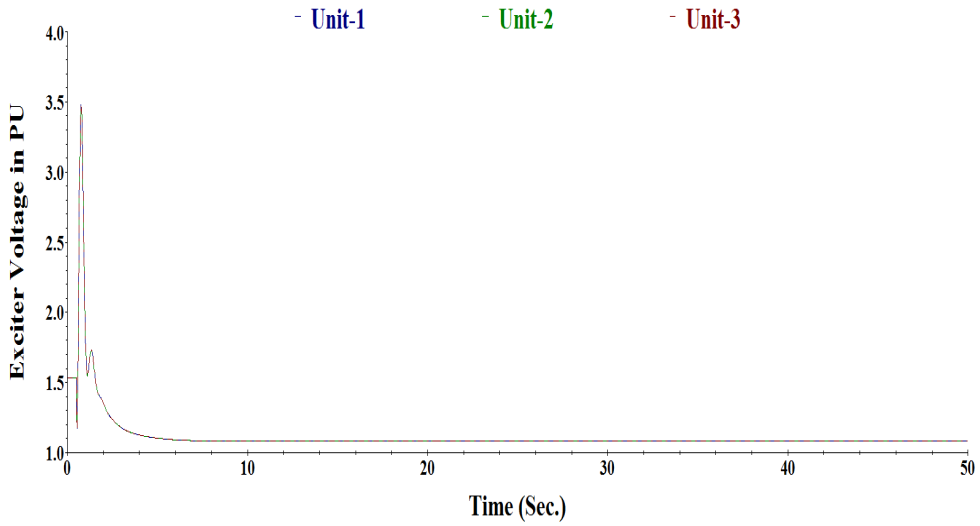

Figure 5.19: Exciter Voltage

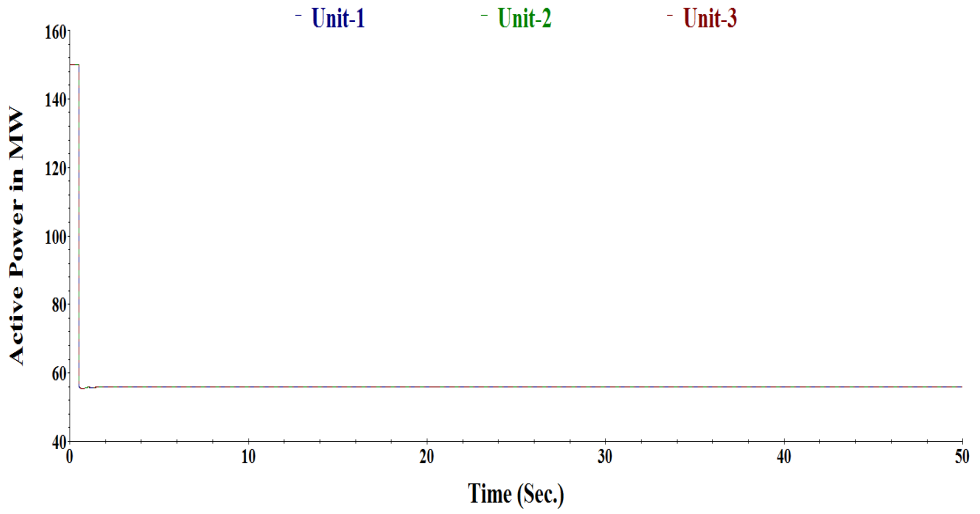

Figure 5.20: Active Power

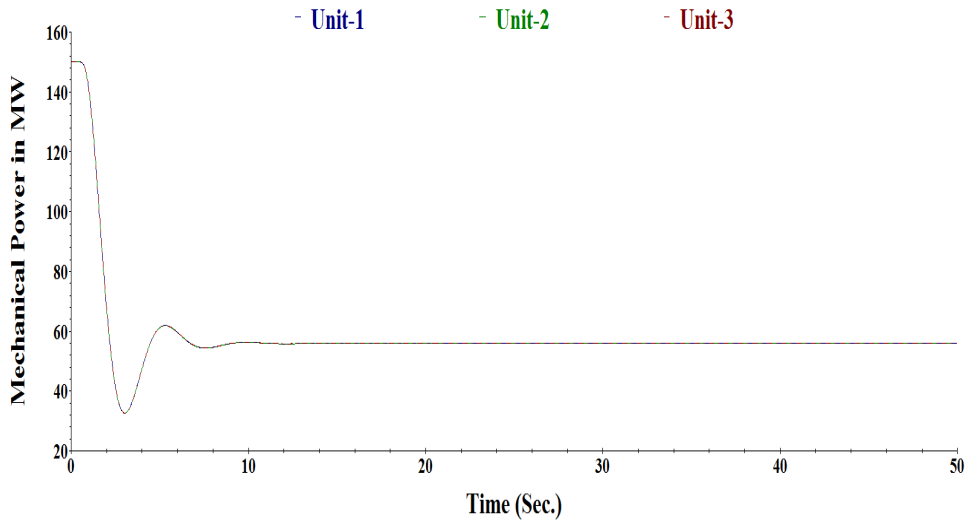

Figure 5.21: Mechanical Power

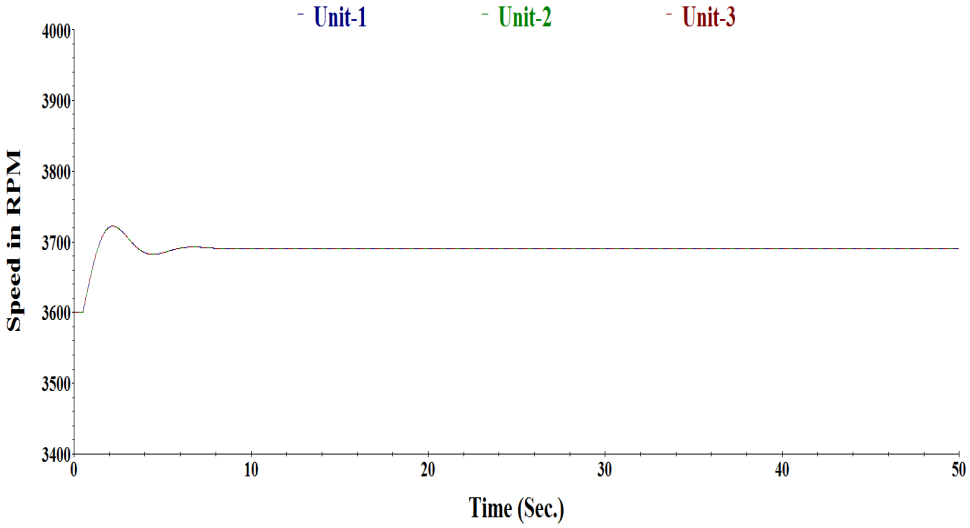

Figure 5.22: Speed

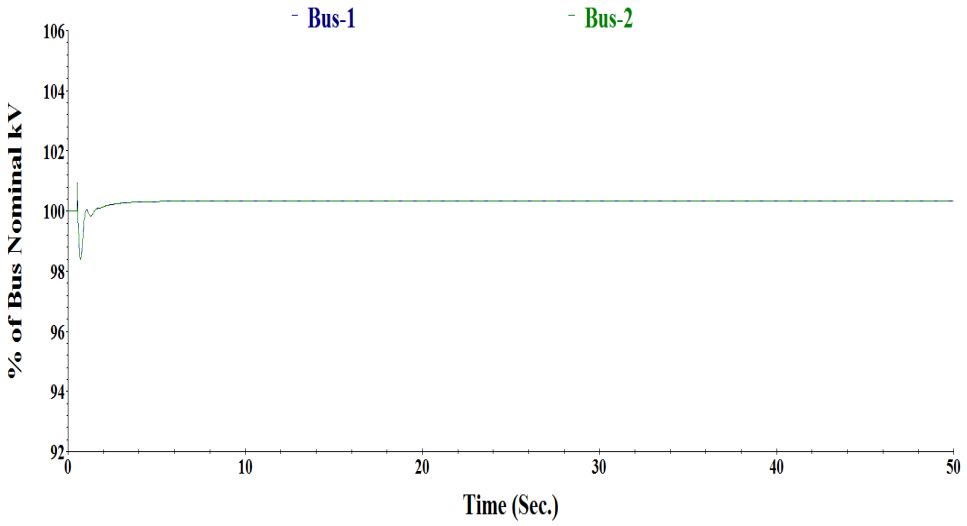

Figure 5.23: Bus Voltage

Chapter 6

SPECIAL PROTECTION SYSTEM

6.1 Introduction

A special protection system (SPS) is designed to identify system conditions that are out of the ordinary, and to correct abnormalities, to ensure no localized or area-wide blackouts. As a result, system reliability is maintained. Changes to load connections, generation levels (MV and MVAR) and system configurations may form a part of this protection system. Included within the special protection system are sensing devices, simple or complex logic, and high-speed communication. The key functions of the special protection system are to:

- Operate the power system closer to its limits.
- Increase power system security, particularly during extreme contingencies.
- Improve power system operation.

Because of cyber security concerns, it is often difficult to learn specific details of special protection systems which are in use. The author has learned of a special

protection system on an island off the coast of New Zealand which exports power to New Zealand via an underwater cable [36]. Upon loss of the interconnection to New Zealand, one or more generators is tripped to achieve a closer balance between generation and the remaining load on the island. The governors then act to achieve the final required balance between generation and load. The author has also learned that, because of multiple interconnections, there are many special protection systems in use in the provincial utility local to this university [37]. One such system protects against the loss of an interconnection which might be exporting upwards of 900 MW. The sensing element is the position of an auxiliary contact on the main contacts of the interconnection circuit breakers. There is a logic which is updated daily depending on loading conditions and current generators synchronized. There is a high speed communication system over a distance of a few hundred kilometres. Finally there is the action to trip circuit breakers to remove generators from operation in order to achieve an approximate balance between generation and remaining load in the islanded power system.

In terms of the SPS actions, the following are some of the commonly used types of SPS:

- System separation.
- Generator runback, or tripping.
- Runback of HVDC interconnections
- Under-frequency load shedding.
- Dynamic braking.

It is possible that actions of more than one type are initiated by an SPS once its operation conditions are met.

There are four methods to implement the SPS:

1. Identify the grid's Circuit Breaker(CB) status.
2. Measuring bus MW.
3. Measuring bus voltage.
4. Measuring bus over-frequency in export case or bus under-frequency in import case.

The frequency method has been used in this study because:

1. Very fast action by tripping the required circuit breakers CB.
2. Bus over-frequency SPS is recommended based on the results.
3. Frequency-based system acts before a voltage-based system.

An over-frequency generator shedding scheme may consider:

1. Tripping stages, each with specific frequency set points, generator shedding percentage, and time delay.
2. Tripping types: generator.
3. Possible under-voltage blocking.
4. Coordination with generation tripping.

An under-frequency load shedding scheme may need to consider some or all of the following factors:

1. Tripping stages, each with specific frequency set points, load shedding percentage, and time delay
2. Tripping types, loads.
3. Possible under-voltage blocking.
4. Coordination with generation tripping.

6.2 Case Study and Simulations

A one-line diagram of the SAPF electrical power system is shown in Figure 6.1. If the export power to the grid is greater than 335 MW, an SPS is necessary to ensure stability of the islanded SAPF if both grid lines are opened. Studies of SAPF electrical system of conditions with 419.6 MW and 335 MW export power show that the instability can be mitigated by tripping 1 or 2 units. A possible SPS can therefore be designed with the following operation logic:

1. If the export power is lower than 335 MW, the SPS will not be activated when both grid lines are opened.

2. If the export power is higher than 335 MW, the SPS is armed in anticipation of the possible event when both grid lines are opened.

3. When the SPS is armed, the two pre-determined generators are tripped once both grid lines are opened.

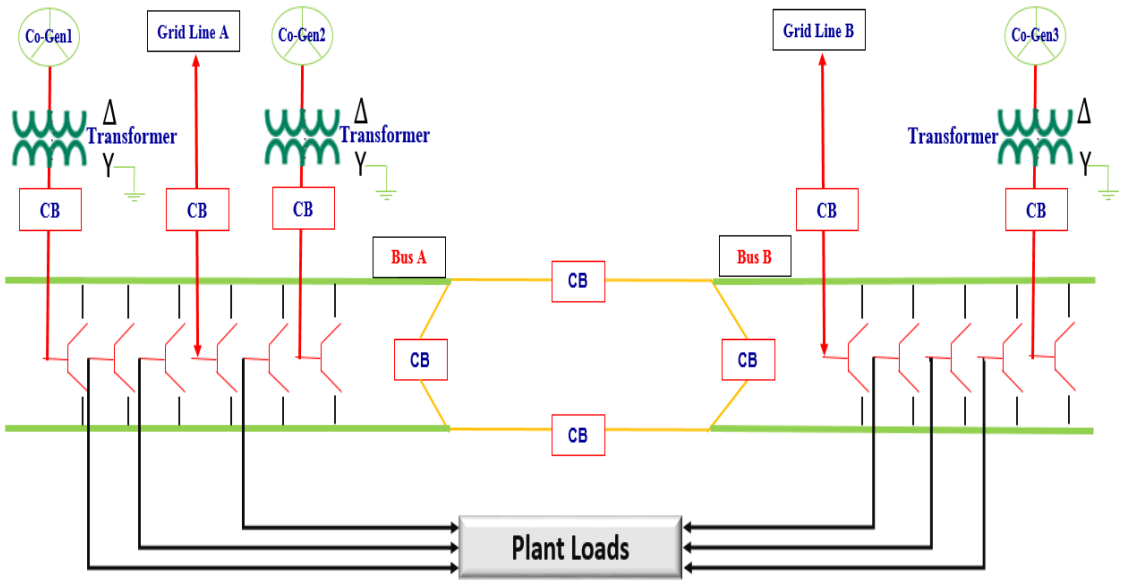

Figure 6.1: Single Line Diagram of Electrical System

Case 1

Each unit was generating 175 MW for a total of 525 MW. The plant consumption was 100.2 MW and 424.8 was exported to grid. Both grid lines were isolated at 0.5 seconds. The over-frequency relay settings are the following:

a) Unit 1: 103% pick-up time is 10 seconds.

b) Unit 2: 103% pick-up time is 20 seconds.

c) Unit 3: 103% pick-up time is 35 seconds.

The SPS actions are summarized in the table below:

Table 6.1: SPS Actions (Case 1)

Time (sec)	Event	Action	Action By
11.197	CB3-Unit1	Open	Freq Relay
21.197	CB4-Unit2	Open	Freq Relay

The effectiveness of the SPS can be verified by observation of the following seven graphs. Conceptually when the islanding mode of operation takes place the speed of the generators will initially rise because the energy being supplied by the turbines is more than that required by the load. The speed increase is detected by the governors which close the fuel valves by the required amount to maintain the required speed. Voltage will initially rise, the increase is detected by the AVR which decreases the excitation by the amount required to maintain output voltage. For this specific case, after the plant was isolated from the grid at 0.5 seconds with 419.6 MW load rejection (80% of the generated power), the speed of the generator increased from 3600 PRM to 3780 RPM and settled down after 6 seconds at 3740 PRM (103.88%). At 10 seconds unit 1 was tripped by the SPS due to over-frequency (62.33 Hz, 103.88%), and after 20 seconds unit 2 was tripped by the SPS due to over-frequency (62 Hz, 103.33%).

Due to the accurate action by SPS, unit 3 survived with the speed settling out at 3678 RPM (61.3 Hz, 102.16%) with the generator power equal to the plant consumption.

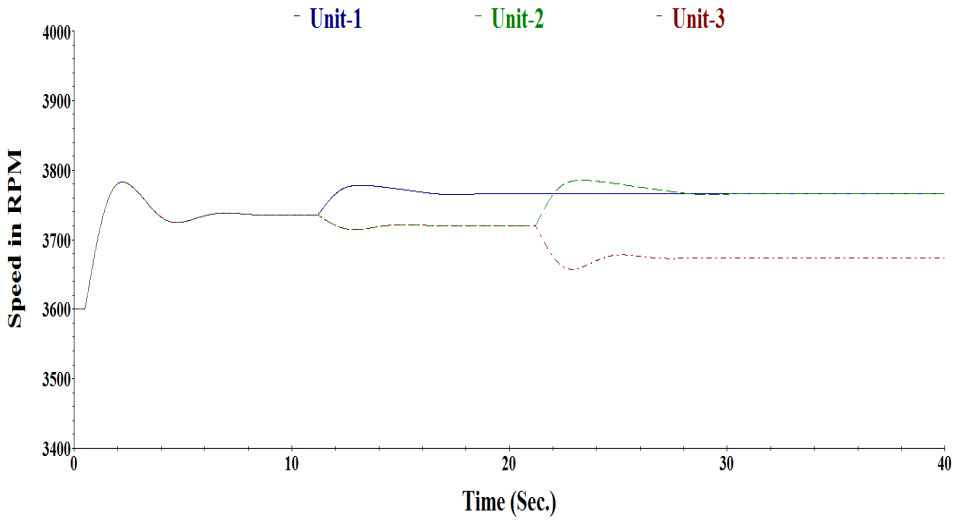

Figure 6.2: Speed

All three units initially survived and operated stably with a small overshoot in mechanical power (Pm). When unit 1 tripped, and then again when unit 2 trips, there was an acceptable over-shoot in mechanical power on unit 3 which nicely settled down 22 seconds after the SPSs took the required actions. The performance is fully satisfactory.

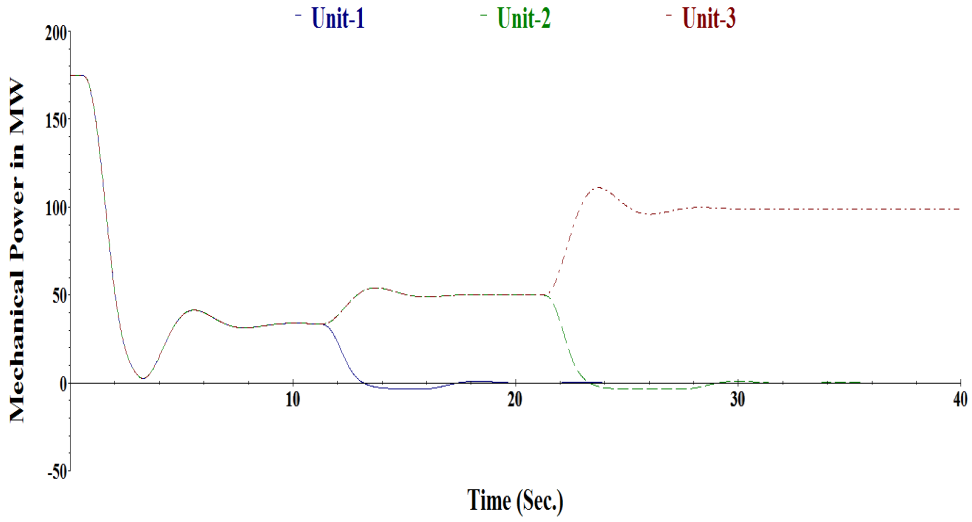

Figure 6.3: Mechanical Power (Pm)

The changes in electrical power (Pe) are initiated by the opening of the unit circuit breakers.

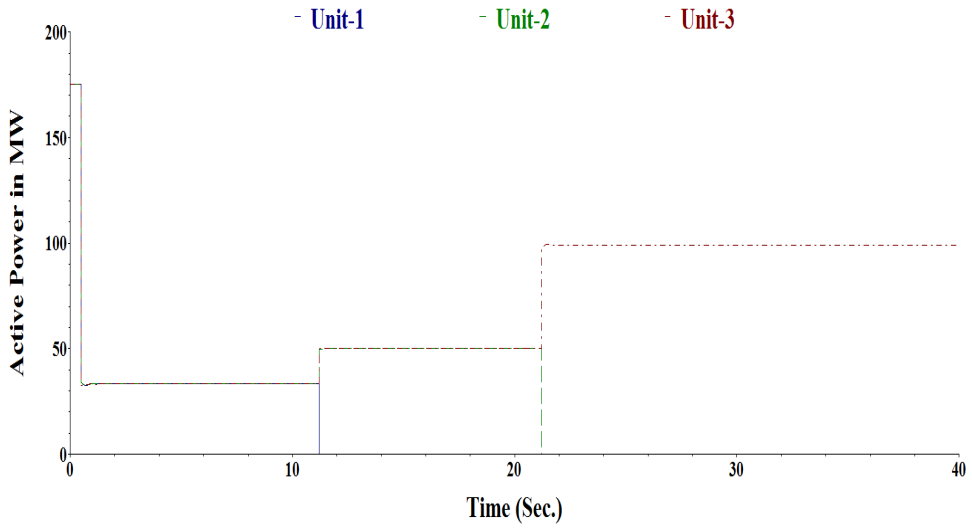

Figure 6.4: Active Power (Pe)

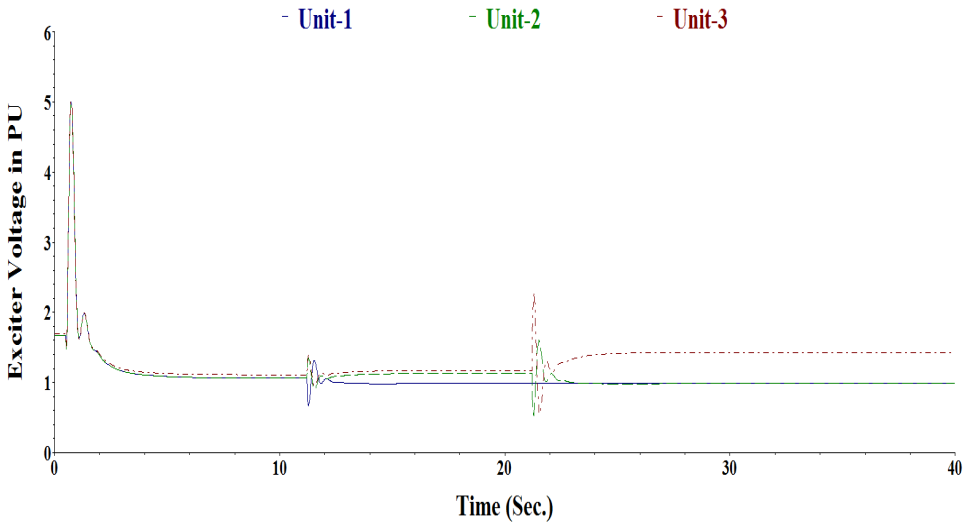

Figure 6.5: Exciter Voltage

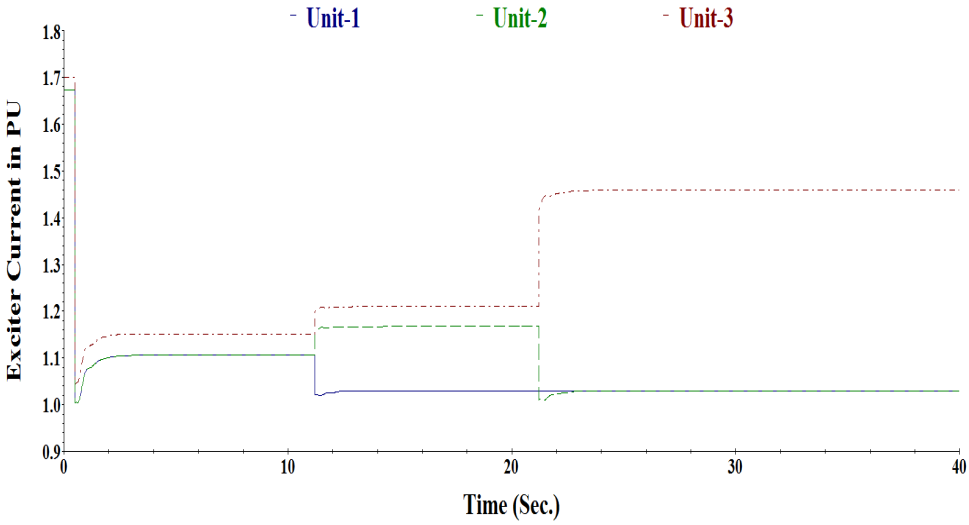

Figure 6.6: Exciter Current

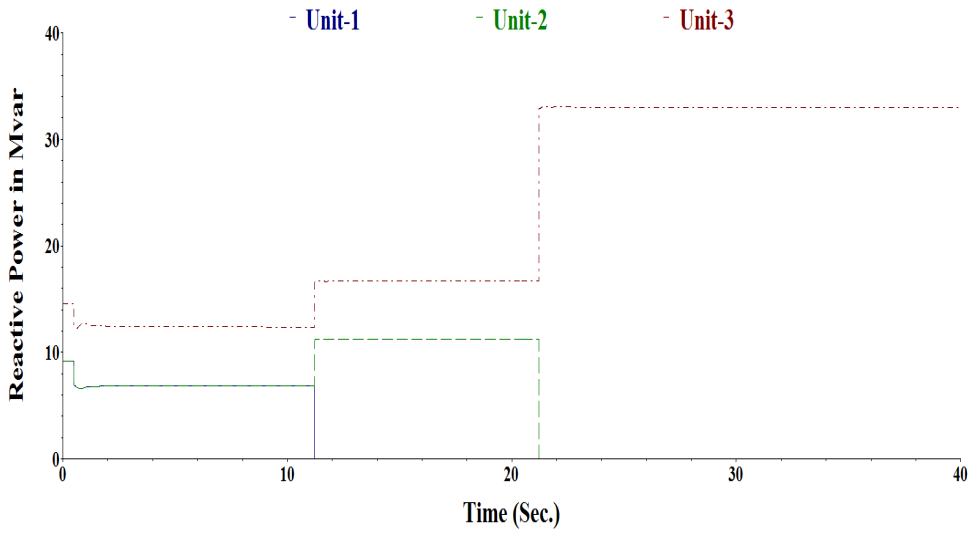

Figure 6.7: Reactive Power

The bus voltage graph requires some comment. Originally each generator was supplying 175 MW, which would cause a large voltage drop in each one. In the final steady state, the one remaining generator was only supplying about 100 MW, which should cause a greatly reduced voltage drop in that generator. The logical conclusion is that the bus voltage should tend to be higher in the final steady state than in the original state. However, it is necessary to look at the MVAR load. The original MVAR loading was about 9 MVAR on unit 1 and unit 2 and about 15 MVAR on unit 3. In the final steady state the MVAR loading on the remaining unit 3 was 33.5 MVAR. The 33.5 lagging MVAR will cause a significant voltage drop in the generator. The AVR increases the exciter current to try to control the voltage and acts within the capability of the proportional controller which it is.

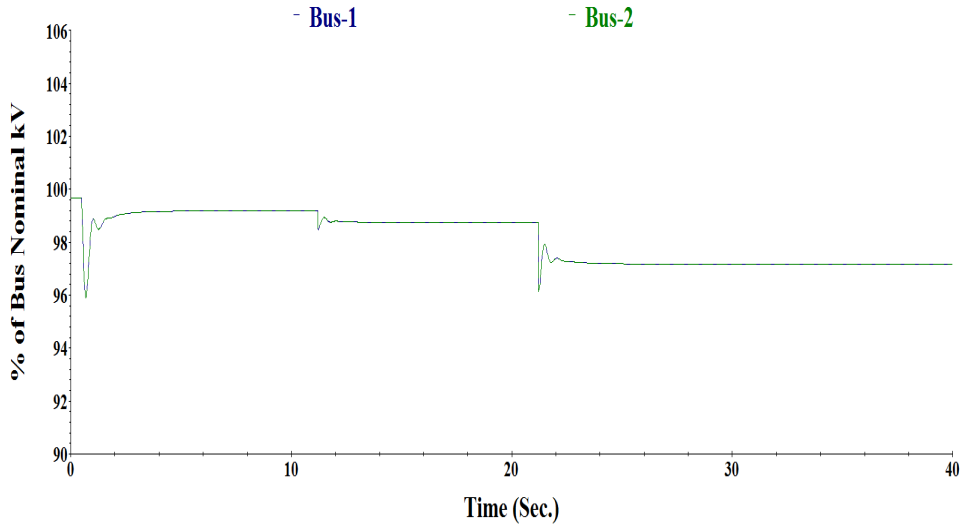

Figure 6.8: Bus Voltage

Case 2

Each unit was generating 150 MW for a total of 450 MW. The plant consumption was 100 MW and 350 MW was exported to the grid. Both grid lines were opened at 0.5 seconds. The over-frequency relay settings are similar to Case 1.

Table 6.2: SPS Actions (Case 2)

Time (sec)	Event	Action	Action By
15.576	CB3-Unit1	Open	Freq Relay

In this case one unit tripped and two units survived because the export power was 77% of the generated power. When the plant was isolated from the grid at 0.5 seconds with 346 MW load rejection (77% of the generate power), the generator speed increased from 3600 PRM to 3740 RPM and settled down after 6 seconds at 3720 PRM (103.33%). At 15 seconds unit 1 was tripped by the SPS due to over-frequency (62 Hz, 103.33%). Because of the action of the SPS, unit 2 and unit 3 survived, with the speed of both of them dropping to 3682 RPM (61.36 Hz, 102.27%). As result of governor action, the generated power is equal to the plant consumption.

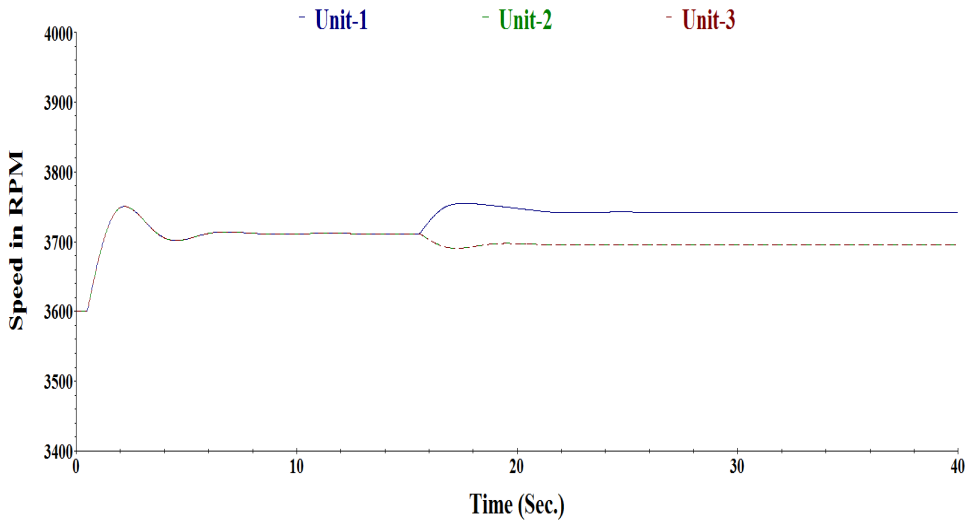

Figure 6.9: Speed

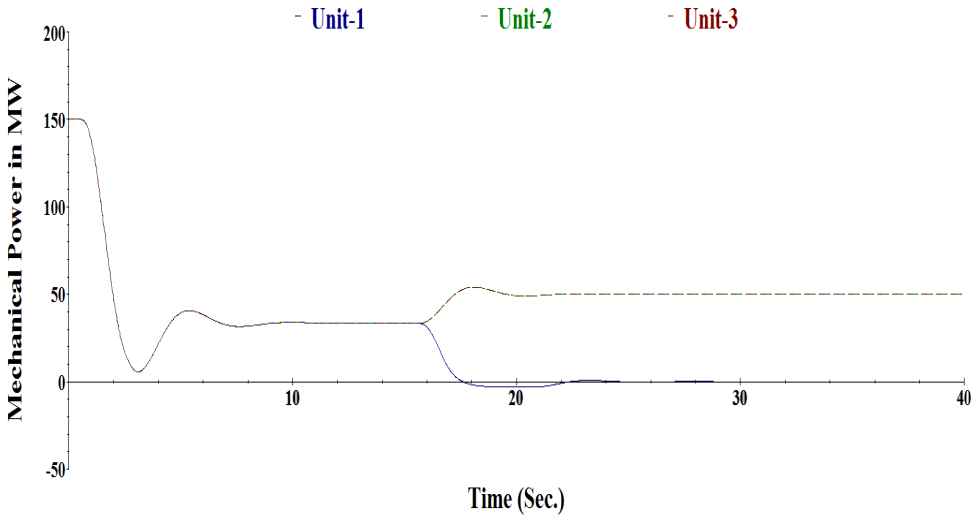

Figure 6.10: Mechanical Power (Pm)

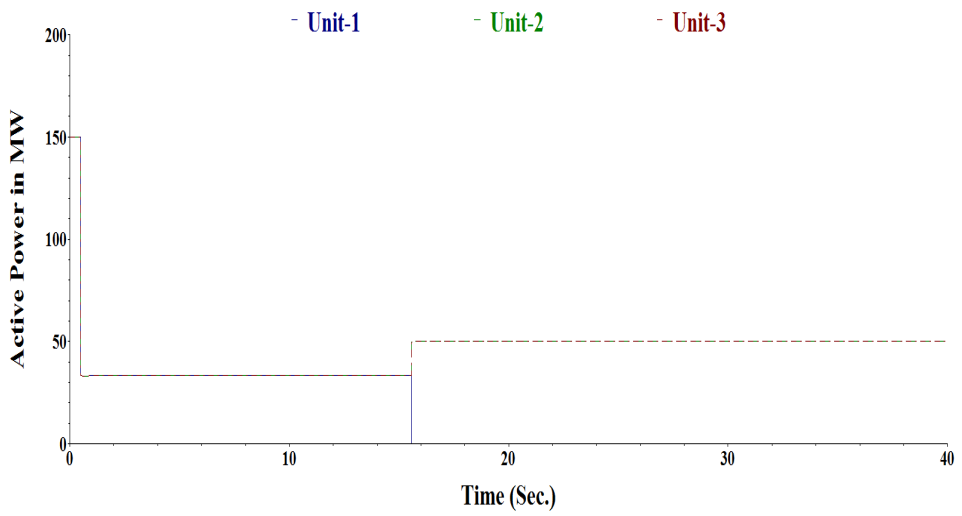

Figure 6.11: Active Power (Pe)

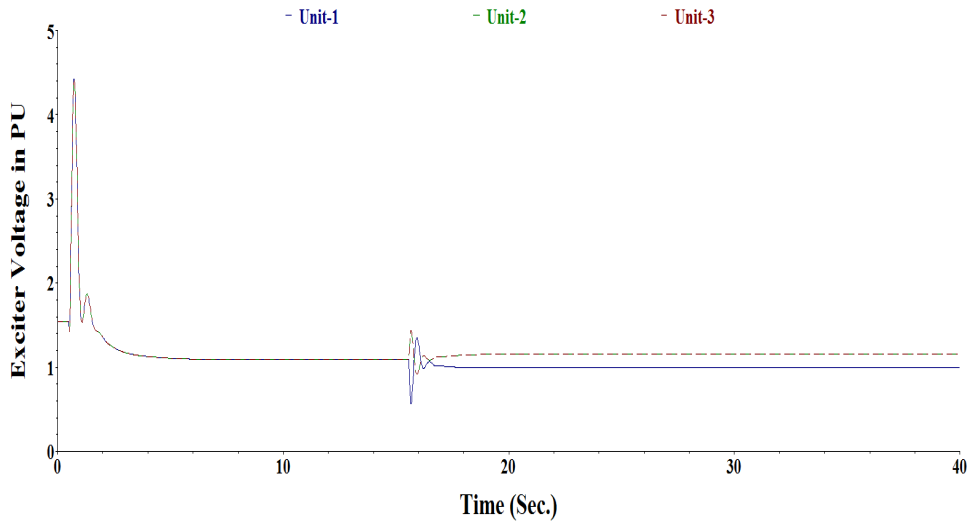

Figure 6.12: Exciter Voltage

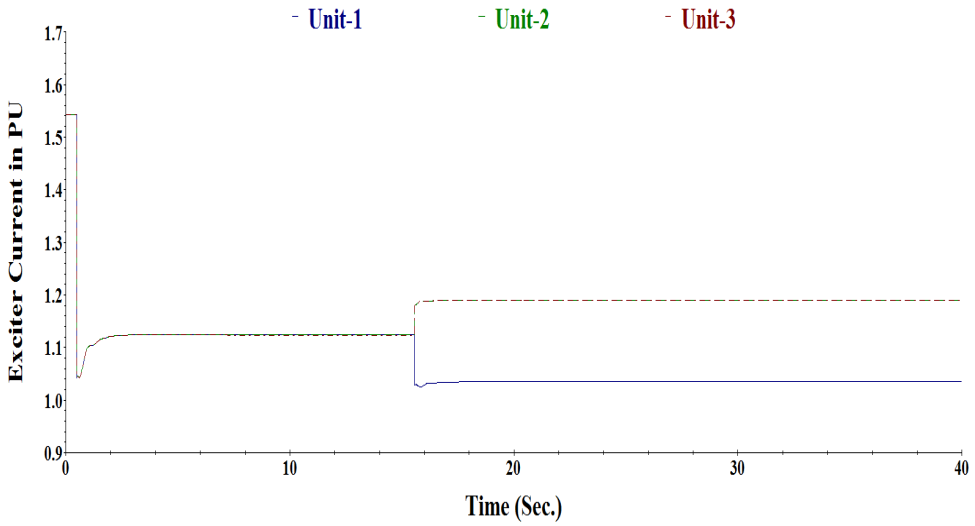

Figure 6.13: Exciter Current

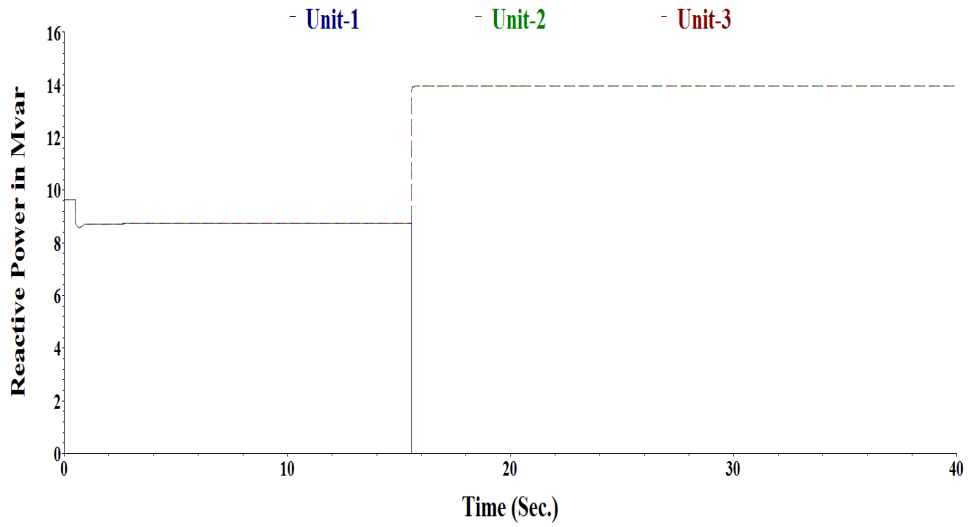

Figure 6.14: Reactive Power

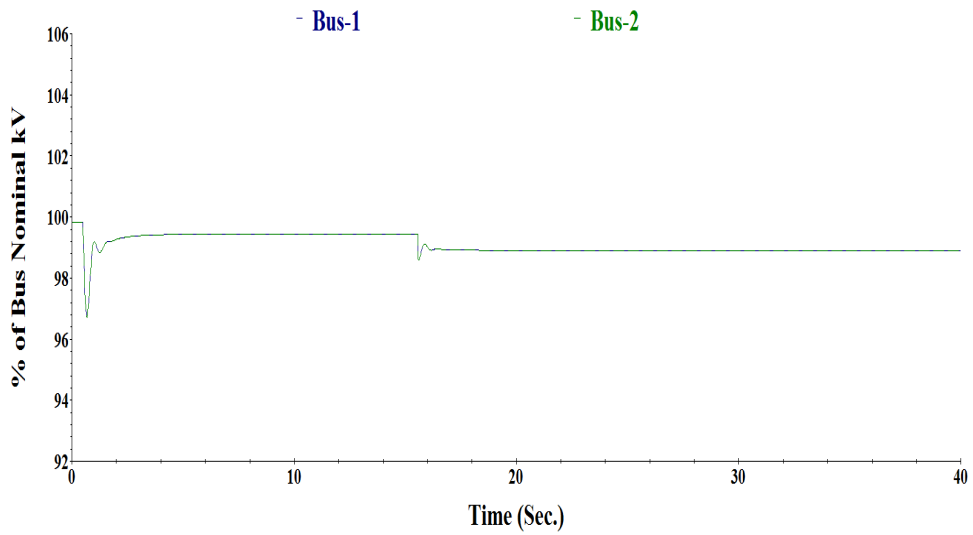

Figure 6.15: Bus Voltage

Case 3

Unit 1 and unit 2 were generating 52 MW each for a total of 104 MW. The plant consumption was 204 MW and 100 MW was imported from the grid. Both grid lines were opened at 0.5 seconds. The under-frequency relay settings are as follow:

Table 6.3: Under-Frequency Relay Settings

Device	Setting (%)	Time Delay,(Sec)
Under-Frequency,relay	94	0.1

A load shedding system (LSS) was used in this case to show the behavior of the units and compare the results with Case 5 of Chapter 5. The LSS setting and action are summarized in the below table:

Table 6.4: LSS Setting and Action

Load Shedding Level/ %		Load to be Shed	Time Delay
Level	Frequency (%)	MW	Seconds
1	99.1	20.2	10

When both grid lines were tripped at 0.5 seconds, the speed decreased gradually until it reached 3571 RPM (99.1%), the LSS under-frequency limit, at 0.961 seconds. The speed further decreased in the 3550 RPM (range) between 6.1-7.76 seconds. The LSS was activated at 11.04 seconds, at which time 20.2 MW of plant load tripped. This resulted in the speed increasing regularly until it reached 3561 RPM at 15.96 seconds.

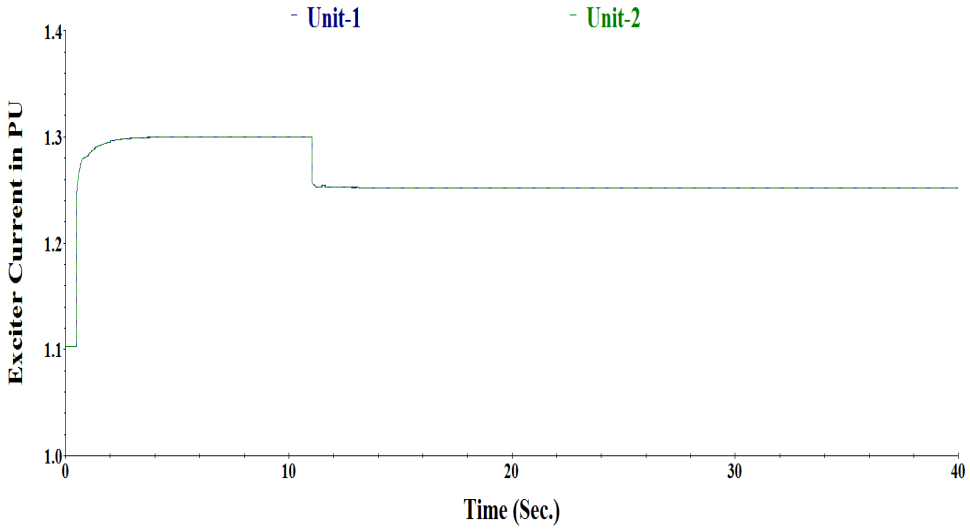

Figure 6.16: Exiter Current

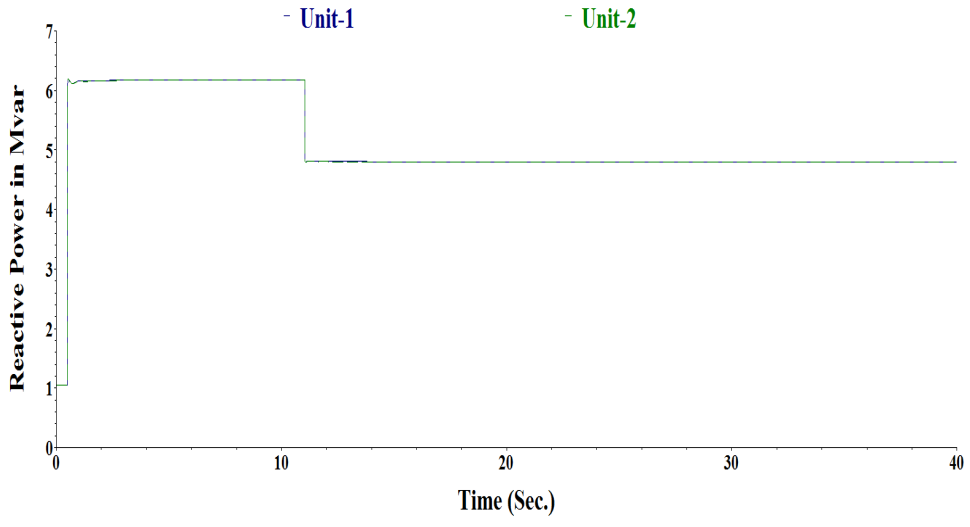

Figure 6.17: Reactive Power

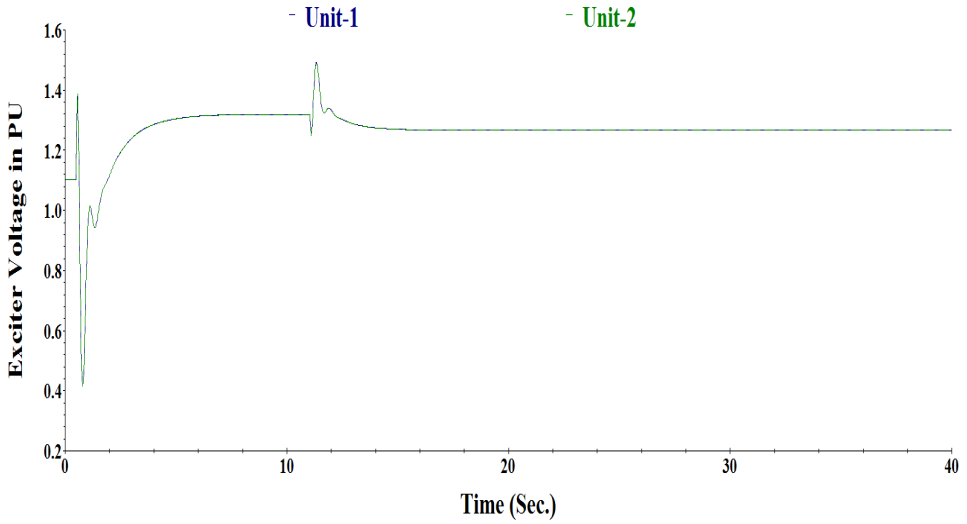

Figure 6.18: Exciter Voltage

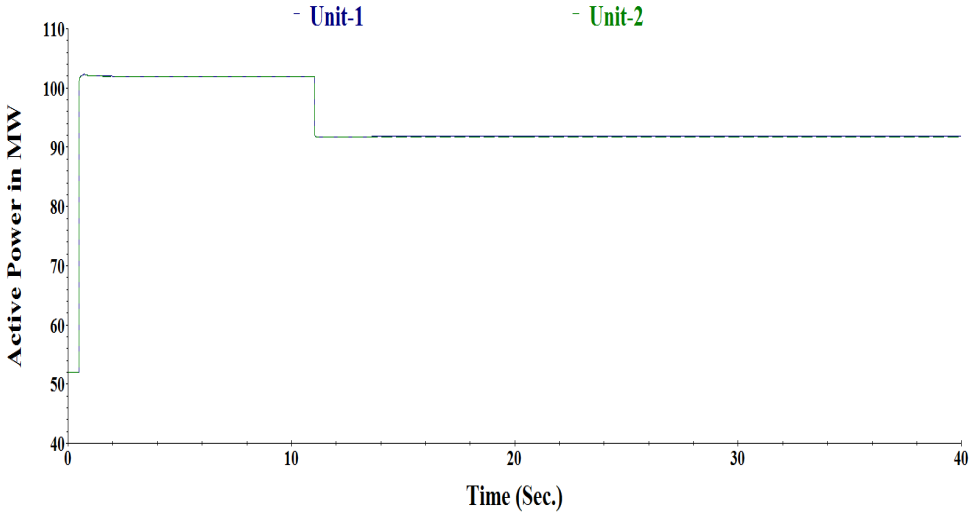

Figure 6.19: Active Power

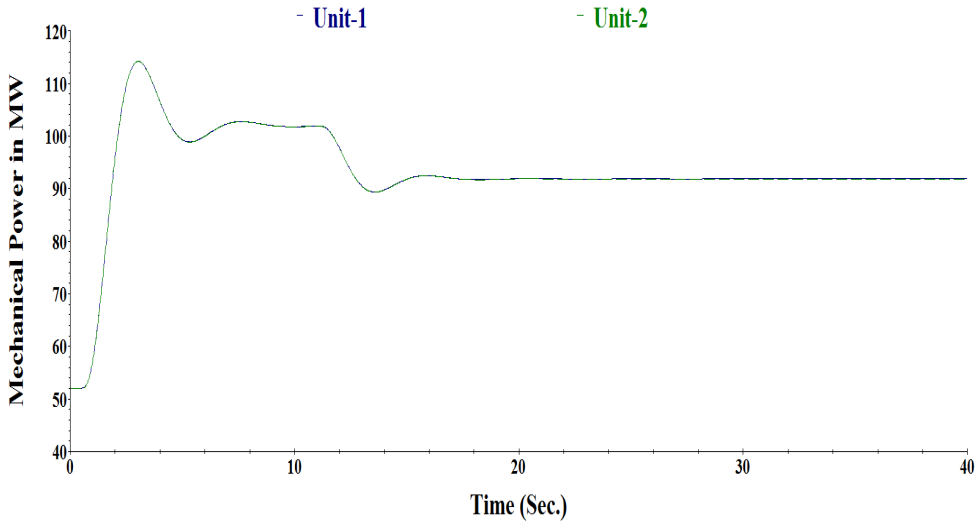

Figure 6.20: Mechanical Power

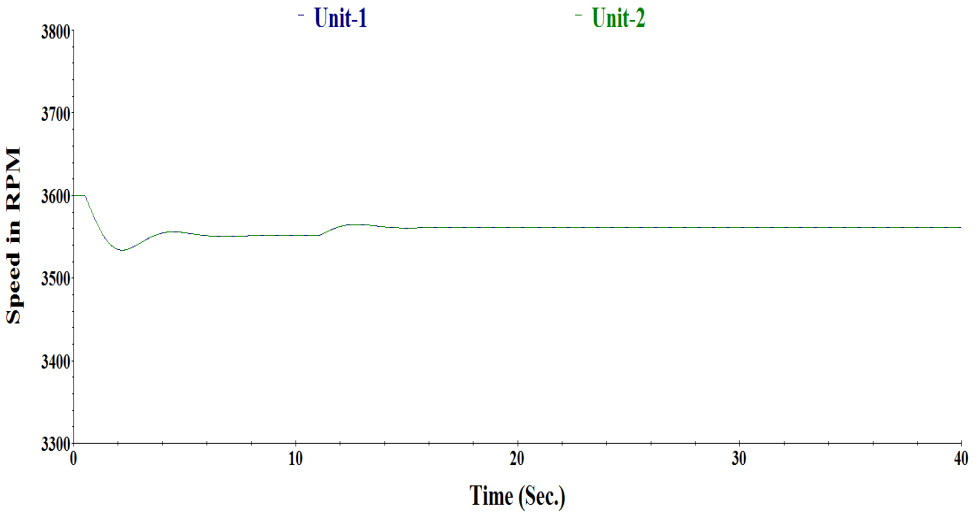

Figure 6.21: Speed

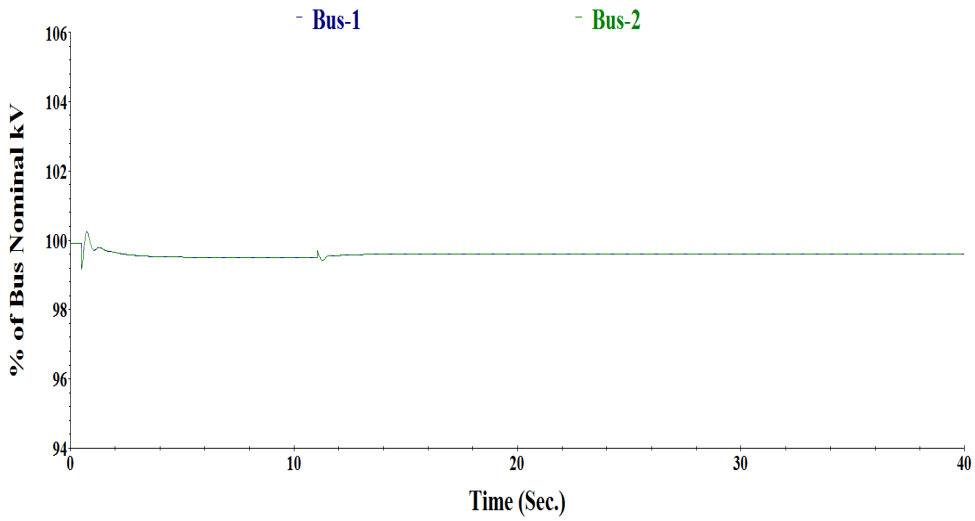

Figure 6.22: Bus Voltage

Chapter 7

CONCLUSIONS AND RECOMMENDATIONS

7.1 Summary

This thesis presents a complete model of the SAPF cogeneration and electrical system. The SAPF electrical power system model has been constructed using both MATLAB and ETAP. The performance of the governor and gas turbine model originally proposed by Rowen has been simulated in isolated mode and in interconnected mode. The exciter and AVR model has been established as per the IEEE Standard. The synchronous generator has been modelled fully in ETAP, and the linearized K1-K6 model originally proposed by Heffron and Philips has been used in MATLAB. Both the islanded and interconnected modes of operation have been modelled in MATLAB and ETAP, via the operation of circuit breakers, allows transition from interconnected to isolated mode. The thesis proposes special protection systems which allow successful transition from interconnected mode to isolated mode for a variety of plant operating conditions, thus increasing the plant reliability.

7.2 Conclusions

It is possible to produce transient instability in two ways, although the results are not shown in the thesis. Using the linearized synchronous machine model in MATLAB, an artificially high value of external reactance between the machine and the infinite bus produced transient instability. With the ETAP software, an improperly tuned power system stabilizer produced continuing small oscillations superimposed on some of the longer term steady state variables.

However, as the results show, the existing SAPF behaves extremely well during disturbances. Transient overshoots on speed and mechanical power are normally relatively small, which is to be expected since a gas turbine more closely resembles a large jet engine than it does a conventional thermal turbine or particularly a hydro turbine. Through plant personnel, the OEM has provided parameters for the gas turbine and generator and their controllers. There are actual time delays in Rowens model of the gas turbine. For the SAPF gas turbines, the combustion reaction time delay and the turbine and exhaust delay are zero seconds, while typical values are 0.01 and 0.04 seconds respectively. As well the SAPF governor lag time constant is 0.05 seconds compared to a typical value of 1 second, and the fuel control time constant is 0.02 seconds compared to a typical value of 0.4 second. In the exciter and AVR, the time constants are sometimes smaller than the typical values provided in the IEEE Standard.

The research has also revealed a significant inconsistency in the SAPF over frequency protective relaying. Presently the over frequency relay is set at 103%. Because the speed reference for a fully loaded machine is 104%, this means that any disturbance which causes the machine to be loaded to less than 25% will always cause a tripping of the generators on over frequency. Based on the stability analysis in Chapter 4, it is shown that the gas turbine control is capable of maintaining the stability of the system with significant load changes. With three units in operation, and an export

of more than 346 MW, presently the loss of the two transmission lines to the grid will cause all three units to trip. A special protection system has been designed in Chapter 6 which, depending on the plant load, will trip one or two units but the third unit will survive and supply the required power to the plant loads. On the other hand, import power from the grid can impact the reliability of the SAPF power system unless a load shedding system is implemented, as shown in Chapter 6.

7.3 Recommendations for SAPF

Based on the result of the simulations and findings of this thesis the following are the recommendations for SAPF:

1. There is no need for an islanding signal based on circuit breaker position to be sent to the turbine control system.

2. There is no need for a live plant MW signal to be sent to the turbine control system.

3. Based on the results in Chapter 5 and 6, a special protection system (SPS) is needed for reliable operation of the SAPF electrical power system.

4. Based on the results in Chapter 5 and 6, a load shedding system based on frequency is needed for the SAPF electrical power system.

5. Based on the results in Chapter 5 and 6, governor droop and over-frequency relay settings need to be reevaluated (currently governor droop is 4%, while over-frequency relay protection setting is 3%).

6. Consideration should be given to activation and optimal tuning of the power system stabilizer (PSS).

7. Black start-up capability is required.

7.4 Recommendations for Future Work

To continue this work, the following topics are suggested:

1. Power system stabilizer (PSS) tuning based on SAPF parameters.

2. Theoretical development of the proposed control strategy for multi-GT in MATLAB.

References

[1] W. I. Rowen, "Simplified Mathematical Representations of Heavy-Duty Gas Turbines," *Journal of Engineering for Gas Turbines and Power*, vol. 105, no. 4, pp. 865–869, 1983.

[2] W. Rowen, "Simplified Mathematical Representations of Single Shaft Gas Turbines in Mechanical Drive Service," *Turbomachinery International*, vol. 33, no. 5, 1992.

[3] D. G. Photovoltaics and E. Storage, "IEEE Application Guide for IEEE Std 1547, IEEE Standard for Interconnecting Distributed Resources with Electric Power Systems," 2009.

[4] T. S. Basso and R. DeBlasio, "IEEE 1547 Series of Standards: Interconnection Issues," *Power Electronics, IEEE Transactions on*, vol. 19, no. 5, pp. 1159–1162, 2004.

[5] H. Jouybari-Moghaddam, S. Hosseinian, and B. Vahidi, "An Introduction to Active Distribution Networks Islanding Issues," in *Electrical Power Distribution Networks (EPDC), 2012 Proceedings of 17th Conference on.* IEEE, 2012, pp. 1–6.

[6] J. C. Vieira, W. Freitas, W. Xu, and A. Morelato, "Performance of Frequency Relays for Distributed Generation Protection," *Power Delivery, IEEE Transactions on*, vol. 21, no. 3, pp. 1120–1127, 2006.

[7] J. C. Vieira, W. Freitas, A. Morelato, and J. Leao, "Dynamic Models of Frequency and Voltage Based Relays for Distributed Generation Protection," in *Power Tech, 2005 IEEE Russia*. IEEE, 2005, pp. 1–5.

[8] T. Younkins, F. deMello, R. Dunlop, F. Fenton, J. Intrabartola, P. Kundur, B. Littman, and T. Russell, "Guidelines for Enhancing Power Plant Response to Partial Load Rejections," *IEEE Trans. Power Appar. Syst.;(United States)*, vol. 102, no. 6, 1983.

[9] H. You, V. Vittal, and X. Wang, "Slow Coherency-Based Islanding," *Power Systems, IEEE Transactions on*, vol. 19, no. 1, pp. 483–491, 2004.

[10] R. Sun and V. A. Centeno, "Wide Area System Islanding Contingency Detecting and Warning Scheme," *Power Systems, IEEE Transactions on*, vol. 29, no. 6, 2014.

[11] N. Senroy, G. T. Heydt, and V. Vittal, "Decision Tree Assisted Controlled Islanding," *Power Systems, IEEE Transactions on*, vol. 21, no. 4, pp. 1790–1797, 2006.

[12] R. Diao, V. Vittal, K. Sun, S. Kolluri, S. Mandal, and F. Galvan, "Decision Tree Assisted Controlled Islanding for Preventing Cascading Events," in *Power Systems Conference and Exposition, 2009. PSCE'09. IEEE/PES*. IEEE, 2009, pp. 1–8.

[13] H.-C. Chen, S.-Y. Chen, S.-C. Shih *et al.*, "Transient Stability Analysis of an Industrial Cogeneration System," 2010.

[14] S. K. Yee, F. Hughes, and J. Milanovic, "Comparative Analysis and Reconciliation of Gas Turbine Models for Stability Studies," in *Power Engineering Society General Meeting, 2007. IEEE*. IEEE, 2007, pp. 1–8.

[15] M. Murty, "Modeling of Gas Turbine and Its Control System," *CEB Power Systems Simulation Training Lectures. Online on: http://www. sari-energy. org.*

[16] L. Hajagos and G. Berube, "Utility Experience with Gas Turbine Testing and Modeling," in *Proc. IEEE PES winter meeting*, vol. 2, 2001, pp. 671–677.

[17] I. Yousefi, M. Yari, and M. A. Shoorehdeli, "Modeling, Identification and Control of a Heavy Duty Industrial Gas Turbine," in *Mechatronics and Automation (ICMA), 2013 IEEE International Conference on.* IEEE, 2013, pp. 611–615.

[18] L. Hannett and A. H. Khan, "Combustion Turbine Dynamic Model Validation from Tests," *Power Systems, IEEE Transactions on*, vol. 8, no. 1, pp. 152–158, 1993.

[19] H. E. Shalan, M. M. Hassan, and A. Bahgat, "Parameter Estimation and Dynamic Simulation of Gas Turbine Model in Combined Cycle Power Plants Based on Actual Operational Data," *Journal of American Science*, vol. 7, no. 5, pp. 303–310, 2011.

[20] P. Mahat, Z. Chen, and B. Bak-Jensen, "Gas Turbine Control for Islanding Operation of Distribution Systems," in *Power & Energy Society General Meeting, 2009. PES'09. IEEE.* IEEE, 2009, pp. 1–7.

[21] P. Kundur, N. J. Balu, and M. G. Lauby, *Power System Stability and Control*. McGraw-Hill New York, 1994.

[22] Y.-n. Yu, "Electric Power System Dynamics," *ACADEMIC PRESS, INC., 111 FIFTH AVE., NEW YORK, NY 10003, USA, 1983, 256*, 1983.

[23] W. Heffron and R. Phillips, "Effect of a Modern Amplidyne Voltage Regulator on Underexcited Operation of Large Turbine Generators [includes discussion],"

Power Apparatus and Systems, Part III. Transactions of the American Institute of Electrical Engineers, vol. 71, no. 1, 1952.

[24] S. Feng, X. Jianbo, W. Guoping, and X. Yong-hong, "Study of Brushless Excitation System Parameters Estimation Based on Improved Genetic Algorithm," in *Electric Utility Deregulation and Restructuring and Power Technologies, 2008. DRPT 2008. Third International Conference on.* IEEE, 2008, pp. 915–919.

[25] Z. Fengge, J. Guanglong, W. Xiuping, and J. Shi, "Research on Performance of Brushless Electric Excitation Synchronous Machine," in *Electrical Machines and Systems (ICEMS), 2013 International Conference on.* IEEE, 2013, pp. 597–601.

[26] D. Sumina, N. Bulić, and S. Skok, "Stabilization of the Electromechanical Oscillations of Synchronous Generator," *Strojarstvo: Časopis za Teoriju i Praksu u Strojarstvu*, vol. 53, no. 3, pp. 209–219, 2011.

[27] E. Rakhshani and J. Sadeh, "Application of Power System Stabilizer in a Combined Model of LFC and AVR Loops to Enhance System Stability," in *Power System Technology (POWERCON), 2010 International Conference on.* IEEE, 2010, pp. 1–5.

[28] H. Guanghui, H. Weiguo, and Z. Dawei, "Research and Implementation on Power System Stabilizer PSS4B Model," *CICED 2010 Proceedings*, pp. 1–4, 2010.

[29] I. Kamwa, R. Grondin, and G. Trudel, "IEEE PSS2B Versus PSS4B: the Limits of Performance of Modern Power System Stabilizers," *Power Systems, IEEE Transactions on*, vol. 20, no. 2, pp. 903–915, 2005.

[30] F. De Mello, D. Ahner, P. Anderson, J. Doudna, P. Kundur, L. Richardson, G. Tandy, C. Taylor, and F. VAN DE MEULEBROEKE, "Dynamics Models for Combines Cycle Plants in Power System Studies," *IEEE Transactions on Power Systems*, vol. 9, no. 3, pp. 1698–1708, 1994.

[31] C. Sharma, "Modeling of an Island Grid," *Power Systems, IEEE Transactions on*, vol. 13, no. 3, pp. 971–978, 1998.

[32] R. A. J. Khan, M. Junaid, and M. M. Asgher, "Analyses and Monitoring of 132 kV Grid Using ETAP Software," in *Electrical and Electronics Engineering, 2009. ELECO 2009. International Conference on*. IEEE, 2009, pp. I–113.

[33] C. Chen, C. Hsu, Y. Lee, J. Huang, H. Chen, and C. Huang, "Under Frequency Relay Setting for Tie Line and Load Shedding of an Industrial Power System with Multiple Cogeneration Units," in *Pulp and Paper, 1999. Industry Technical Conference Record of 1999 Annual*. IEEE, 1999, pp. 184–189.

[34] T. Sengupta, A. Das, and A. Mukhopadhya, "Development of On-line Real-time PC Based Frequency Meter and Frequency Relay for Monitoring, Control and Protection of HV/EHV Power System," in *Power Engineering Conference, 2005. IPEC 2005. The 7th International*. IEEE, 2005, pp. 1–22.

[35] F. P. Demello and C. Concordia, "Concepts of Synchronous Machine Stability as Affected by Excitation Control," *IEEE Transactions on Power Apparatus and Systems*, vol. 88, no. 4, pp. 316–329, 1969.

[36] Dr. Eugene F. Hill, "Private Email to E. F. Hill from an Electrical Engineering Colleague in Bhutan in 2012."

[37] Dr. E. F. Hill, "Work Experience of E. F. Hill with the Local Provincial Utility in 2012."

Appendix A

ROWENS MODEL for HDGT INCLUDING IGV

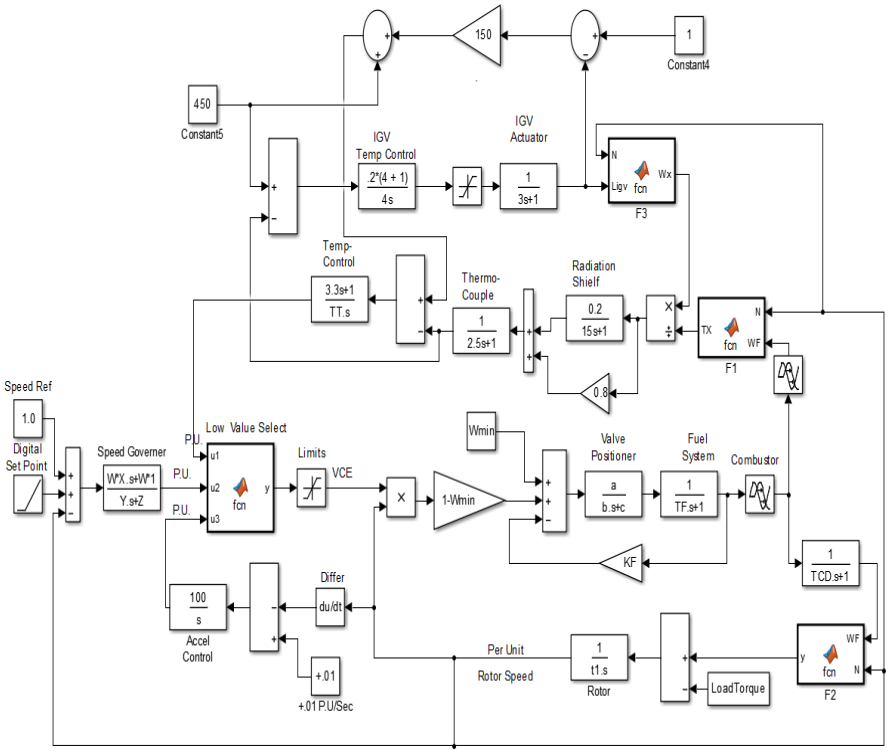

Figure A.1: Rowens Model for HDGT Including IGV

Appendix B

SYSTEM EQUATIONS

B.1 Moment of Inertia J

$$J = \frac{WR^2}{32.2} * 1.356 \ (kg.m^2) \tag{B.1}$$

B.2 Inertia Constant H

$$H = 5.48 * 10^{-}9 \frac{J(RPM)^2}{MVArating} \ (MW \cdot s/MVA) \tag{B.2}$$

Appendix C

SYSTEM PARAMETERS

Synchronous Generator Data	
MVA	175.24
MW	148.954
kV	16.5
PF	0.85
# of Poles	2
RPM	3600
X_e (Strong Grid)	0.257
X_e (Weak Grid)	0.40
$X_{d'}$	0.138
X_d	1.26
X_q	1.01

Table C.1: Exciter Parameters

Exciter Parameters	
Type	AC5A
VRmax	20.53
VRmin	-12.8
Efdmax	5
KA	135.6
KE	1
KF	0
TA	0.001
TE	0.055

Table C.2: PSS Parameters

PSS Parameters	
Type	PSS1A
KS	0.75
VSTmax	0.05
VSTmin	-0.05
A1	0
A2	0.008
T1	0.14
T2	0.01

Appendix D

CALCULATION OF $K_1 - K_6$

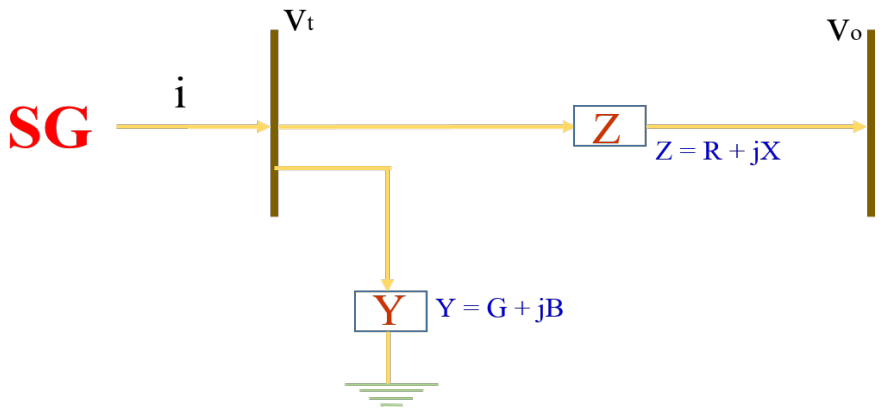

Figure D.1: A One Machine Infinite Bus Power System

$$\begin{bmatrix} K_1 \\ K_2 \end{bmatrix} \begin{bmatrix} 0 \\ i_{q0} \end{bmatrix} + \begin{bmatrix} F_d & F_q \\ Y_d & Y_q \end{bmatrix} \begin{bmatrix} (x_q - x_d^{'}) i_{qo} \\ e_{q0}^{'} + (x_q - x_d^{'}) i_{qo} \end{bmatrix} \tag{D.1}$$

$$K_3 = 1/[1 + (x_d - x_d^{'}) Y_d] \tag{D.2}$$

$$K_4 = (x_d - x_d^{'}) F_d \tag{D.3}$$

$$\begin{bmatrix} K_5 \\ K_6 \end{bmatrix} \begin{bmatrix} 0 \\ v_{q0}/v_{q0} \end{bmatrix} + \begin{bmatrix} F_d & F_q \\ Y_d & Y_q \end{bmatrix} \begin{bmatrix} -v_d^{'} v_{q0}/v_{t0} \\ x_q - x_d v_q 0/v_{t0} \end{bmatrix} \tag{D.4}$$

Appendix E

SAPF ISLANDING SCENARIOS

Table E.1: SAPF Islanding Scenarios

#	Online Unit	Individual Total generate Power (MW)	Plant Load (MW)	Grid (MW)	Disturbance (Seconds)	Comments
1	1,2,3	57.1/171.3	171	0	Both Grid Lines open at 0.5	This is a reference case.
2	1,2,3	57.1/171.3	171	0	One Grid Lines open at 0.5	This is a second reference case, with one line remaining in service.
3	1,2,3	57.1/171.3	171	0	Both Grid Lines open at 0.5 Load (701-A) 20.2 MW trip open at 2	Loss of both lines, followed by an in-plant load change.

4	1	180/180	217.2	+ 38	Both Grid Lines open at 0.5	The nominal rating of the generator is 150 MW. However if the ambient temperature for the gas turbine is 15-20 degrees C it can produce 180 MW
5	1,2	52/104	203.6	+100	Both Grid Lines open at 0.5	More import power than Case 4.
6	1	52	229.5	+178	Both Grid Lines open at 0.5	This is the highest import case.
7	1	130	99.7	-30	Both Grid Lines open at 0.5	This is an export case.
8	1,2	175/350	170.9	-177.1	Both Grid Lines open at 0.5	This case is increasing the export MW.
9	1,2,3	175/525	100.2	-419.6	Both Grid Lines open at 0.5	This is the very highest export case.

10	1,2,3	150/450	100	-346.6	Both Grid Lines open at 0.5	This case shows the maximum export MW under normal ambient conditions.
11	1,2,3	150/450	170	-277.1	Both Grid Lines open at 0.5	This is a normal operation.
12	1,2,3	150/450	170	-277.1	Both Grid Lines open at 0.5 And Load (701-A) 20.2 MW trip at 5	Export case, followed by an in-plant load change.
13	1,2,3	150/450	170	-277.1	Grid Line # 2 open at 0.5 , Bus tie Breaker open at 5 { Load on the Bus-2 =97.2MW}	Export case, followed by one line tripped and bus-2 separation. (tie Breaker tripped).
14	1,2,3	150/450	170	-277.1	Grid Line #2 open at 0.5 , Bus tie Breaker open at 30 (load on Bus-2 = 134.3MW)	Similar to case 13, but the total load on bus-2 is higher.

Appendix F

TRANSIENT STABILITY AND OVER-FREQUENCY RELAY ACTIONS

Table F.1: Transient Stability and Over-frequency Relay Actions

Device #	Action	Action By	Time (Sec)
Grid-1 CB	Trip	Study Case	0.5
Grid-2 CB	Trip	Study Case	0.5
Unit-1 CB	Trip	Over-Frequency Relay	40.576
Unit-2 CB	Trip	Over-Frequency Relay	40.576
Unit-3 CB	Trip	Over-Frequency Relay	40.576

Vita

Candidate's Full Name:	Bader Saud Alkhaldi
University Attended:	California State University of Long Beach, 1250 Bellflower Blvd, Long Beach, CA 90840, United States Bachelor of Engineering in Electrical Engineering. 2003-2006
Employer:	Saudi Aramco Oil Company (Kingdom of Saudi Arabia)